AN ABSTRACT OF THE THESIS OF

Shawn M. Wicks Freilinger for the dual degree of Master of Science in Civil Engineering and Forest Products presented on January 30, 1998. Title: Short-Term Duration of Load and Cyclic Performance of Metal-Plate-Connected Truss Joints.

Signature redacted for privacy.

Abstract approved: _____

Rakesh Gupta

Signature redacted for privacy.

_____

Thomas H. Miller

The objective of this research was to evaluate the duration of load factor for metal-plate-connected (MPC) truss joints subjected to various cyclic loading conditions. Heel and tension-splice joints from a standard 30-foot span Fink truss constructed from nominal 2x4 Douglas-fir lumber were tested. A testing frame similar to that developed by Gupta and Gebremedhin (1990) was used to test the joints under several different loading conditions. A static ramp load of 780 lbs./min. was applied to ten joints (both tension-splice and heel joints) until failure was reached. This test group served as the control group for comparison with joints tested under several cyclic loading regimes, with ten joints (per joint type) in each sample group. At the end of these cyclic loadings, the joints were ramped to failure (if they survived the cyclic loading). Results were evaluated by comparing the ultimate loads and stiffnesses from the control group specimens to those from the cyclic loading groups. An evaluation of the damage resulting from the cyclic loads is also discussed. Reductions in the stiffness and strength of the joint after the cyclic loading are related to the number of cycles, and the amplitude of the cycles. The results of this research show that the current duration of load factor of 1.6 for earthquake loading used in the design of MPC joints is adequate.

Short-Term Duration of Load and Cyclic Performance of Metal-Plate-Connected Truss Joints

by

Shawn M. Wicks Freilinger

A THESIS

submitted to

Oregon State University

in partial fulfillment of
the requirements for the
degree of

Master of Science

Completed January 30, 1998
Commencement June 1998

Master of Science thesis of Shawn M. Wicks Freilinger presented on January 30, 1998

APPROVED:

Signature redacted for privacy.

Co-Major Professor, representing Forest Products

Signature redacted for privacy.

Co-Major Professor, representing Civil Engineering

Signature redacted for privacy.

Head of Department of Forest Products

Signature redacted for privacy.

Head of Department of Civil, Construction and Environmental Engineering

Signature redacted for privacy.

Dean of Graduate School

I understand that my thesis will become part of the permanent collection of Oregon State University libraries. My signature below authorizes release of my thesis to any reader upon request.

Signature redacted for privacy.

Shawn M. Wicks Freilinger, Author

ACKNOWLEDGMENT

I would like to thank my major professors, Dr. Rakesh Gupta and Dr. Thomas H. Miller for their guidance in this research. I would also like to thank Frank Lumber Company and Alpine Engineered Products for their help in supplying the materials needed in this research. Finally, I would like to especially thank Milo Clauson for his technical assistance with the MTS hydraulic control system.

TABLE OF CONTENTS

TABLE OF CONTENTS, CONTINUED

TABLE OF CONTENTS, CONTINUED

LIST OF FIGURES

LIST OF FIGURES, CONTINUED.

LIST OF FIGURES, CONTINUED.

LIST OF TABLES

LIST OF APPENDIX FIGURES

LIST OF APPENDIX TABLES

DEDICATION

This thesis is dedicated to our Creator from whom all this is possible, my wife and parents for their constant encouragement and drive, and my son, Kyler, who gave me my purpose and meaning.

SHORT-TERM DURATION OF LOAD AND CYCLIC PERFORMANCE OF METAL-PLATE-CONNECTED TRUSS JOINTS

1. Introduction

1.1. Background

Metal-plate-connected (MPC) wood trusses are used in residential and light commercial applications. By prefabricating the trusses, time and labor costs can be saved in the construction of intricate roof systems. While MPC trusses are widely used in the construction industry, very little is known about the dynamic characteristics of their joints. Design requirements found in both the National Design Specification (AFPA 1991) and the Truss Plate Institute (TPI 1985) specification are based on static loading and do not account for degradation due to the cyclic nature of wind and seismic loading conditions.

Wood structures have repeatedly demonstrated that wood has beneficial qualities with regard to dynamic loading and load rate effects. Timber structures can dissipate the energy imparted to them from earthquake and wind events through their connections and material properties (USDA 1987). The connections used in timber construction often are key contributors in the absorption of energy in seismic events.

Traditionally, timber connections have been designed based on an understanding of their monotonic properties. The monotonic design values are based on 10-minute static testing and these values are then transformed to 10-year design values using a 1.6 duration of load factor from the Madison Curve (AFPA 1991). For Metal-Plate-Connected truss joints, a factor of safety of 1.875 is also applied to the 10-minute static value to determine the 10-year allowable design values for MPC joints (1.875 in the 1991 National Design Specification).

Figure 1-1. Typical Residential Construction using MPC Joints.

When these allowable design values are used for seismic or wind event design, they are transformed back to a shorter time duration by using the appropriate duration of load factor (C_D) from the 1991 National Design Specification (AFPA 1991).

The 1991 National Design Specification (NDS) uses the C_D adjustment factor to transform the 10-year allowable design values to 10-minute values for both seismic and wind events (C_D=1.6). The increase in the design allowable accounts for the beneficial properties of wood for short-duration loading. Past editions of the NDS specified that allowable design values should be transformed from the 10-year values to 1-day values for both seismic and wind loadings. The duration of load factor for 1-day is 1.33. Building code agencies have questioned the change in this C_D value. The 1994 Uniform Building Code (UBC 1994) adopted the new duration for wind events, but did not adopt the same duration for seismic events (seismic: C_D = 1.6 and wind: C_D = 1.33).

The literature review in chapter 2 contains a general discussion of the duration of load factor and how it impacts the design of metal-plate-connected truss joints.

This research will investigate the appropriateness of the 10-minute duration of load factor (C_D = 1.6) for the seismic design of metal-plate-connected truss joints and the effects of short-term cyclic loads on these joints.

1.2. Objectives

The following are the objectives of this research:

1. To evaluate the duration of load factor of 1.6 for metal-plate-connected truss joints by subjecting tension-splice and heel joints to a cyclic loading that has been proposed to simulate seismic events.
2. To evaluate strength and stiffness degradation from this cyclic loading by investigating the cyclic stiffness, and the reduction in ultimate strength following the cyclic loading.
3. Determine a conservative estimate for the duration of load factor for seismic loadings.

2. Literature Review

The study of the performance of metal-plate-connected truss joints subjected to dynamic loading is a relatively new research area. Most of the research associated with metal-plate-connected joints deals exclusively with the response to static loads. Dynamic loading of joints has received some additional attention in the recent past (Dagher et al 1991, Leiva 1994, Kent 1995), and researchers have gained an increased understanding that structural properties of joints can change under dynamic and cyclic loading conditions.

Most dynamic testing of wood joints has involved nailed and bolted connections. This chapter will review several aspects of the overall behavior of metal-plate-connected truss joints. The first section will give a general overview of the dynamic behavior of wood structural systems. The rest of this chapter will highlight the existing research on static testing of metal-plate-connected truss joints, fatigue of metal-plate-connected truss joints, and studies of nailed and bolted connections and metal-plate connected joints under dynamic and cyclic loads.

2.1. Behavior of Wood Structures Subjected to Dynamic Loads

While relatively few studies have been accomplished on the dynamic properties of wood joints, several have examined the dynamic properties of other timber structural systems.

Polensek and Schimel (1991) investigated the behavior of connections in wood structural systems. Their study investigated the changes in stiffness and damping coefficient as displacement amplitudes of the test cycles were varied. In three other papers presented at the 1994 Pacific Timber Engineering Conference (Ceccotti et al 1994, Leiva 1994, Deam and King 1994), stiffness, viscous damping ratios, ductility,

and energy dissipation were discussed for wood systems. In an article by Foliente and Zacher (1994), there is a detailed discussion of timber joints and timber structures subjected to seismic loads. It covers energy dissipation, hysteresis behavior and damping characteristics and provides an excellent discussion of timber joint testing under dynamic loads. These articles provide an excellent background to the study of wood connections subjected to dynamic loads, and the research demonstrated the beneficial energy dissipation (damping) properties of wood structures and wood connections.

2.2. Wood Connection Research

2.2.1. Influence of Strain Rate on Strength of Wood Joints

This section describes two studies that discuss load rate and strain rate effects on wood joints. While these are similar, load rate refers to the rate of applied load and strain rate refers to the rate of strain (displacement) in the joint. Girhammar and Anderson (1988) investigated the loading rate of connections and effects on the strength of the joint. They investigated several joint types and configurations and found that all were affected by the loading rate. There was a significant increase in strength at the higher load rates. The second study, by Bodig and Farquhar (1988), investigated the strain rate and its effect on structural properties. This study also found a similar significant effect due to the strain rate. Joints subjected to a higher strain rate had an increase in strength when compared to tests at slower strain rates.

2.2.2. Static Testing of MPC Joints

While there is no standard for the dynamic testing of metal-plate-connected truss joints, standards exist for the static testing of metal-plate-connected truss joints. ASTM D1761 (ASTM 1994) provides a method of static loading for tension-splice joints. For MPC joints, the Truss Plate Institute specification (TPI 1985) exclusively addresses static loading.

Gupta and Gebremedhin (1990) reported on the load-displacement characteristics and failure modes of actual MPC wood truss joints. Their study investigated tension-splice joints, web at the bottom chord joints, and heel joints. They obtained information regarding strength, stiffness, and failure mechanisms for MPC joints under static loads. Gupta and Gebremedhin (1990) found the failure of the heel joint to be ductile and the failure of the tension-splice joint and the web at the bottom chord joint to be brittle. They found that tension-splice joints tended to fail at approximately 6000 lbs. They also found that the joints showed a combination of wood and tooth failure.

Gupta (1994) also investigated MPC wood truss joints under combined tension and bending loading. Gupta (1994) examined six different loading conditions: pure axial tension, pure bending, and four combined cases with varying degrees of eccentricity of an axial load. This study showed that the axial capacity of a tension-splice joint decreased by approximately 200 lbs. for each 1,000 lb.-in of bending moment applied. All of these joints failed in tooth withdrawal. Wolfe et al. (1991) also investigated combined loading conditions for MPC joints. They employed eccentric axial loads to produce bending within the joint. Wolfe et al. (1991) also found that there was a decrease in strength with an increased applied moment. The joints failed in tooth withdrawal and plate yielding. These studies illustrate the

importance of joint alignment in testing. If the axial load applied to the joints is out of alignment, one can expect lower strengths.

Static loading studies have been accomplished to determine the influence of wood and joint properties on the strength of the joints. These include the previously mentioned study by Gupta and Gebremedhin (1990). In addition to this study, Nielson and Rathkjen (1994) also tested tension-splice joints subjected to tension loads. They provide many graphs of load-displacement relationships, and their load-displacement curves proved to be similar to ours. They investigated the influence of plate placement, loading rate, and grain orientation. Their results show a strength increase due to higher load rates.

These static studies provide a background for the dynamic testing of MPC joints. They also provided insight into the importance of proper fabrication of the joints and how they should be accomplished in our study.

2.2.3. Dynamic Testing of MPC Joints

Currently, accepted test standards do not exist for the dynamic testing of wood joints. Dolan (1994) presented the Sequential Phased Displacement (SPD) Procedure originally proposed by Porter (1987) and similar to that of Reyer and Oji (1991). This standard was proposed for the study of nailed and bolted connections. The first half of this overall research project, described in Kent (1995), examined the effects of an SPD loading, a historical earthquake loading, and an artificial earthquake loading on the strength and stiffness of MPC tension-splice and heel joints.

This portion of the project will apply a load-controlled method to MPC joints. The load-controlled method was originally proposed by Dolan, Gutshall and McLain (1995) for nailed and bolted joints. The proposed method attempts to quantify the load duration factor for nailed and bolted connections. To demonstrate that the load duration factor of 1.6 is conservative, their study began by loading bolted and nailed

joints with 30 cycles at 1.6 and 1.75 times the allowable design value, respectively. All cycles were applied at 1 Hz. The 30 cycles represented 4 design level earthquakes in the life of the joint and were based on Dolan's (1989) study of shearwalls subjected to a simulated 1954 Taft earthquake (Dolan 1995b). They found that nailed and bolted joints did not experience any damage when subjected to the 30 cycles. They then loaded the joints at 1.0 times the design load for 30 cycles and 1.6 times the design load for 15 cycles. This was to represent 4 smaller earthquakes and 2 design level earthquakes in the life of the joint. This loading regime also did not cause any damage. The nailed and bolted joints were then subjected to 1.0 times the design load for 30 cycles, 1.6 times the design load for 15 cycles and 2.0 times the design load for 8 cycles. This was to represent 4 smaller earthquakes, 2 design level earthquakes, and 1 overload event in the life of the structure. This conservative loading regime did not cause any damage either. Due to the conservative approximation of the life span loading, it was concluded that the use of 1.6 for the duration of load factor was adequate for nailed and bolted connections. A similar approach was applied here for MPC joints.

The previous studies of nailed and bolted connections did not include a representative dead load. To produce a more realistic loading function, the joints in this project were loaded to a theoretical dead load before cycling (900 lbs. for the tension-splice joints and 1550 lbs. for the heel joints). In order to maintain consistency in the overall project, the dead load was based on the dead load used in Kent (1995).

A few studies have investigated the mechanical properties of MPC joints subjected to cyclic loading. Besides the previously mentioned Kent (1995) research, Leiva (1994) investigated the stiffness changes in MPC joints due to cyclic loading. Leiva (1994) found that the stiffness decreased with increasing cycles. Emerson and Fridley (1996) also published research based on Dolan and Gutshall's work with nailed and bolted connections (Gutshall 1994). Their study did not pre-load the joint to dead

load (as this study does) and the joints never went into compression and were only cycled in tension. They noted minimal strength losses, and a slight stiffness loss due to the cycles.

2.2.4. Fatigue Characteristics of MPC Joints

Dagher et al. (1991) investigated the fatigue strength of MPC joints. They observed two modes of failure: tooth withdrawal and metal fatigue. Tooth withdrawal occurred when larger magnitude loads were used to fail the joints and metal fatigue occurred when small magnitude loads applied. The tests in this study involved high magnitude (between 2820 lbs. and 4750 lbs. for the tension-splice joints and between 3470 lbs. and 5390 lbs. for the heel joints) loading for a short time period. Thus, we expected tooth withdrawal failures.

Tokuda, et al. (1977) studied the behavior of MPC joints subjected to repetitive tension forces. Their research found that repetitive tension loads of up to 60% of the static ultimate load did not affect the static strength of joints. Hayashi et al (1980) studied tension-splice joints subjected to cyclic tension at a frequency of approximately 1 Hz. This and other research (Hayashi and Sasaki 1979) has centered on repetitive tensile loading or tension cycling. Our joint loading cycles will extend into the compression region and present buckling possibilities in our joints as well.

Sletteland, et al. (1977) investigated the fatigue life of MPC joints used in roof trusses and subjected to tension and compression cyclic loading. They found that Bostich-type nailed plates subjected to 80% to 140% of the design load exhibited no fatigue failures. Gismo-type plates failed at approximately 50,000 cycles of loading (at design load). The gang-nailed plates failed when the metal teeth sheared. This was followed by the remaining teeth failing in tooth withdrawal. This occurred at approximately 39,000 cycles at the design load.

2.3. Duration of Load Research

Wood (1951) did the first testing of duration of load effects on small clear specimens. In that study, Wood proposed a hyperbolic model for the relationship between strength and duration of load. This model is known today as the Madison Curve (Rosowsky and Fridley 1992). The Madison curve is the same model that is used today in the National Design Specification for Wood Construction (AFPA 1991) for determining duration of load effects on timber structures.

Several models have been studied recently to predict the duration of load effects on structural lumber. Most of these involve cumulative damage theory, but some have been based on fracture mechanics and strain energy (Rosowsky and Fridley 1995). Cumulative damage models seem the most appropriate for failure of wood applications because it is known that wood is influenced by time and cumulative damage (i.e. creep) (Rosowsky and Fridley 1995). This type of model was first proposed by Gerhards (Gerhards and Link 1987, Gerhards 1979) for small clear specimens and then extended to full-size lumber (Rosowsky and Fridley 1995).

The idea of a critical load or threshold limit has also been proposed. Barrett and Foschi (1978) first proposed a threshold limit under which no damage was accumulated. Rosowsky and Fridley (1992) investigated the influence of random loadings on duration of load effects. They found that damage accumulation seemed to be governed by a single load event based on a combination of critical magnitude and duration (Rosowsky 1992). Recent studies have suggested that this is true (Rosowsky and Fridley 1995). While this model seems very appropriate for full-size lumber (Foschi 1982), it is unsure whether it is also appropriate for connection mechanics. Rosowsky (1992) suggests that the duration of load effect is more critical in connections than in structural lumber. Since the typical design procedures for wood structures result in ultimate failures at the connections, duration of load effects for dynamic loadings are most critical in connections (Rosowsky and Fridley 1995).

Gutshall (1994) accomplished the most recent duration of load research on nailed and bolted joints. By comparing capacities and ductilities of joints with and without prior cyclic loading, it was concluded that the use of C_D =1.6 for nailed and bolted joints is adequate.

The duration of load factor (C_D) is used to account for time-related effects on wood strength. It is used to transform loads from one time duration to another. C_D is specifically used to modify the allowable design values determined using the National Design Specification (AFPA 1991). The 10-year allowable design values for metal-plate-connected truss joints are obtained through static testing (AFPA 1991). For MPC truss joints, allowable design values are obtained by taking the ultimate strength from a 10-minute test and dividing it by the 10-minute duration of load factor (1.6) and a factor of safety (1.875). This transforms the ultimate strength test value into a 10-year design value (AFPA 1993). This process is summarized in the NDS by simply taking the lesser of the ultimate static load divided by 3.0. The alternate definition of the design load (in the NDS) is based on the load associated with 0.03" wood-to-wood slip divided by 1.6 (AFPA 1991).

$$Y_{10\_year} = \frac{Y_{10\_minute}}{C_D * F.S.},$$

Y_{10_year}=10-year strength,
Y_{10_minute}=10-minute strength,
C_D= duration of load factor
F.S. = Factor of Safety

In 1951, Wood developed an equation that described the increase in wood strength due to decreased duration of loading. The curve that developed from the equation is referred to as the Madison Curve. Some common points along the Madison Curve are given below:

Table 2-1. Typical Duration of Load Factors (AFPA 1991).

Duration of Load	Duration of Load factor (C_D) to transform a 10-year allowable strength to the specified duration.
2 months	1.15
1 day	1.33
10 minute	1.6

In the NDS, the application of the duration of load factor to connection design is identical to wood members (AFPA 1993). Allowable design values determined by the 1991 National Design Specification (AFPA 1991) are based on a member " fully stressed to its maximum allowable design value cumulatively or continuously for a period of ten years or less during the life of the structure in which the member is used" (AFPA 1993). This implies that the cumulative damage of the joint loading is being assumed for the design of wood structures. Therefore, if a loading representing a 10-year loading could be applied in a shorter time period, one could assume that the resulting ultimate load is the 10-year strength value. By comparing this " 10-year" strength value to that from a 10-minute static test, we can determine a conservative estimate of the duration of load factor that transforms the 10-minute static test value to the " 10-year" value.

The load-controlled testing done by Dolan, Gutshall, and McLain (1995) used an approximation of a representative 10-year loading. The loading was designed to represent several seismic events in the life of the structure (Dolan 1995b). By assuming that this represents the cumulative loading during a 10-year period, a test can be produced that evaluates the duration of load factor used in design (Dolan 1995b).

The development of the representative 10-year loading function was based on load-control tests done at Virginia Tech (Gutshall 1994). These were based on Dolan's (1989) study on shearwalls, which concluded that 6-8 cycles (1 Hz.) at the 10-year NDS design load represented the accumulated damage during a " reasonable" seismic

event (Dolan 1995b). Applying this assumption, Gutshall (1994) performed various load-control tests on nailed and bolted joints. Gutshall's test design included a loading function that cycled at 1.0 times the allowable design load for 30 seconds (1 Hz.), 1.6 times the allowable design load for 15 seconds, and 2.0 times the allowable design load for 8 seconds (Gutshall 1994). It was concluded that these tests were a conservative estimate of the loading during the structure's lifetime (Dolan 1995b). To quantify how this function may break down into specific seismic events, Dolan surmises that the first stage (30 seconds at 1.0 times the NDS allowable design value) simulates 4 events that are minor in magnitude (i.e. minimum design level), the second stage (15 seconds at 1.6 times the NDS allowable design value) simulates 2 seismic events at the design level, and the third stage (8 seconds at 2.0 times the NDS allowable design value) simulates a single major seismic event (Dolan 1995b).

The magnitudes of the first and last stages of the representative 10-year loading are approximations of minor and major events, respectively. The seismic design level event (or second stage of the representative 10 year loading) is based on the current National Design Specification's (AFPA 1991) determination of member or (in our case) connection capacity. The seismic design capacity of a connection is the allowable design value (10-yr. Value from NDS) times the duration of load factor (C_D) of 1.6. If we are trying to determine an appropriate duration of load factor for design, we can vary the magnitude of the second stage until we obtain a duration of load factor that produces a final ultimate load (when ramped to failure) that is within some acceptable factor of safety to the allowable design value determined from the NDS.

If we use this method to specifically investigate the duration of load factors that are currently being used in the NDS, we can determine a factor of safety for that duration of load factor.

$$FS = \frac{Ultimate\_load\_following\_cycles}{Allowable\_Design\_Value\ From\_the\_NDS}$$

By comparing the NDS 10-year design value (static ultimate strength/3.0) with the ultimate load following the cyclic loading, we can determine the factor of safety for a given C_D value (Dolan, Gutshall, and McLain 1995).

It is very important to remember that the NDS 10-year allowable design value represents a member " fully stressed to its maximum allowable design value cumulatively or continuously for a period of ten years or less during the life of the structure" (AFPA 1993). By comparing the ultimate strength (load at failure from the cyclic test) of the cumulative loading function with the ultimate static strength (load at failure for the 10-min. test), one can determine if the MPC joints in this study experienced any adverse effects due to the load history. Since the cumulative loading function approximates the loading over a 10-year period, one can compare it with the ultimate 10-minute strength and determine a conservative approximation of the duration of load factor to transform between a 10-minute duration and a 10-year duration.

The representative 10-year loading function in this study of MPC joints was developed in a similar manner. In Gutshall's (Gutshall 1994) research, 1.0 and 2.0 times the NDS allowable design load were used as estimates of minor and major magnitude seismic events and 1.6 times the NDS allowable design load represented the application of the C_D factor used in the NDS for design. By multiplying the 10-year NDS allowable design value by $C_D = 1.6$, we can transform the 10-year NDS design value back to a 10-minute strength value used for seismic design. The 10-minute strength is the cumulative or continuous maximum load described in the NDS Commentary (AFPA 1993) and can therefore be used as the maximum load due to the

cyclic event (seismic). This 10-minute strength could be assumed to be the magnitude of a design level event. Therefore, it is used in the development of the representative 10-year loading function. Figure 3-1 steps through this development of C_D and the representative 10-year loading function.

As with Gutshall's (Gutshall 1994) study of nailed and bolted connections, a similar evaluation of duration of load affects can be accomplished for metal-plate-connected (MPC) truss joints. In this study of MPC joints, we actually took Gutshall's (Gutshall 1994) concept a step further. The MPC joints could not survive the same severity of loading as nailed and bolted joints did. Therefore, it was necessary to develop an approach to approximate the adverse effect that the cycles seemed to have on the joints. Two possible approaches were considered: 1) lower the C_D value, or 2) lower the NDS allowable design value. By lowering the C_D factor associated with a 10-minute test, we would be recognizing the fact that there may be a smaller strength gain during a short duration cyclic event for a connection than for structural members. To test the use of lower C_D values, different C_D values were used in the development of a representative 10 year loading function (i.e. $C_D = 1.0$, and 1.33). By using smaller duration of load factors in the development of the representative 10-year loading function, we reduced the magnitude of the design level events and the severity of the loading.

The load-controlled tests described were used to determine a number of cyclic properties. We also compared the static ultimate load to the ultimate load following the cyclic loading to determine the strength degradation. By comparing the static and cyclic load-deflection curves we approximated stiffness degradation due to the cyclic loading history. These tests added to the understanding of MPC truss joint behavior.

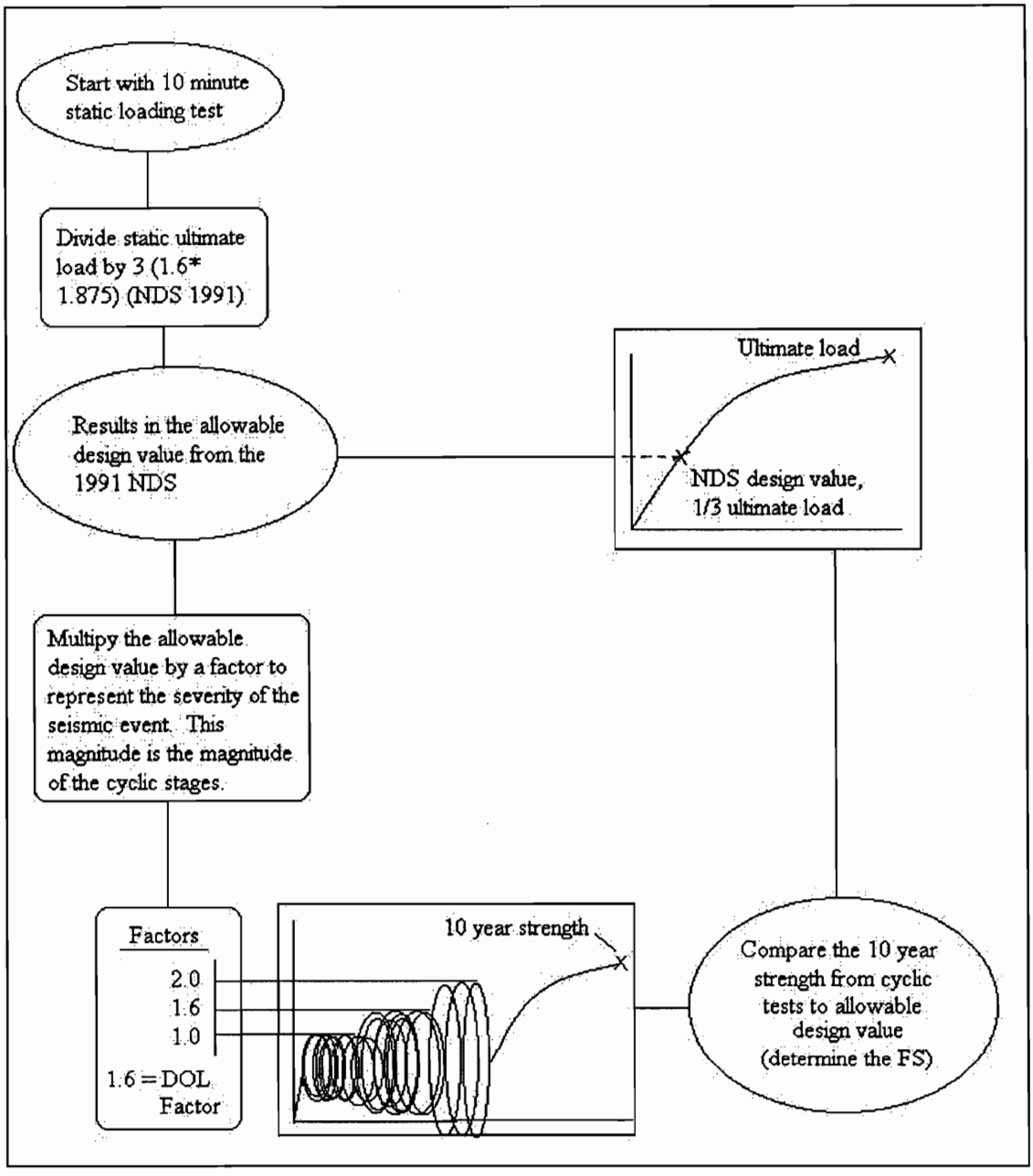

Figure 2-1. C_D Flow Chart.

3. Experimental Methods

3.1. Experimental Procedures

3.1.1. Sampling Method

Ten-foot long nominal 2 x 4 members were obtained from Frank Lumber Company. Each board was assigned a number and its modulus of elasticity was measured with a vibration method using a Metricguard, Model 390. The boards were then randomized based on random computer generated numbers. The random number assignments determined which boards would be used for tension-splice joints and which boards would be used for heel joints. From each board, 2-3 joints were made. Each of these joints was marked according to which board they were taken from. They were randomized again using generated random numbers to determine which testing regime they would be assigned to. If a joint was inadequately fabricated (gaps in the joint, poor plate contact), the next joint was moved up in the loading case assignment. This procedure provided a thorough mixing of the joints for testing.

The following equation was used to determine the ideal sample size.

$$n = (\frac{t}{0.05} CV)^2$$

For a CV = 7% and 95% confidence interval, the sample size should be 9. This is based on the assumed that the t statistic is equal to 2.101 (18 degrees of freedom).

3.1.2. Materials and Fabrication

Test specimens were fabricated from machine stress rated (MSR) Douglas-fir (1800f-1.6E). The lumber was conditioned in a standard room to approximately 14% moisture content. Alpine Engineered Products, Inc., Pompano Beach, FL Beach, supplied the metal plates used in the fabrication of the joints. The properties of the metal plates are summarized in Table 3-1. The tension-splice joints were connected using 20-gauge, 3" x 4" metal plates as shown in Figure 3-1. The heel joints were connected using 20-gauge, 3" x 5" metal plates. The heel joints were fabricated at a slope of 4:12 with the placement of the metal plate as shown in Figure 3-2.

Kent (1995) found that some variation in joint properties seemed to occur due to different manufactured batches of plates. Therefore, all tension-splice joints and heel joints were fabricated from plates taken from the same manufactured batch to limit a source of variability. The plates were pressed into the joints using a 450-ton Cliffton hydraulic press until the teeth were completely embedded into the wood. They were then visually inspected to insure that over-pressing and under-pressing of the plates were avoided. After fabrication, the joints were placed in a standard room at approximately 14% moisture content. The joints remained in the standard room for several months until the testing took place. This allowed a much greater time for the relaxation of the teeth in the wood than is required (7 day minimum), as suggested by Arbek (1979). Bolt holes to hold the joint the testing apparatus were drilled within days of the testing.

Table 3- 1. Physical Properties of MPC Plates (Alpine Engineered Products, Inc.)

Property	Value
Yield Strength	51.5 ksi
Ultimate Strength	60.5 ksi
Thickness	0.036 in.
Percent Elongation at Failure	31.5%
Tooth Length	0.25 in.
Tooth Width	0.12 in.
Slot Length	0.25 in.
Slot Width	0.12 in.

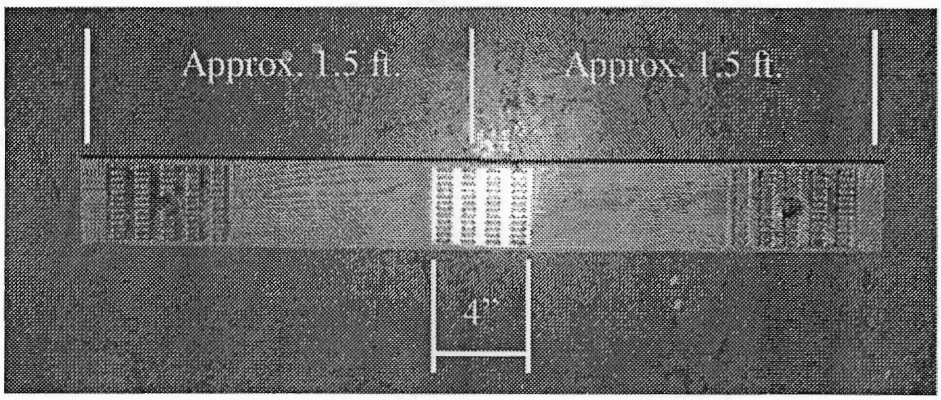

Figure 3- 1. Typical Tension-Splice Joint.

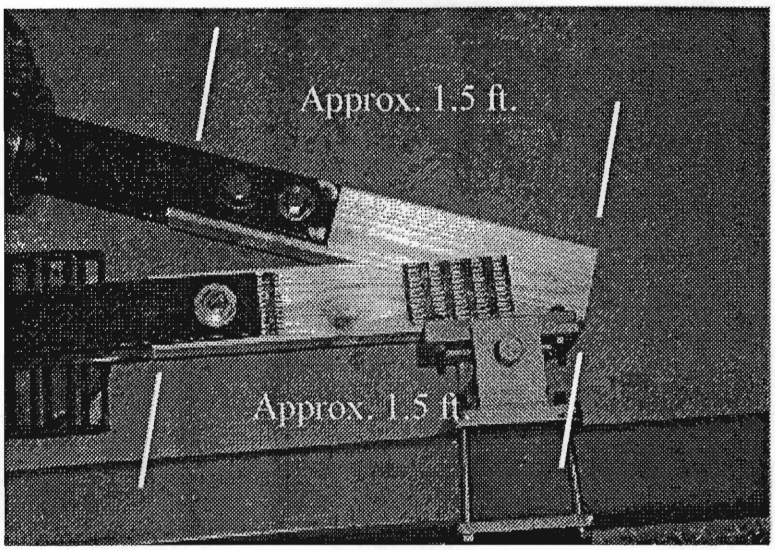

Figure 3- 2. Typical Heel Joint.

3.1.3. Apparatus

The joints were tested using a trapezoid-shaped frame similar to that developed by Gupta and Gebremedhin (1990). The frame allows for various joint configurations to be tested in the horizontal plane. To apply the load, an 11,000 lb. capacity Materials Testing System (MTS) dynamic hydraulic actuator was used. Several bracing fixtures were developed to reduce loading eccentricities the testing. The bracing helped provide consistent alignment of the test joints. Care was taken to place the test joint in a location where the frame would supply the stiffest reaction and reduce energy dissipation in the test frame. Bracing members were also added to increase the frame's stiffness. Figures 3-4 and 3-5 show the schematic of the test set-ups for the tension-splice and heel joints.

The axial load on the tension-splice joint was measured using a 20,000-lb. capacity Sensotec load cell. It was placed between the hydraulic actuator and the

support for one end of the joint (Figure 3-3). The load cell required a 5-volt input. Two similar Sensotec load cells were used in the testing of the heel joints. One was placed between the joint and the hydraulic actuator (in the top chord) and one was placed between the joint and a frame fixture (to measure force in bottom chord (Figure 3-4).

The relative displacements on either side of the tension-splice joint were measured using direct current linearly variable differential transducers (LVDTs) (Figure 3-3). The LVDTs were fastened to the test specimen using aluminum fixtures that helped to center the LVDTs on the side of the joint and hold them secure (Figure 3-5). In the testing of the heel joints, two LVDTs were used. One LVDT measured the axial displacement across the metal plate and the other LVDT measured the rotation of the top chord away from the bottom chord of the joint (Figure 3-6). The LVDTs required a 5-volt power source and had a range of 1-inch.

Figures 3-7 and 3-8 are photographs of the complete setup before testing.

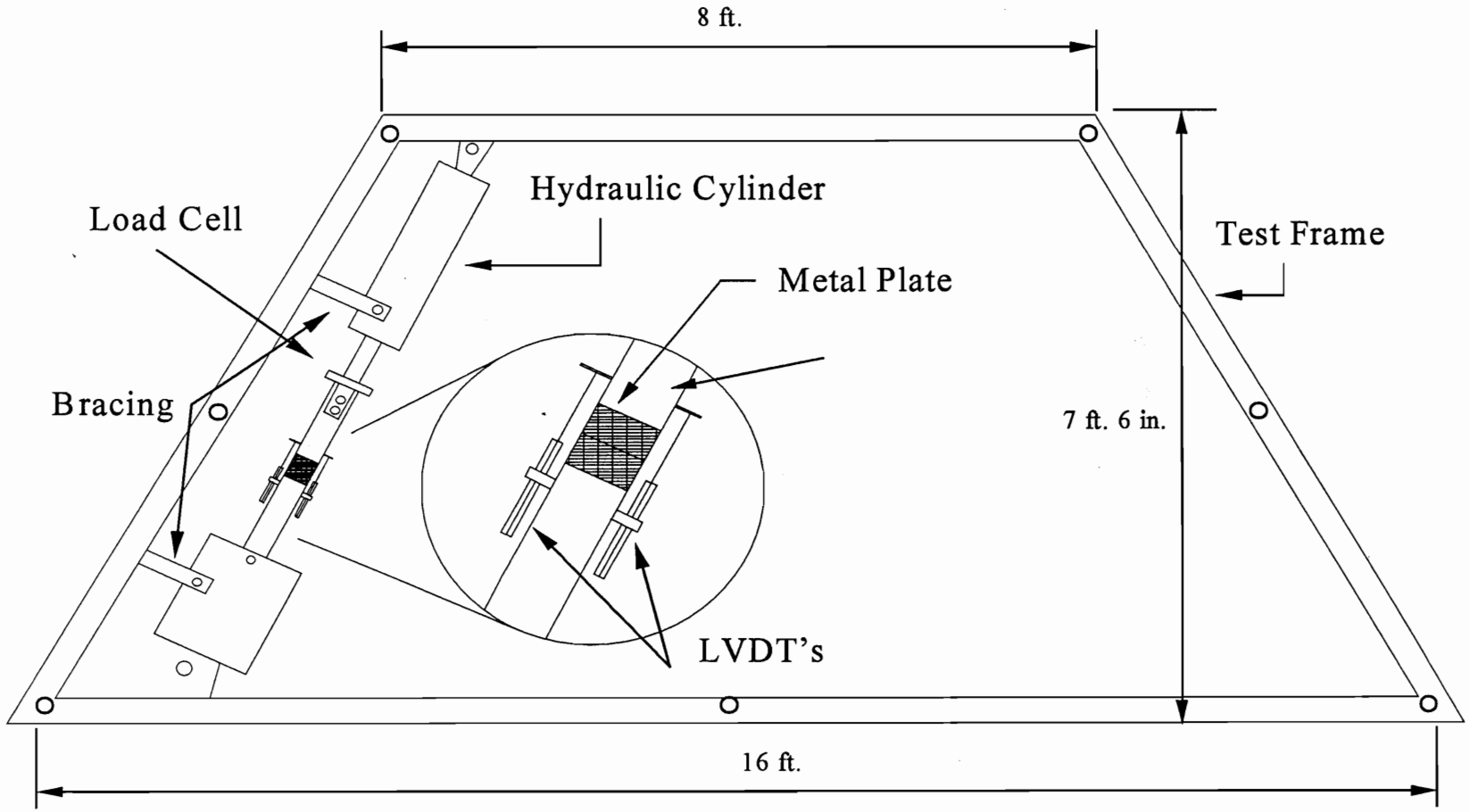

Figure 3- 3. Schematic of Test Setup With Tension-Splice Joint.

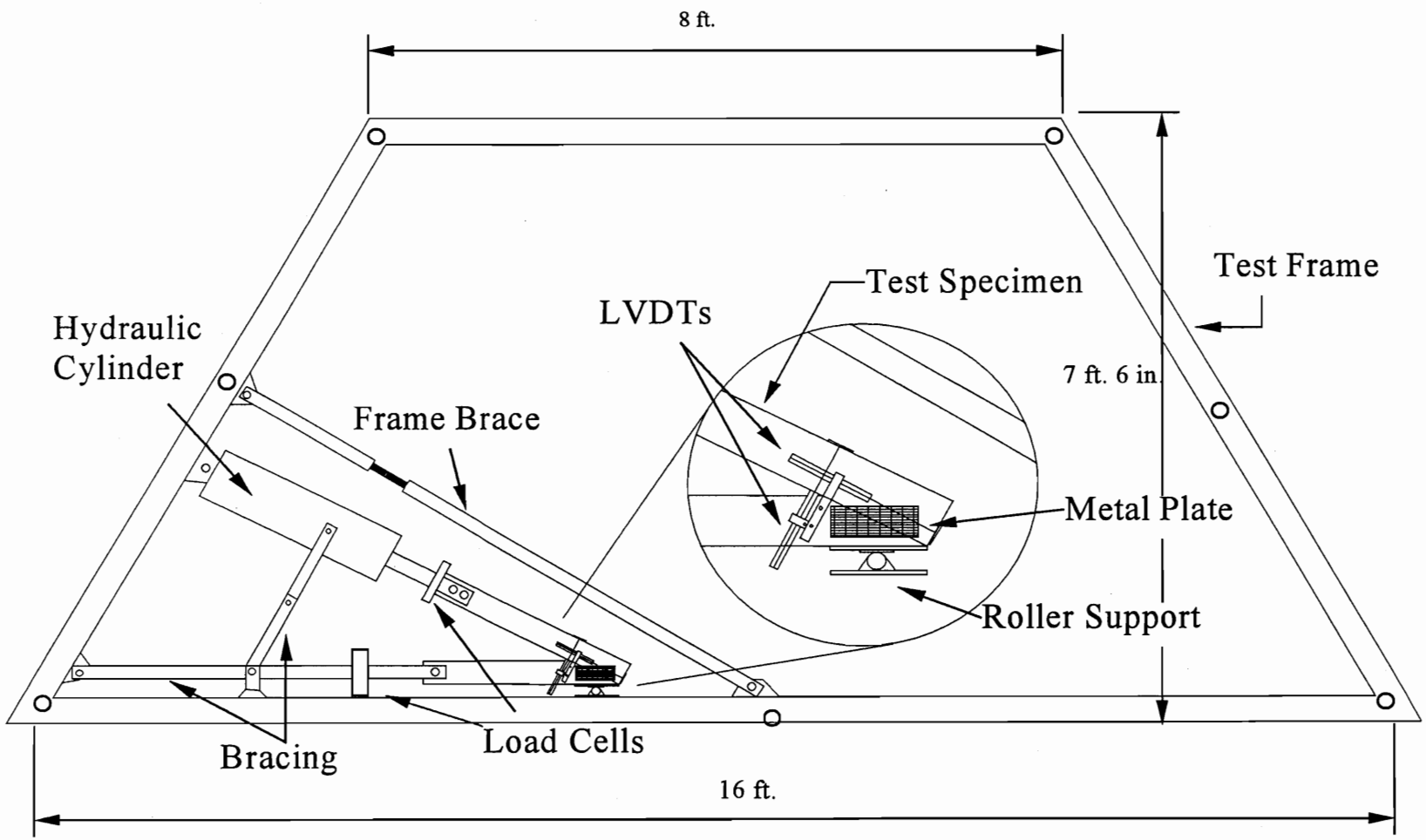

Figure 3- 4. Schematic of Test Setup with Heel Joint.

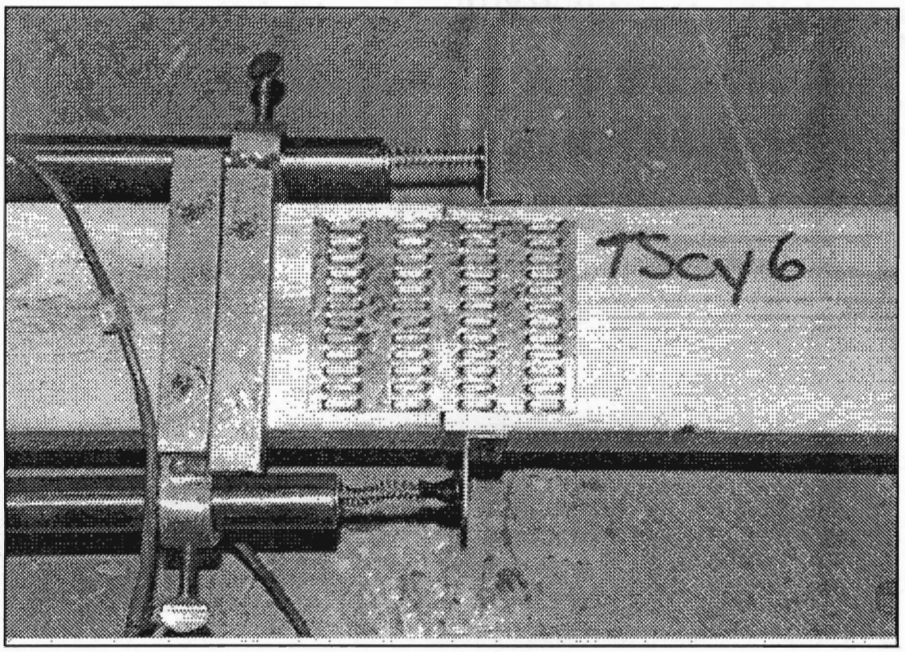

Figure 3- 5. Tension-Splice Joint LVDT Layout.

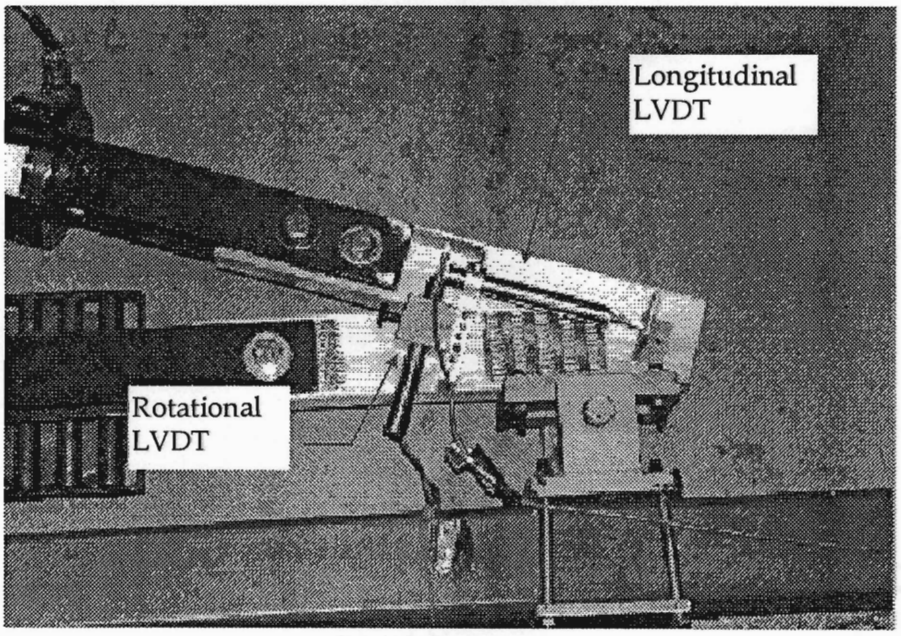

Figure 3- 6. Heel Joint LVDT Layout.

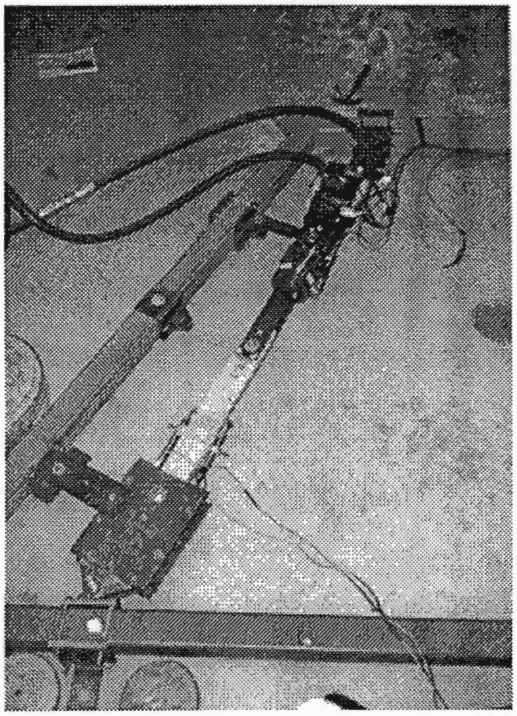

Figure 3- 7. Tension-Splice Joint Loading Setup.

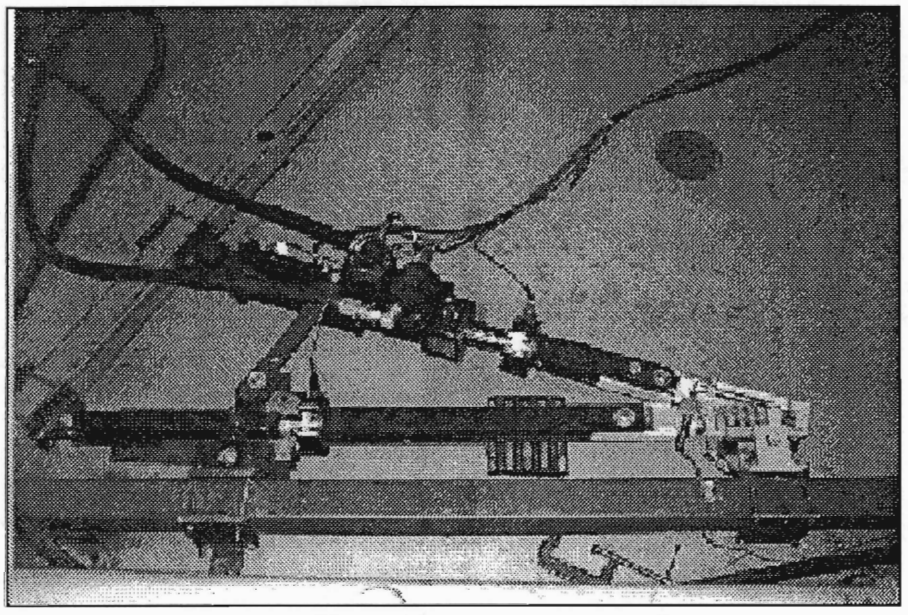

Figure 3- 8. Heel Joint Loading Setup.

The response voltages from the LVDTs were recorded using an analog-to-digital card attached to a personal computer with an 80386 microprocessor. The load cell response voltages were sent directly to an MTS 403.11 Controller. After comparing the response voltage from the load cell and the required voltage from the control function, the controller adjusted the voltage supplied to the hydraulic actuator, thereby changing the load observed by the load cell. The controller then sent the load cell response voltage to the analog-to-digital card to be recorded.

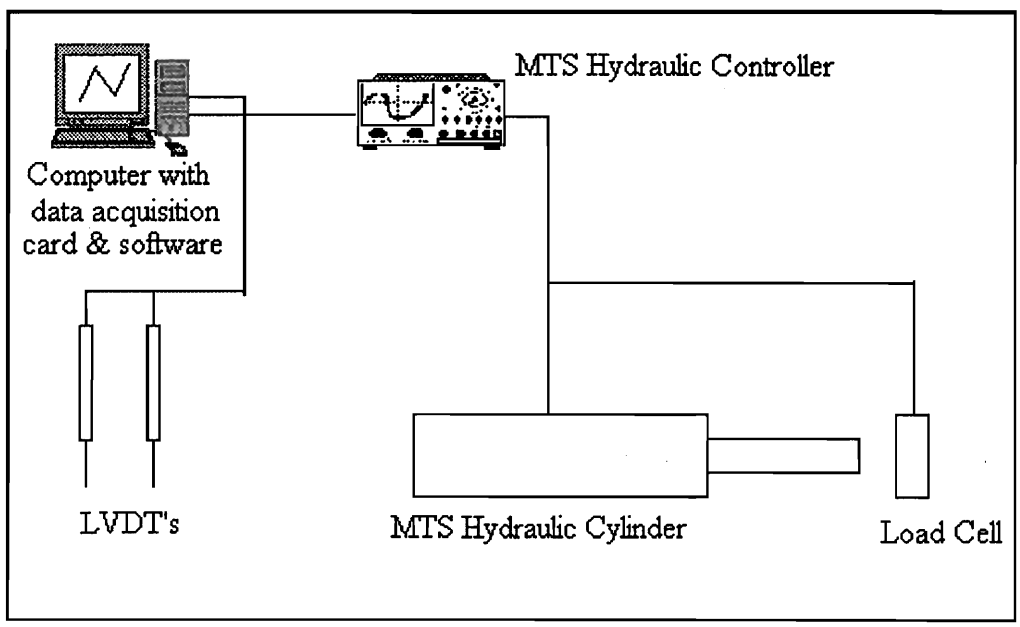

Figure 3- 9. Test Setup Schematic.

3.2. Test Procedures

The tension-splice joints were tested under seven different loading regimes as shown in Table 3-2. The first loading regime was a static loading test used as a control. The next six loading regimes tested the joints under

various cyclic loading conditions. These loading regimes were variations based on Dolan, Gutshall, and McLain (1995). Two additional loading regimes did not track the control function from the computer properly. The results from these two test regimes were unreliable, therefore one load case was repeated and the other was eliminated from the study completely. The eliminated tests are discussed in Appendix A. Dolan used the cyclic loadings to simulate seismic events in the life of a joint. Dolan assumed that 1.0 times the design load simulated a minor event, 1.33, 1.6, and 1.8 times the design load were used to approximate various possible design events and 2.0 times the design load was assumed to simulate a major event (Dolan 1995b). Our tests were similar to Dolan's test except a dead load (based on Kent 1995) was added before the cycles were applied. This was done to produce a more realistic loading on the joints. The tension-splice joint dead load was 900 lbs. and the heel joint dead load was 1550 lbs. These loads were applied with the hydraulic system at the same location as the cyclic loads.

The personal computer used Workbench 2.0 software (1991) for the data acquisition and control signal generation. Using a Strawberry Tree Workbench interface, the response voltages from the LVDTs and the load cell were viewed during the test and recorded in a standard ASCII text file. The Strawberry Tree Workbench interface also generated the required voltage (for control) sent to the MTS 403.11 Controller. The required voltage (for control) was generated based on the forcing function for the specific loading case using appropriate mathematical expressions within the Strawberry Tree program. Figure 3-9 above is a complete schematic of the testing control system.

The heel joints were tested under four loading regimes. The first loading regime was a static loading test used for a control. The next three loading regimes

tested the joint under various cyclic loading conditions based on Dolan, Gutshall, and McLain (1995) with an additional pre-load representing the dead load. Again, these cyclic loadings were used to simulate seismic events in the life of the joint in the same manner as for the tension-splice joint loading regimes.

3.2.1. Static Load Tests

A tensile static ramp load of 780 lbs./min was applied to ten joints for the tension-splice joints. The tensile ramp load was applied axially to the tension-splice joints and caused failure in 7 to 10 minutes. For the heel joints, a compressive static ramp load was applied to the top chord of the heel joints and caused failure in 7 to 10 minutes. The response voltage from the LVDTs and load cells were averaged using a boxcar filter with a duration of 0.05 seconds to reduce noise. The design load was then calculated for use in the cyclic loading regimes by dividing the average ultimate load by 3. This is the standard practice used in both the NDS and the TPI standards (AFPA 1991, TPI 1985).

3.2.2. Cyclic Loading Tests

The cyclic loading tests are variations on Dolan, Gutshall, and McLain (1995). Table 3-2 indicates which tests were performed for the tension-splice and heel joints. Table 3-3 outlines each test that was performed. The stages in Table 3-3 refer to the example loading function shown in Figure 3-10. The tension-splice joint dead load was 900 lbs. and the heel joint dead load was 1550 lbs. This dead load was applied at the same point as the cyclic load (based on Kent 1995). If a joint survived the cyclic tests, the joint was then ramped to failure.

Table 3- 2. Tension Splice and Heel Joint Tests Performed.

	Tension	*Heel*
Static	X	X
C1	X	
C6	X	
C16	X	X
C132	X	
C8	X	
C162	X	X
C18		X

Table 3- 3. Loading Factors for Cyclic Loadings.

	Stage 1 (30 sec)	*Stage 2 (15 sec)*	*Stage 3 (8 sec)*
Static	N/A	N/A	N/A
C1	1.0	--	--
C6	1.6	--	--
C16	1.0	1.6	--
C132	1.0	1.33	2.0
C8	1.8	--	--
C162	1.0	1.6	2.0
C18	1.0	1.8	--

Notes: Each digit refers to the factors used in each load stage, explained in Table 3-3. All loads were applied at 1 Hz.

C1 provides a baseline comparison for all the cyclic tests. This loading condition is assumed to represent four minor seismic events (1.0 times the allowable design load). C6 investigates the use of the current duration of load factor of 1.6. This test was designed to replicate the loading due to four design level events in the life of the truss. This test is the simplest evaluation of the duration of load factor, and it does not include any additional minor or major loading events in the life of the joint. The duration of load factor of 1.6 is currently used for wind and seismic design in the 1991 NDS (AFPA 1991). The UBC uses a duration of load factor of 1.6 for wind and 1.33 for seismic (UBC 1985). C16 (CH16 similar) provides more conservative

evaluations of C_D=1.6 by adding 4 minor events before testing the joint for 2 design level events. C162 (CH162 similar) provide the most conservative investigation of the NDS duration of load factor of 1.6. This cyclic case is similar to the most conservative case investigated by Gutshall (1994). This test was designed based on a number of seismic events in the life of the structure. The first step of the loading simulates four minor events, the second step simulates two design events and the last step simulates a major seismic event in the life of the structure.

The previous tests indicated that C_D=1.6 may be sufficient for design, but it did not provide the same level of confidence as shown for Gutshall's (Gutshall 1994) nailed and bolted connections. C132 was performed to evaluate the load duration factor of 1.33. It is based on the same loading model as C162, but evaluates the load duration factor of 1.33. It uses a factor of 1.33 (from the old NDS code (AFPA 1993) rather than 1.6 to determine the magnitude of the second stage of loading. The UBC (1985) is based on the old NDS code (AFPA 1993). Therefore, this test simulates four minor events, two UBC (1985) seismic design events, and one major event. By performing this test we showed that the degradation observed for C162 and C132 was due to the major event loading and not the increased load duration factor of 1.6. Both these cases showed degradation while all others did not.

C8 was done to investigate the use of a duration of load factor of 1.8. The purpose of this test was to evaluate the possibility that the load duration

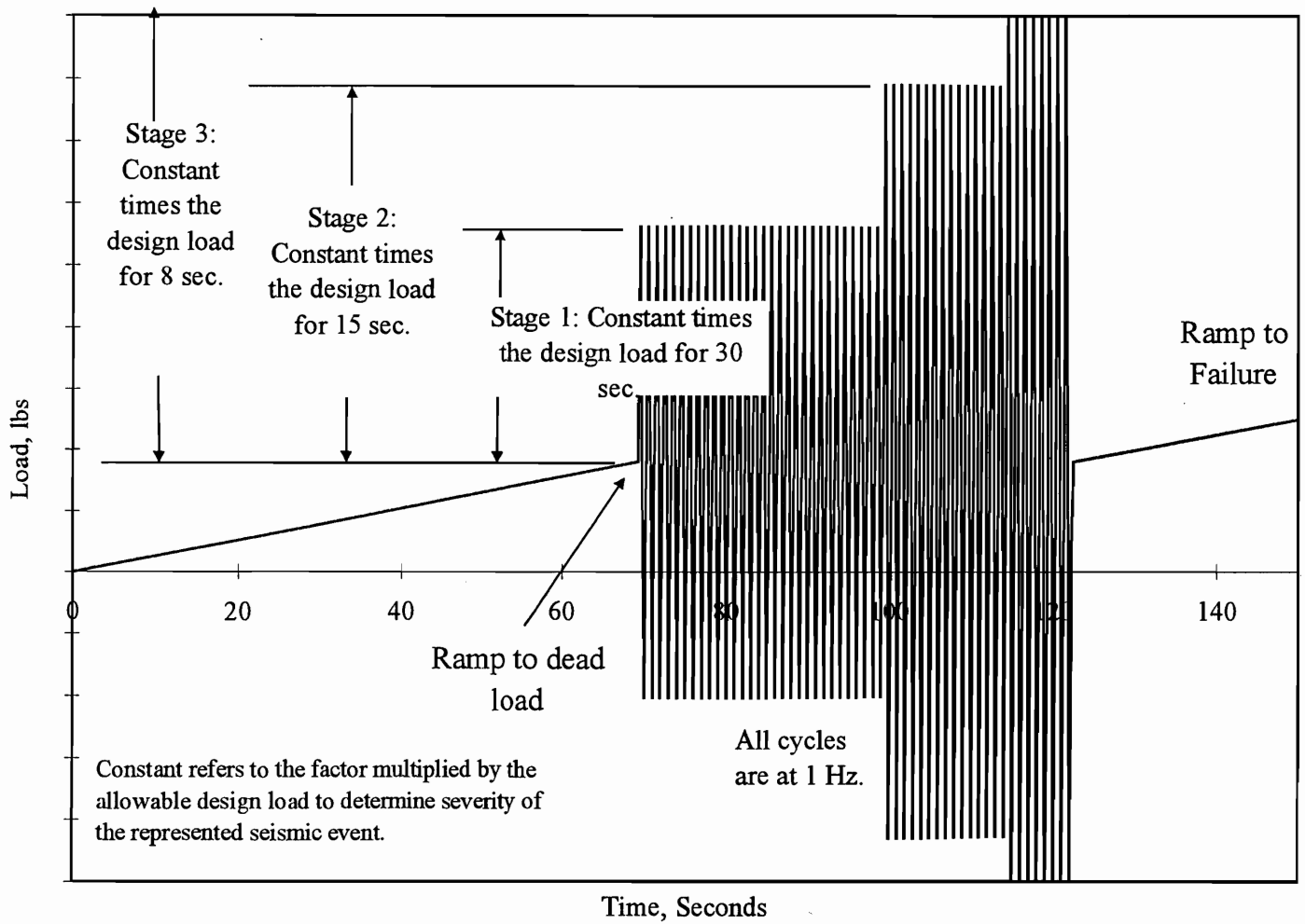

Figure 3- 10. Example Cyclic Loading Function.

factor could in fact be as large as 1.8 for the tension-splice joint. This test simulates four design events at a higher severity of 1.8 times the design load. CH18 provides a similar evaluation for a load duration factor of 1.8 for the heel joint. This loading simulates four minor events, and two design events in the life of the structure based on a duration of load factor of 1.8.

3.2.3. Property Evaluation and Calculation

The ultimate load and stiffness results were determined based on the data from the testing. In cases where the joints failed during the cyclic loading, the maximum load experienced by the joint was used as the ultimate load. This was done to include the failed joint in the average ultimate strength. These same joints were eliminated from the Design Load Stiffness calculations because they failed to reach the design load following the cycles and therefore no point of reference for the stiffness calculation existed. These joints were included in the Hysteretic Stiffness calculations (both described in the next paragraph) for each cycle of each test.

P-value comparisons were made at a 95% confidence interval. The p-value comparisons tested the null hypothesis that the difference in two populations means is zero.

$$h_o: \quad \overline{\upsilon_1} = \overline{\upsilon_2} \qquad \overline{\upsilon_1} : Mean \;\; Population \quad 1, \overline{\upsilon_2} : Mean \;\; Population \quad 2$$

Several methods were used to determine and compare the stiffnesses of the joints. The Dead Load Stiffness was calculated by taking the slope of a secant line between the base (or beginning) of the load-deflection curve to the common dead load of 900 lbs. (or 1550 lbs. for heel joints). The Design Load Stiffness was calculated by taking the slope of the secant line between the load after the cyclic region (which is the same as the dead load before the cycles) and the average design load of 1920 lbs. (1/3 of the average ultimate load from the static tests). The Offset Stiffness reported in Tables 4-1 and 4-6 is defined as the stiffness between the base of the load deflection curve and the design load, including the cyclic portion of the curve.

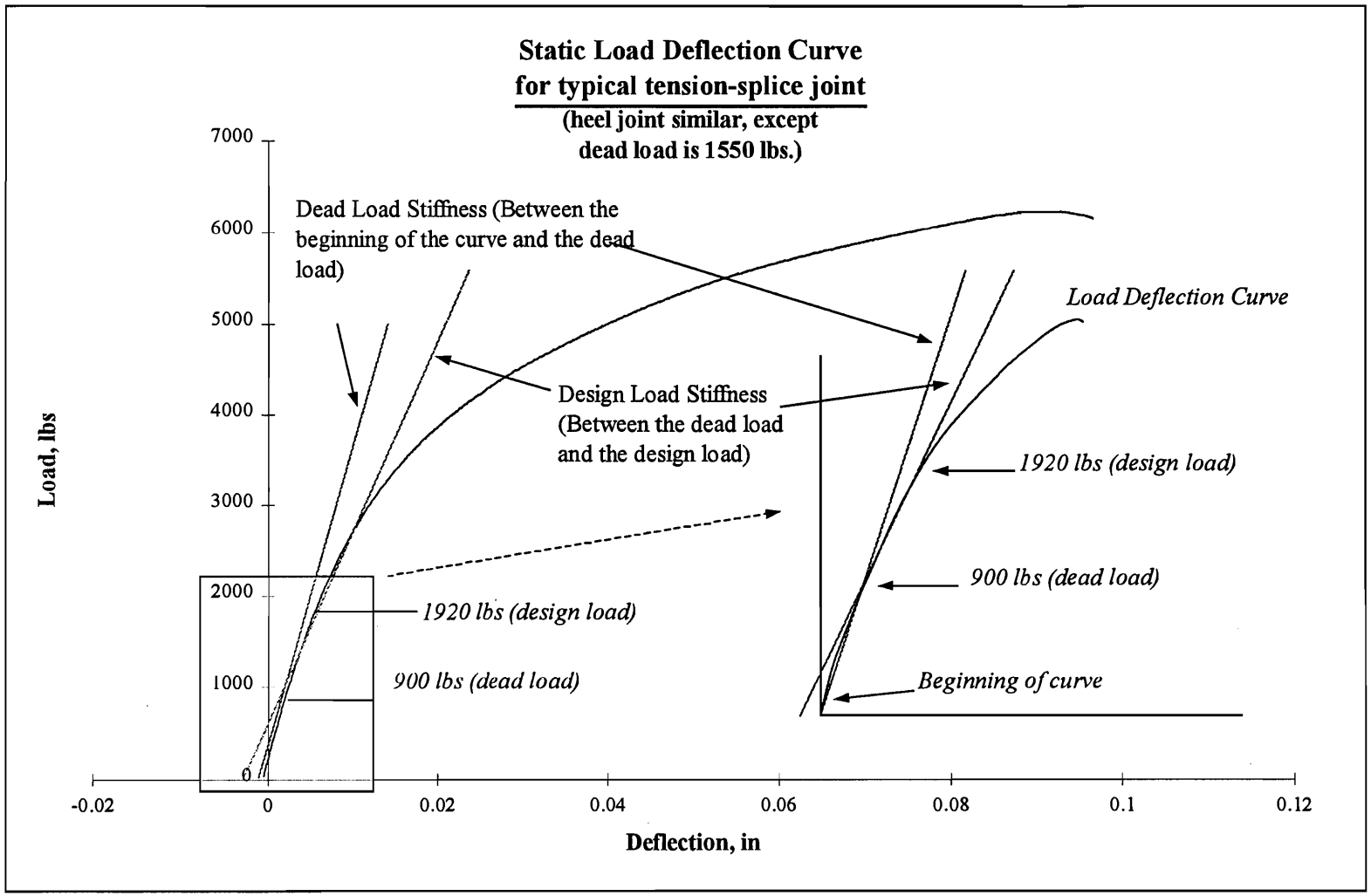

Figure 3- 11. Static Load-Deflection Curve for Tension-Splice Joint.

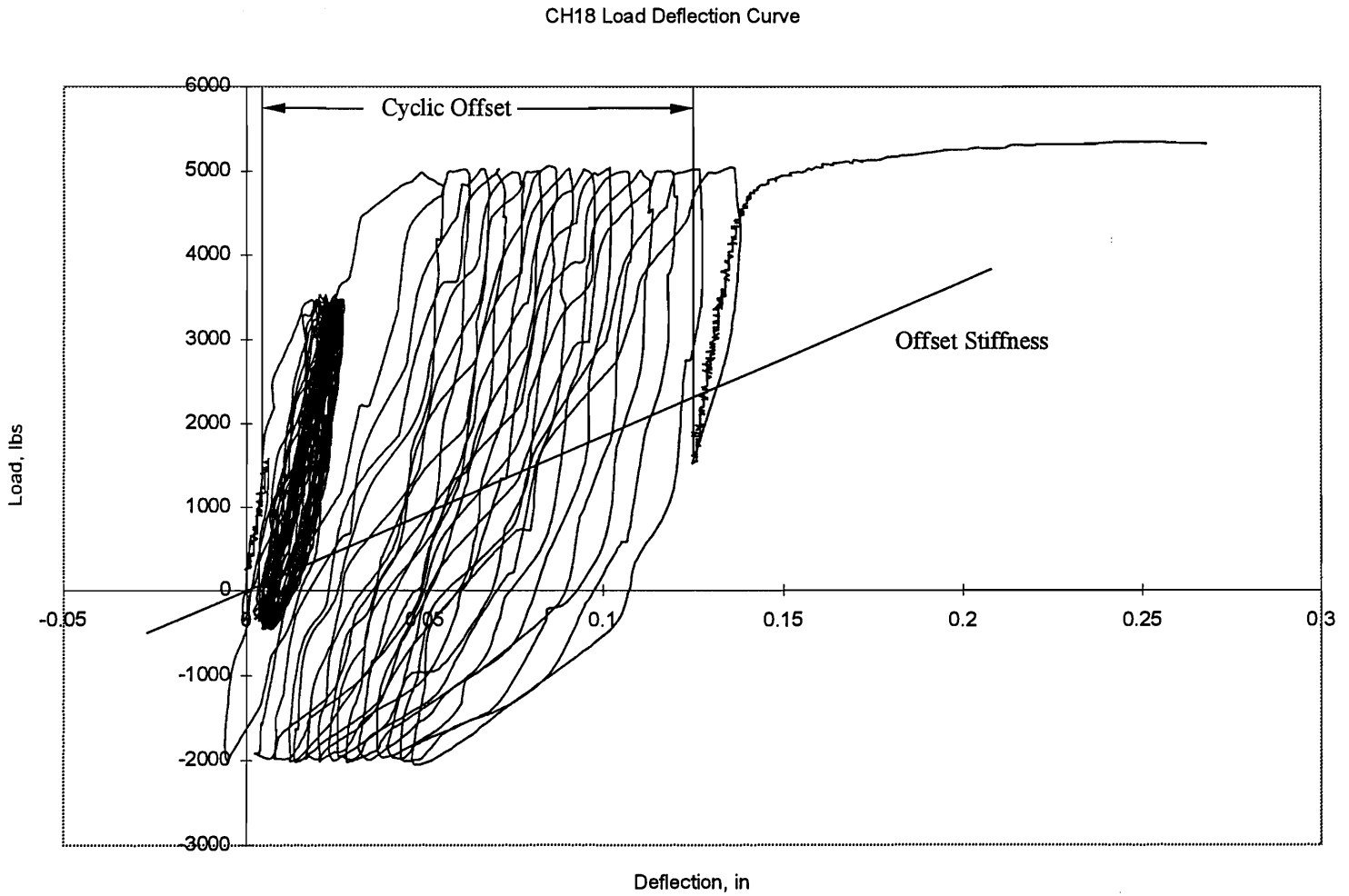

Figure 3- 12. Cyclic Load Deflection Curve for a heel joint.

The average design load for the heel joints was also 1920 lbs. The static stiffness results were calculated similarly except that the cyclic region did not exist (See Figure 3-11). For each joint, a stiffness decrease was calculated as the percent difference between the Dead Load Stiffness and the Design Load Stiffness. In cases where the joints did not survive the cyclic loading, it was assumed that the stiffness decrease was 100%. This was done to include the failed joints in the stiffness decrease average. The stiffness decrease was used evaluate the stiffness degradation.

A second method was also used to determine the stiffness degradation of the joints. The stiffness for each hysteresis curve (cycle) was calculated and plotted versus the number of cycles (See Chapter 4, Results). This clearly illustrated the stiffness degradation that occurred during the cycles. The Hysteretic Stiffness was approximated by taking the average of two extreme approximation methods. The first was obtained by taking the slope of the line between the two load extremes of a typical cycle (shown in Figure 3-13, by points A and B). The second was determined by taking the two displacement extremes of a typical cycle (points C and D in Figure 3-13). These two approximations provided bounds on the hysteretic stiffness, and an average of these two extreme approximations was used. The Hysteretic Stiffnesses for the second cycle and the second from the last cycle for each stage of a loading regime are reported in Appendices B and C. These cycles were chosen to eliminate slight variations that may occur during the transitions of the first and last cycles.

The energy dissipation was also calculated for each cycle of each load regime. The area enclosed by the hysteresis curve is the energy dissipated during the cycle. The Energy Dissipation of the second cycle and the second from the last cycle for each stage of a loading regime are reported in Appendices B and C.

The cyclic offset of a cyclic test is the deflection that occurred during the cyclic portion of the test (Figure 3-12).

Other material properties were measured: modulus of elasticity, specific gravity, ring count, percent latewood, and grain orientation (Tables B-1 and C-1). Specific gravity and moisture content were determined by cutting a 1 to 2 inch sample from each failed joint and weighing, drying and re-weighing it (ASTM D2395-93, ASTM D4442-92). The volume was determined using a hand caliper. The ring count was determined by visually counting the rings within one inch. The grain orientation was determined by drawing tangent lines on the samples at the middle of the cross-section. A protractor was then used to approximately measure the angle. Percent latewood was obtained from a visual approximation of the latewood percentage in a typical ring.

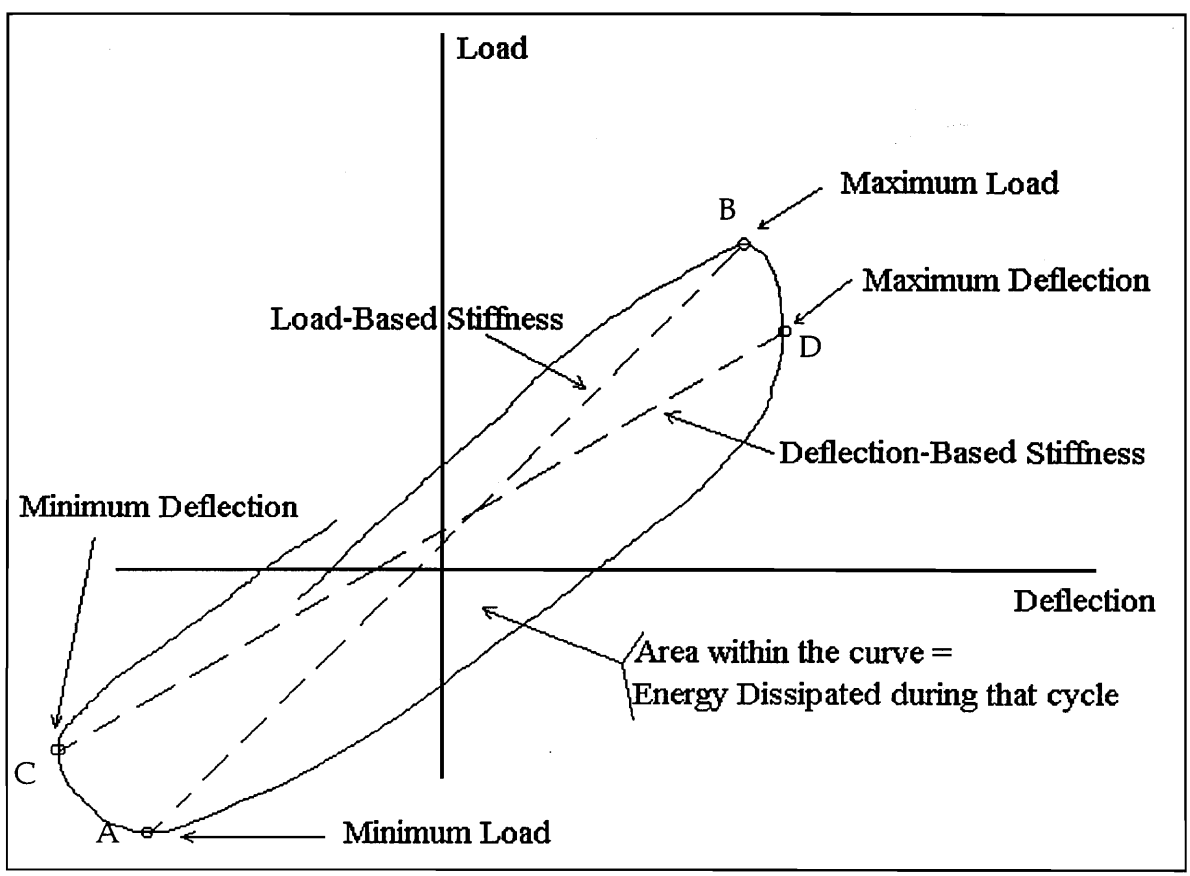

Figure 3- 13. Theoretical Hysteresis Loop.

4. Results

4.1. Tension-Splice Joint Results

A summary of tension-splice joint test results is provided here and individual test results are discussed in the following sections and sub-sections. Table 4-1 shows the average strength and stiffness for tension-splice joints under static and six different types of cyclic loading conditions. The strength is after the cyclic loading. The stiffness reported here is the Design Load Stiffness. The coefficient of variation (COV) for the strength results varies greatly due to 1 or 2 high test values that could not be eliminated as outliers.

Table 4- 1. Tensile Test Summary

Test	*Strength, lbs. (N, COV)*	*Design Stiffness, *10^5 lbs./in (N, COV)*	*Offset Stiffness, *10^5 lbs./in (N, COV)*
Static	5760 (10, 12%)	2.06 (10, 17%)	2.68 (10, 17%)
C1	5639 (10, 24%)	2.59 (8, 30%)	1.88 (8, 43%)
C6	5624 (10, 29%)	1.66 (7, 25%)	1.14 (7, 43%)
C16	6111 (10, 18%)	1.92 (9, 28%)	1.08 (9, 39%)
C8	4794 (9, 25%)	2.11 (1,-)	1.54 (1,-)
C132	4499 (8, 6%)	0.98 (4, 21%)	0.51 (4, 19%)
C162	4924 (10,16%)	1.30 (4, 18%)	0.685 (4, 25%)

Note: The above stiffness is based on the secant line between the base of the load-deflection curve and the design load (including the cyclic offset). The joints that failed during the cyclic portion of the curve were eliminated from the stiffness results.

4.1.1. General Characteristics

Several general characteristics regarding each joint were recorded. The characteristics that were recorded and investigated included ultimate load, modulus of elasticity, moisture content, specific gravity, rings per inch, percent latewood, grain orientation, Dead Load Stiffness, Design Load Stiffness, Dead Load/Design Load Stiffness Decrease, ultimate displacement and cyclic offset. These properties are defined and actual measurements are shown in Appendix B. Failure mode for each joint is also noted. Figure 4-1 shows the three observed failure modes: tooth withdrawal, plate failure, and combined tooth withdrawal and wood failure. Only one joint failed in the plate, while the rest of the joints failed initially due to tooth withdrawal with varying amounts of wood failure. Kent (1995) and Gupta and Gebremedhin (1990) observed similar failure modes.

4.1.2. Tension-Splice Joint Tests

4.1.2.1. Static Results

A total of ten tension-splice joints were tested statically. The average ultimate strength was 5760 lbs. with a coefficient of variation of 12%. This coefficient of variation is slightly higher than the 10% COV observed by Kent (1995). The design load was determined by dividing the average ultimate strength for the statically tested tension-splice joints by 3 (AFPA 1991). This results in an average design load of 1920 lbs. (Table B-1a. A typical load-deflection curve is shown in Figure 4-2.

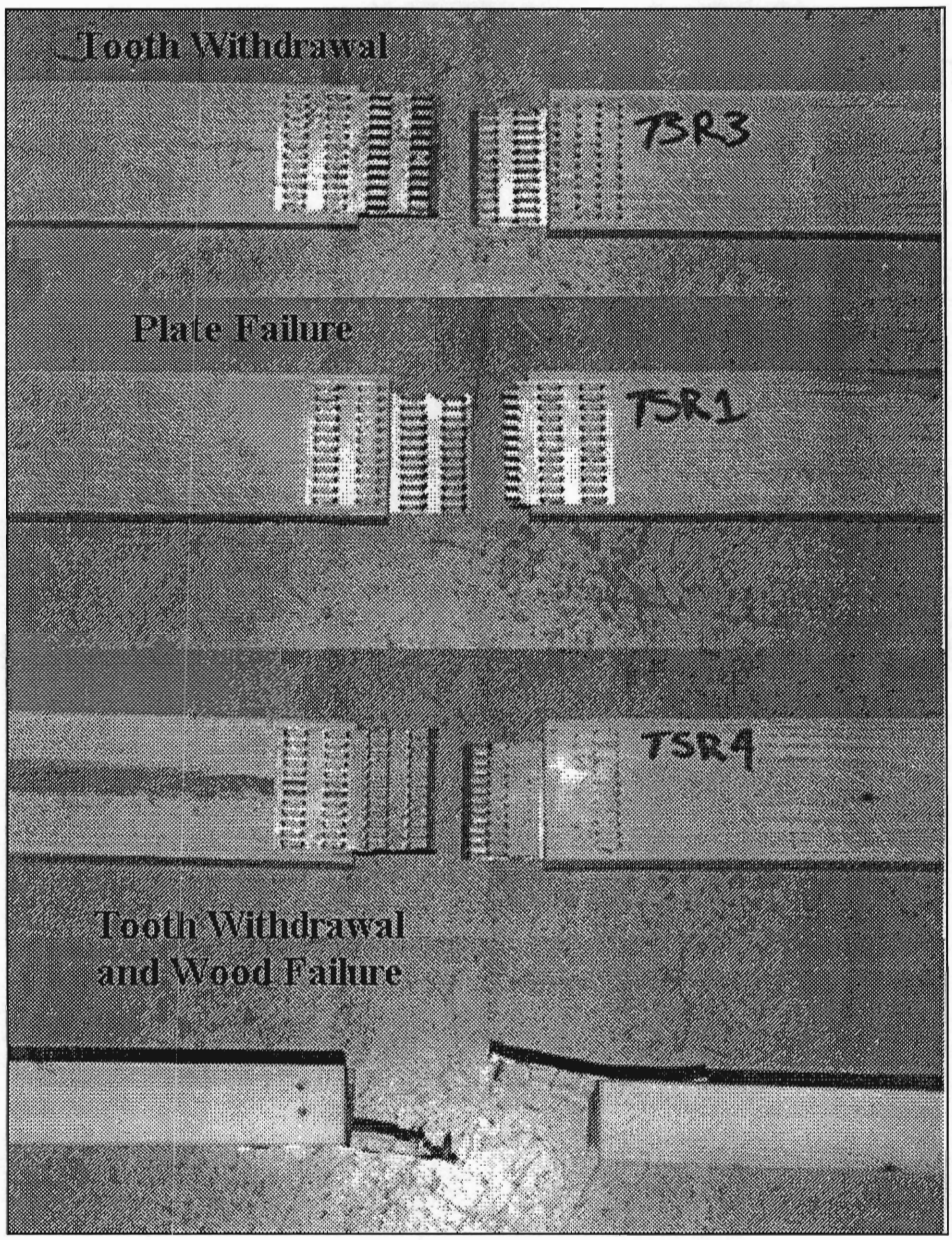

Figure 4- 1. Observed failure modes for Tension-Splice Joints.

The ultimate strengths resulting from the static ramp load testing were slightly lower than those observed by Kent (1995). Kent's average ultimate strength for example, was 6712 lbs. Several variables could have played a part in these differences (fabrication technique, type of plate, and wood variability). Specifically, variations include the degree to which the plates were pressed, the care taken for plate orientation, and the batch from which the plates came. Specific gravity for these test results was comparable to Kent (1995). Kent (1995) discusses the possible variations that were observed during his tests.

The Dead Load Stiffness is defined as the slope of the secant line between the beginning of the load-deflection curve and the defined dead load (900 lbs.). The Design Load Stiffness is defined as the slope of the secant line between the dead load and the average design load (1920 lbs.).

The average Dead Load Stiffness was 3.06×10^5 lb./in. and the average Design Load Stiffness was 2.06×10^5 lb./in. (COV = 16% and 17%, respectively). The average ultimate displacement of the joint at failure was 0.074 inches. All joints failed in tooth withdrawal. There was approximately a 32% decrease in stiffness from the Dead Load Stiffness to the Design Load Stiffness. These results are summarized in Table B-2a in Appendix B. This decrease in stiffness is a relative measure of the stiffness loss under static loading. By comparing the relative stiffness loss that was observed during the static case to the stiffness loss observed from a cyclic case, we can speculate that the additional stiffness loss is due to the cyclic loading. The Dead Load Stiffness and the Design Load Stiffness are shown on the typical static load-deflection curve in Figure 4-2.

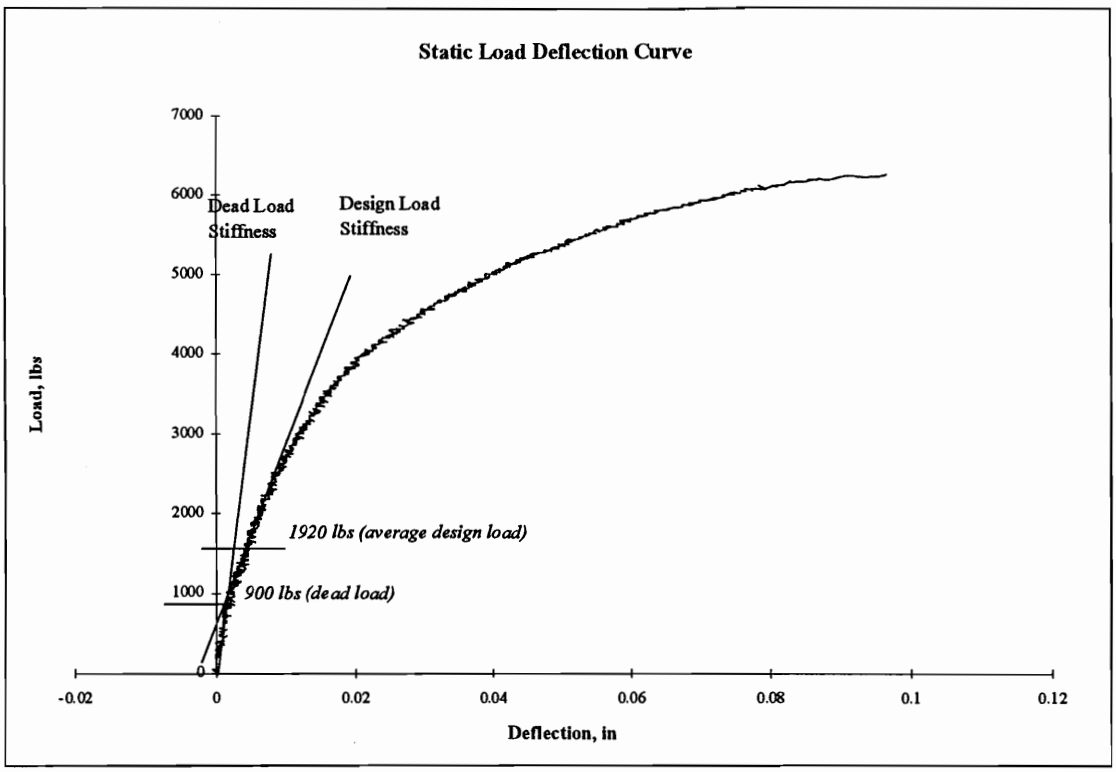

Figure 4- 2. Load-Deflection Curve For A Typical Static Tension-Splice Test.

4.1.2.2. Cyclic Testing Results (C1)

A total of ten tension-splice joints were tested under the C1 loading case. The average ultimate strength was 5639 lbs. with a coefficient of variation of 24%. The COV for this set of tests was high because of one joint that failed during the last cycle of the load case, and the ultimate load was based on the maximum load achieved over the cycles. Nine of the joints survived the cyclic tests and were ramped to failure following the cycles.

Figures 4-3 and 4-4 show a typical load-deflection curve and the isolated hysteresis loops for a typical test. The hysteresis loops were used to define how the cyclic stiffness and the energy dissipation of the joint changed during the test. An Excel/Visual Basic program was written to extract the stiffness for each hysteresis loop. Data obtained from this software are shown in Figures 4-5 and 4-6.

The average Dead Load Stiffness was 3.22 x 10^5 lb./in. and the average Design Load Stiffness was 2.59 x 10^5 lb./in. (COV = 28% and 30%). There was a 31% decrease in stiffness from the Dead Load Stiffness to the Design Load Stiffness. The comparison of the stiffness degradation of C1 (31%) and the static load case (32%) suggests that there was no significant change in the degradation due to the cycles in this load case. The average ultimate displacement of the joint at failure was 0.067 inches. The average cyclic offset that occurred during the tests was 0.006 inches. The cyclic offset is defined as the displacement associated with the cyclic portion of the test.

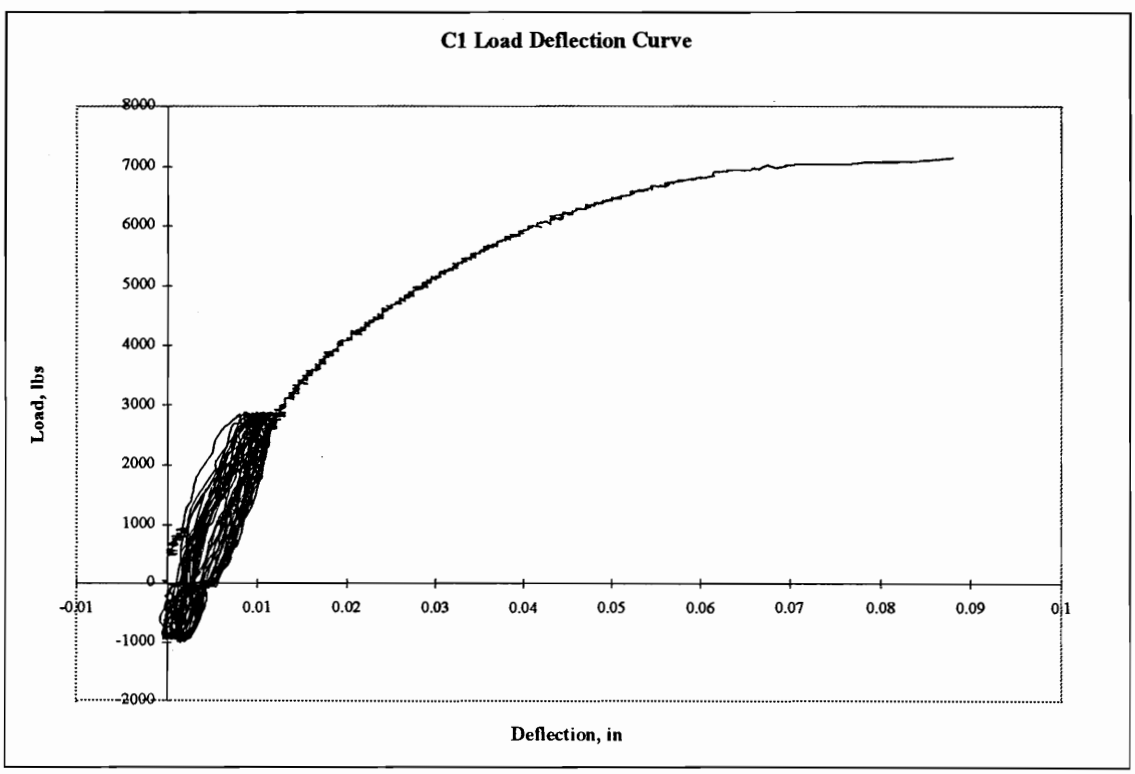

Figure 4- 3. Complete Load-Deflection Curve for Typical C1 Test (test C1-1).

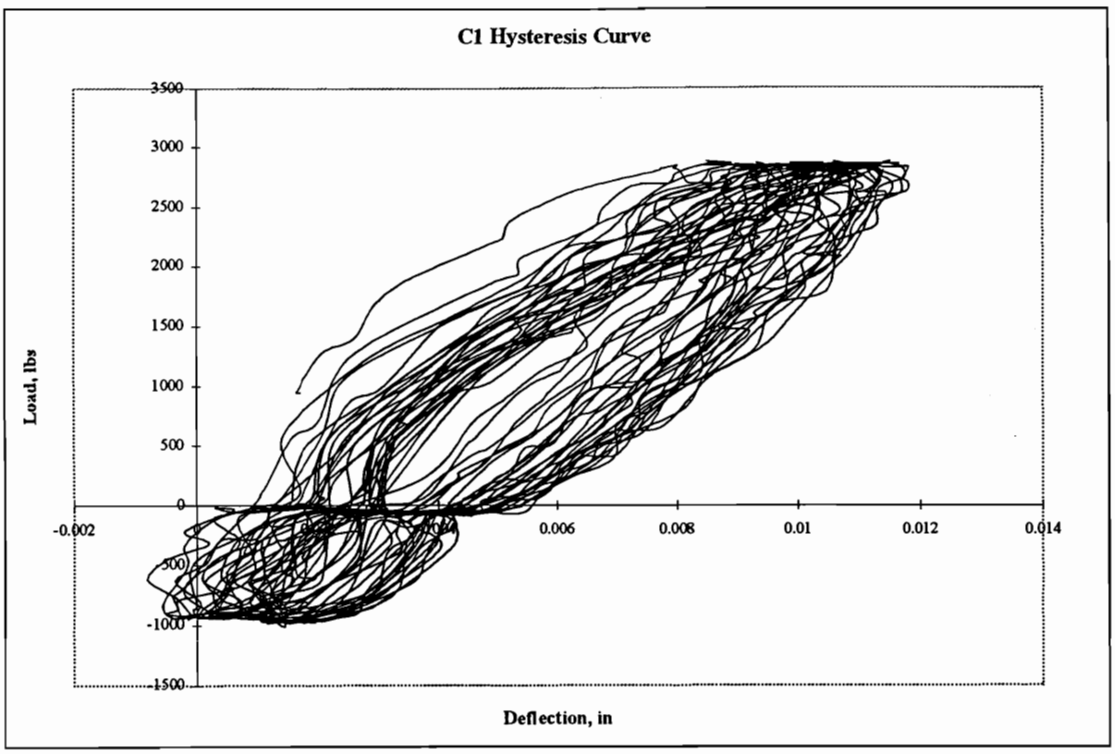

Figure 4- 4. Isolated Hysteresis Curves for Typical C1 Test (test C1-1).

The percent stiffness decrease during the cyclic portion of the test was defined as the difference between the stiffness of the first cycle and the stiffness of the last cycle and dividing it by the stiffness of the first cycle. The first and last cycles were taken as one cycle from the actual ends to reduce variability caused by the loading transition. For C1, the average decrease in stiffness during the cyclic portion of the test was 16.9%. The average energy dissipation of the first hysteresis loop increased by 186% by the end of the test. The energy dissipation is the area within the hysteresis loop (See Figure 3-13). These results are summarized in Table B-2a.

Figures 4-5 and 4-6 show the stiffness degradation and energy dissipation in relation to the displacement of the joint in the direction of the load. The overall displacement of a particular cycle (point in the stiffness and energy dissipation plots) was taken as the average displacement of that cycle. A regression analysis of the data in Figure 4-5 and Figure 4-6 does not suggest that any statistical trend exists (R^2=0.68

for stiffness degradation, R^2=0.69 for energy dissipation). While no statistical evidence exists, visual inspection of the data does suggest that the stiffness decreases as the displacement increases and energy dissipation increases as displacement increases.

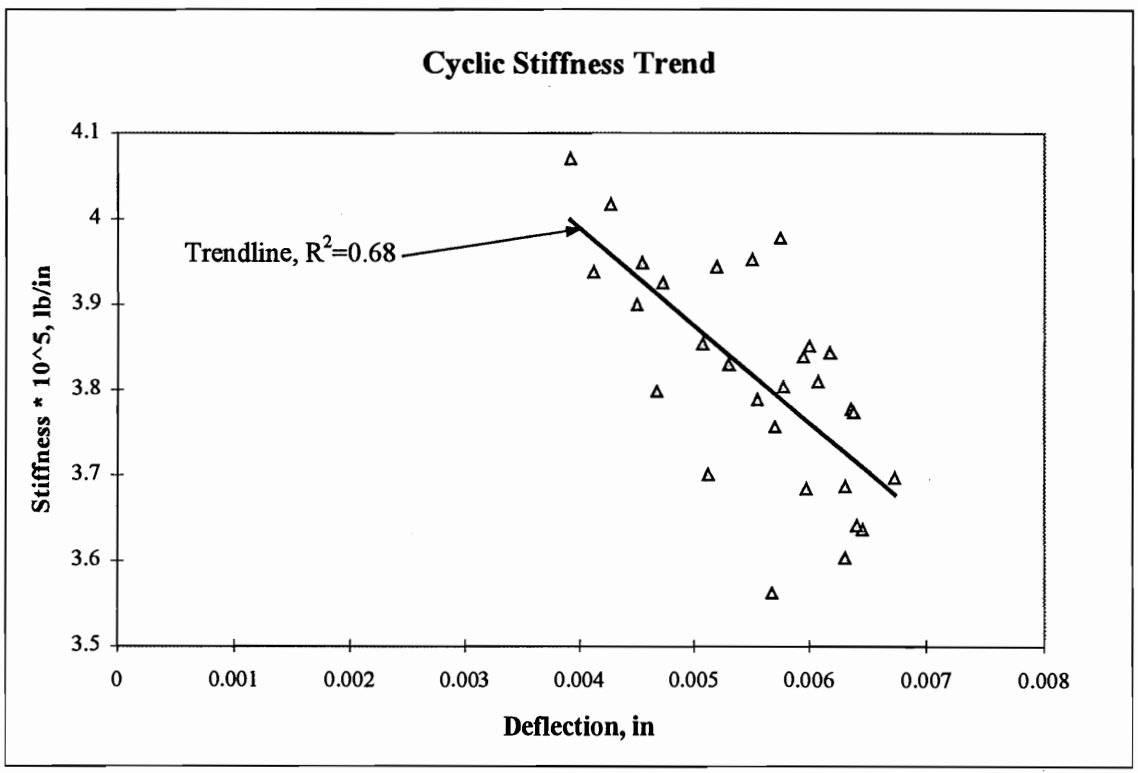

Figure 4- 5. Stiffness During Typical C1 Test (C1-1).

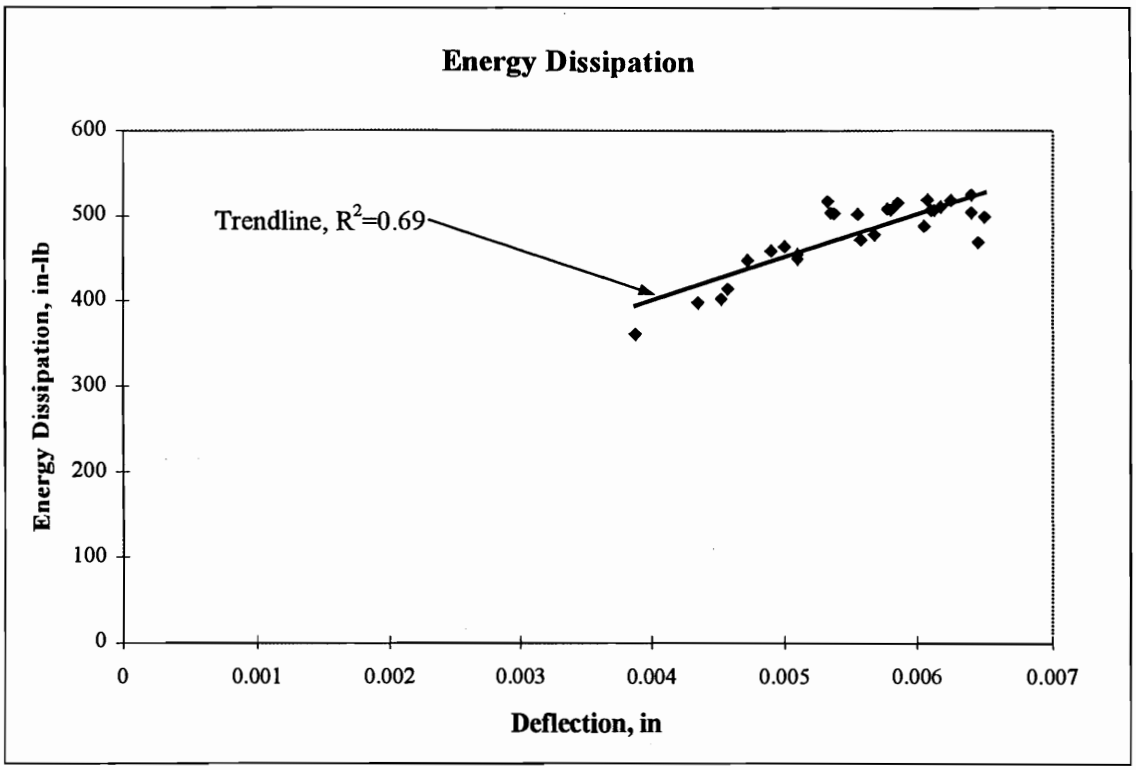

Figure 4- 6. Energy Dissipation During Typical C1 Test (C1-1).

4.1.2.3.Cyclic Testing Results (C6)

A total of ten tension-splice joints were tested under the C6 loading case. The average ultimate strength was 5624 lbs. with a coefficient of variation of 29% (Table B-1a). Eight of the joints survived the cyclic tests and were ramped to failure following the cycles. Two of the joints failed during the cycles. The high COV was due to these two joints which were much weaker than the rest of the population. The comparison of C6 to C1 and the static case reveals no strength degradation due to the increase in the amplitude of the loading function (Table 4-2). The p-value was 0.9825 for this comparison.

Figures 4-7 and 4-8 show a typical load-deflection curve and the isolated hysteresis loops for the same test.

The average Dead Load Stiffness was 3.66 x 10^5 lb./in. and the average Design Load Stiffness was 1.66 x 10^5 lb./in. (COV = 27% and 25%). The average ultimate displacement of the joint at failure was 0.077 inches. The average cyclic offset that occurred during the tests was 0.015 inches. There was a 59% decrease in stiffness from the Dead Load Stiffness to the Design Load Stiffness. This stiffness decrease is twice the decrease experienced in the static and C1 tests. The difference in stiffness decrease between C1 and C6 is due to the increase cyclic magnitude (the number of cycles in the test was the same). The average decrease in stiffness during the cyclic region of the test was

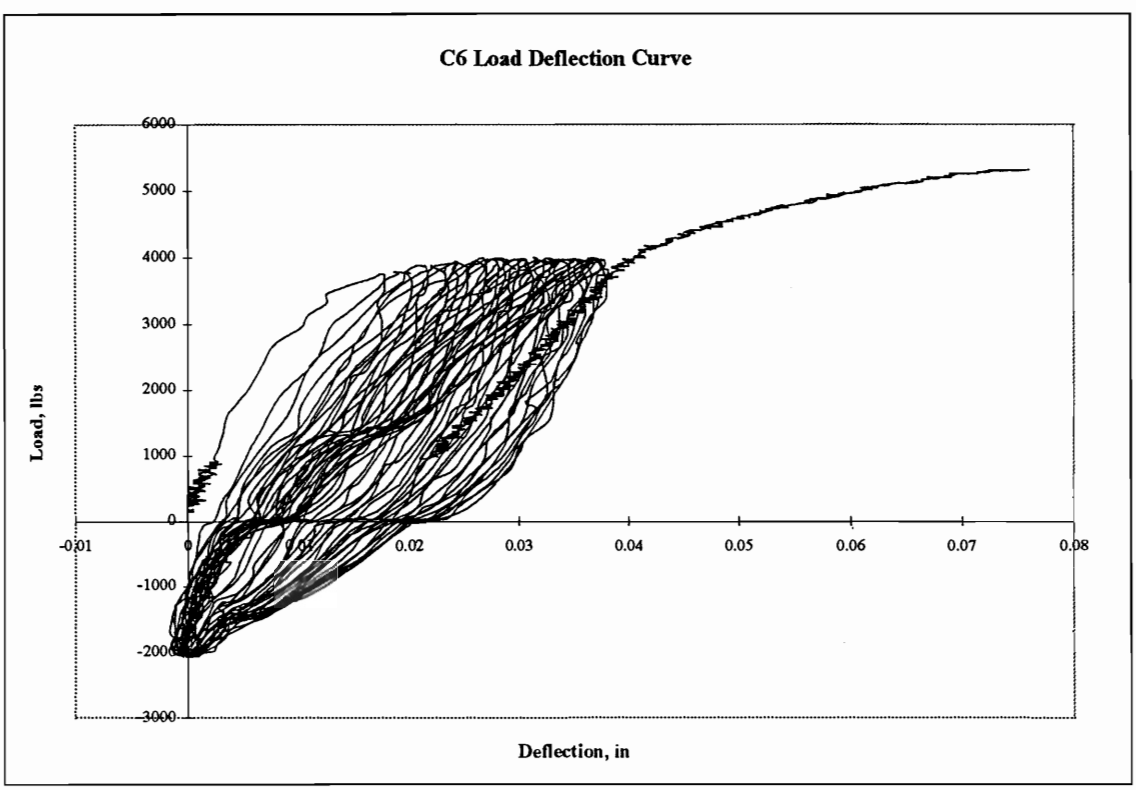

Figure 4- 7. Complete Load-Deflection Curve for Typical C6 Test (test C6-8).

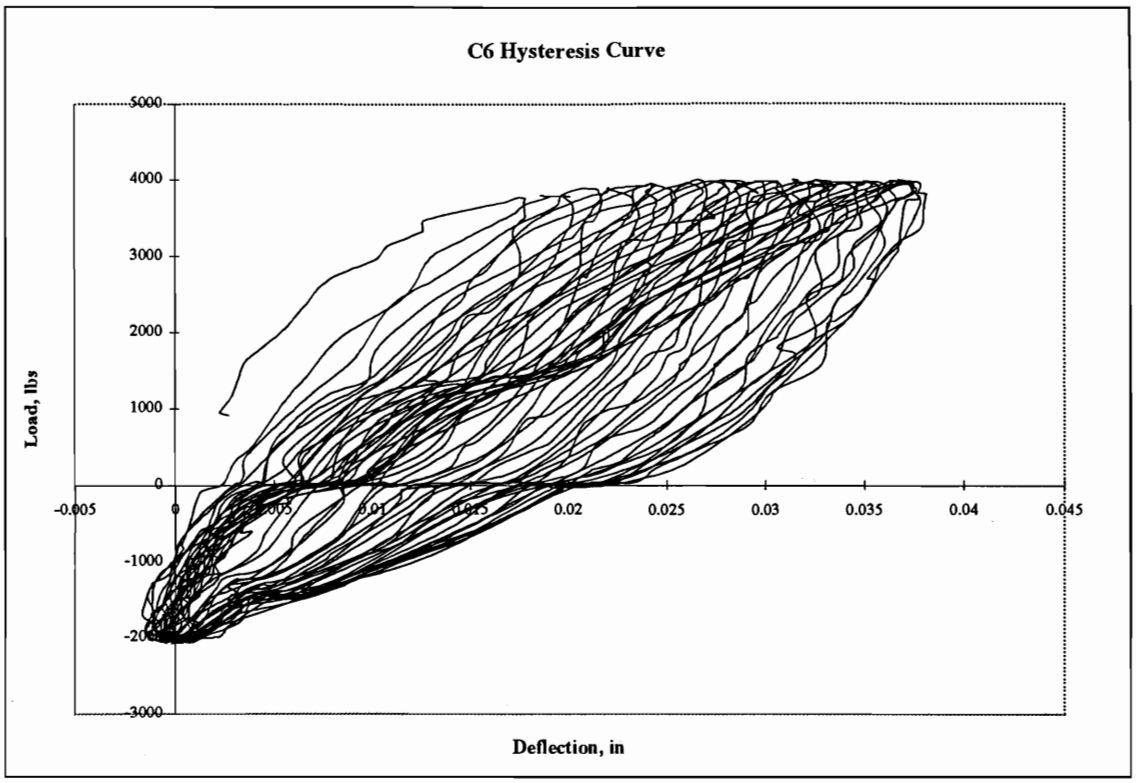

Figure 4- 8. Isolated Hysteresis Curves for Typical C6 Test (test C6-8).

36.8% (extracted from the hysteresis loops). This decrease is over 50% of the total stiffness decrease of 59% for the test. Therefore, most of the stiffness degradation occurred during the cycles. The energy dissipation increased by 189% between the first hysteresis loop and the final hysteresis loop. These results are summarized in Table B-2a.

Figures 4-9 and 4-10 show typical stiffness degradation and energy dissipation versus the displacement in the joint. There is statistical evidence that the stiffness is related to the deflection in the joint (R^2=0.92). The same statistical evidence does not exist for energy dissipation (R^2=0.86), but visual observation of the data would suggest that a trend does exist (Table B-3a).

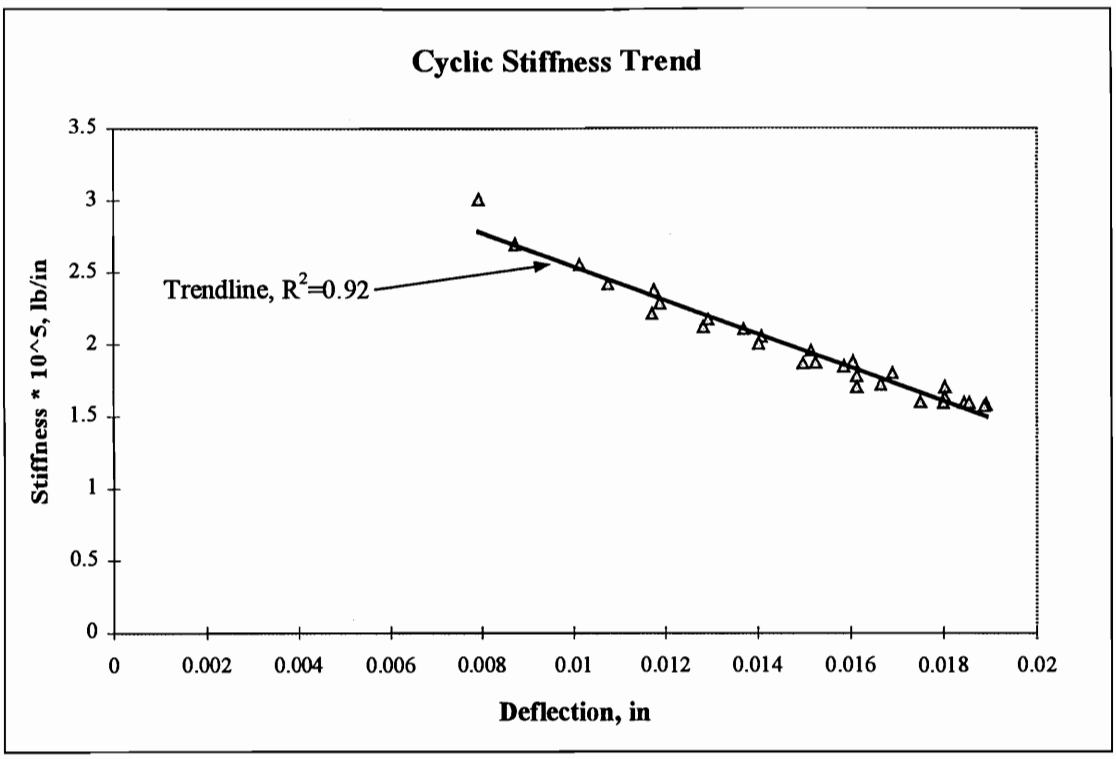

Figure 4- 9. Stiffness During Typical C6 Test (test C6-8).

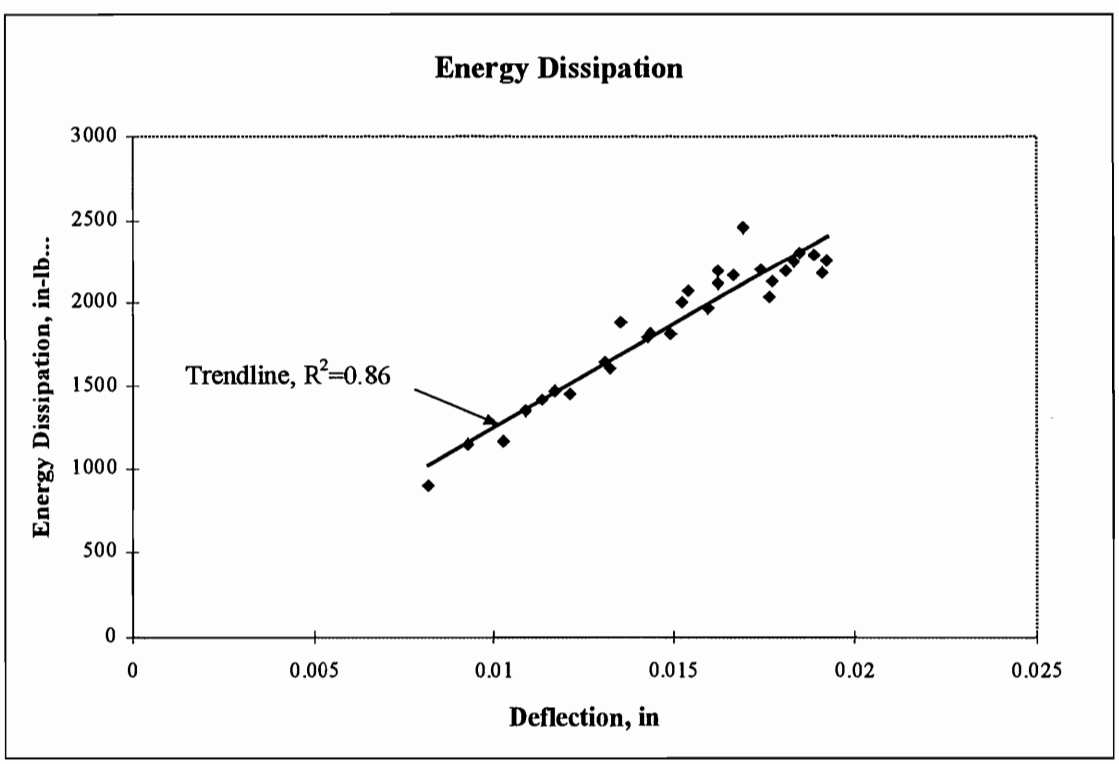

Figure 4- 10. Energy Dissipation During Typical C6 Test (test C6-8).

4.1.2.4.Cyclic Testing Results (C16)

A total of ten tension-splice joints were tested under the C16 loading. The average ultimate strength was 6110 lbs. with a coefficient of variation of 18%. Nine of these joints survived the cyclic tests and were ramped to failure following the cycles. One of the joints failed during the second step of the load case. The high COV was affected by one high ultimate load and one low load (the joint that failed during the cycles). This loading case showed no evidence of strength degradation between this load case and the static load case (p-value = 0.396). This fact provides support for a duration of load factor equal to 1.6. C16 is one possible representation of a ten-year load. Since no degradation is observed, this suggests that 1.6, which this load case uses to approximate a ten-year test, is adequate. It could be argued that this load case does

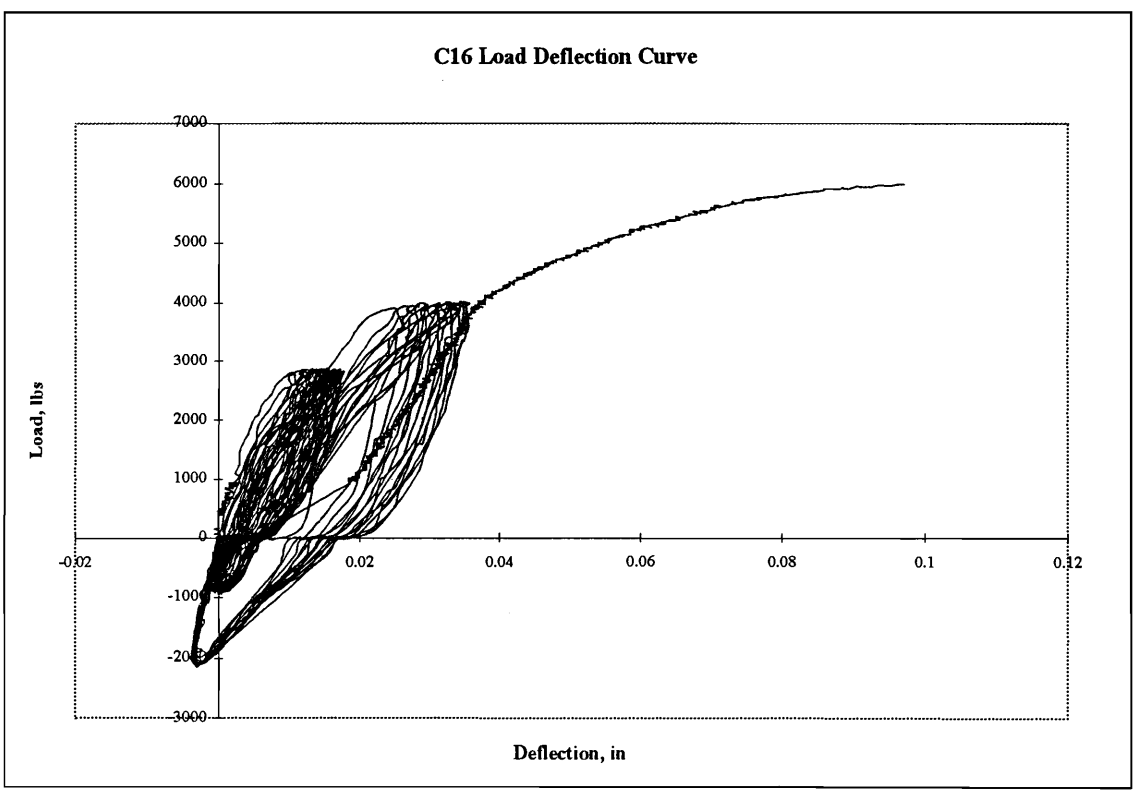

Figure 4- 11. Complete Load-Deflection Curve for Typical C16 Test (test C16-7).

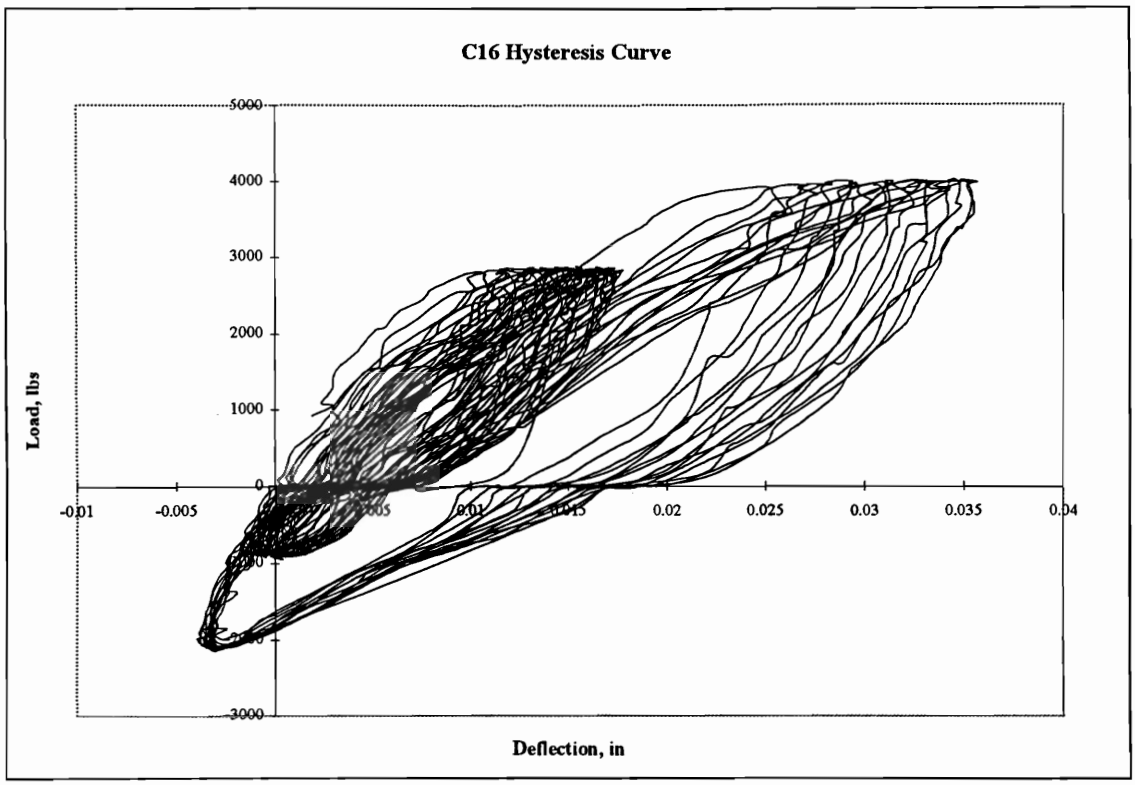

Figure 4- 12. Isolated Hysteresis Curves for Typical C16 Test (test C16-7).

not adequately represent a ten-year load, therefore further load cases are investigated (namely C162).

Figures 4-11 and 4-12 show a typical load-deflection curve and the isolated hysteresis loops for the same test.

The average Dead Load Stiffness was 3.08 x 10^5 lb./in. and the average Design Load Stiffness was 1.92 x 10^5 lb./in. (COV = 27% and 28%). There was a 43% decrease in stiffness from the Dead Load Stiffness to the Design Load Stiffness. The average decrease in stiffness during the first stage of the test was 19.4% and 18.2% in the second stage. The stiffness decrease is only slightly higher than the static (p-value = 0.261) and C1 (p-value = 0.873) degradation, but lower than C6 (p-value = 0.005). The average ultimate displacement of the joint at failure was 0.079 inches. The average

cyclic offset that occurred during the tests was 0.013 inches. These results are summarized in Table B-2a.

In comparing the stiffness degradation associated with C16 and C6, there seems to be some differences. There are fewer number of cycles in C6 than C16. C16 was tested for more cycles (45), but only 15 of those cycles were at 1.6 times the design load. On the other hand, C6 consisted of 1.6 times the design load for 30 cycles. Since C6 had more stiffness degradation, it would seem that the number of cycles at a significant loading level directly affects the stiffness degradation. This would also suggest that there was a significant difference in the stiffness degradation due to the change in cyclic magnitude. C16 had many more cycles, but since a majority of them took place at a lower level (1.0 times the design load), the stiffness degradation was lower. These comparisons suggest two possible variants for the influence on stiffness degradation. The remainder of the cyclic tests will be used to investigate these influences further.

The energy dissipation increased by 169% between the first hysteresis loop and the final hysteresis loop of the first stage. The energy dissipation between the first hysteresis loop of the final stage and the last cycle of the test increased 119%. In comparing the two stages of C16, the first stage (1 times the design load) shows the greatest increase (even though the magnitude was significantly higher). There is a difference in the number of cycles for these two stages, but by comparing the first stage energy dissipation (in C16, 169%) to the energy dissipation in C6 (189%), we see that there is only a slight difference due to the increase in cyclic magnitude. It would seem that energy dissipation is related to the number of cycles and magnitude has less of an effect. These results are summarized in Table B-3a.

Figures 4-13 and 4-14 show typical stiffness degradation and energy dissipation versus the displacement in the joint. Statistical evidence shows that the stiffness degradation is related to deflection during the second stage ($R^2 = 0.905$) but

not the first stage ($R^2 = 0.778$). Neither stage shows any statistical correlation between energy dissipation and deflection, but both illustrate a general increasing trend ($R^2 = 0.617$, and 0.761, respectively) (Table B-3a).

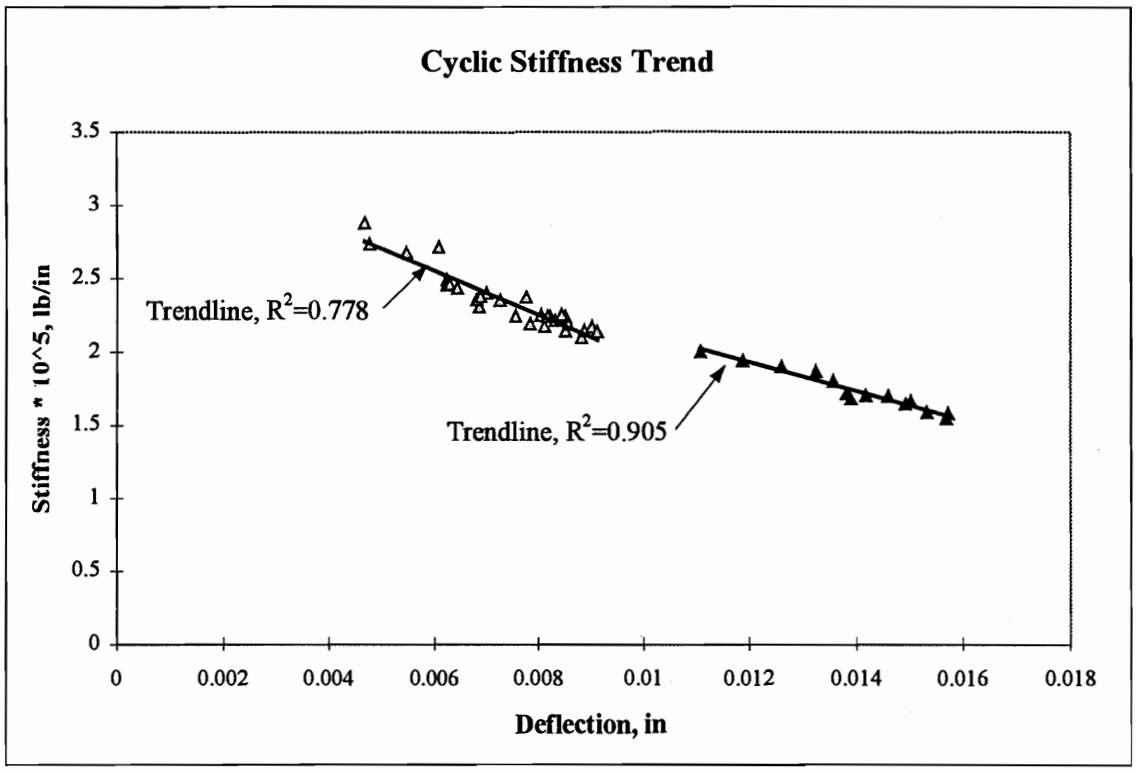

Figure 4- 13. Stiffness During Typical C16 Test (test C16-7).

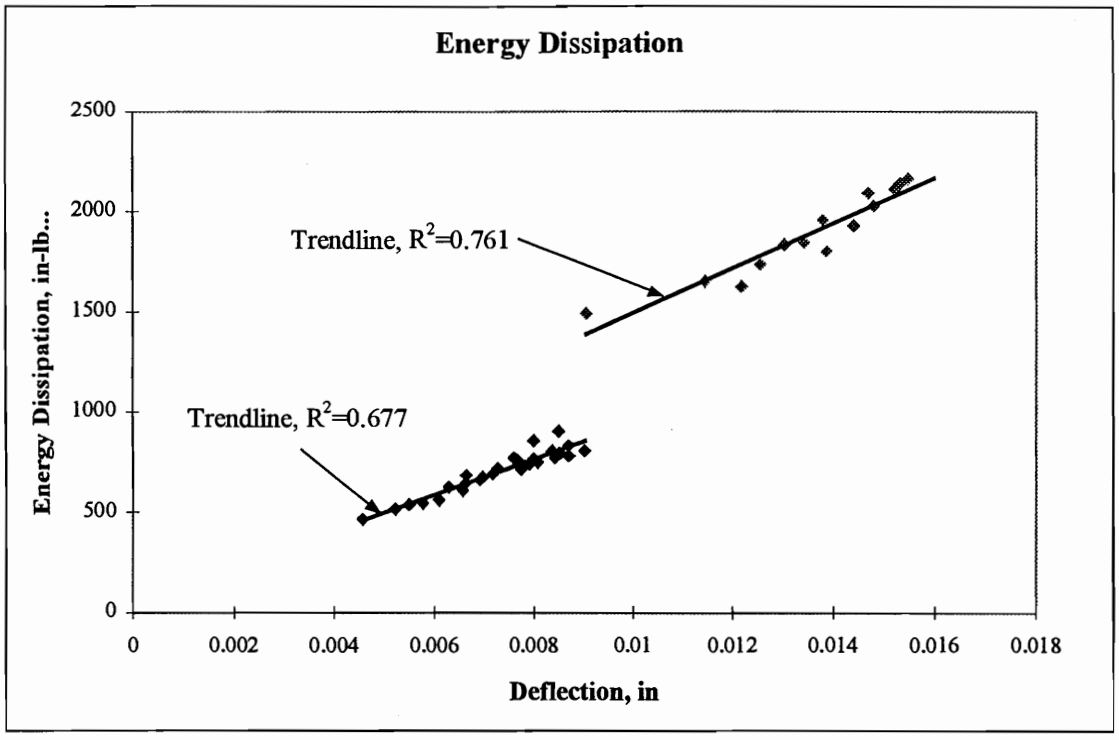

Figure 4- 14. Energy Dissipation During Typical C16 Test (test C16-7).

4.1.2.5. Cyclic Testing Results (C132)

A total of nine tension-splice joints were tested under the C132 loading. The average ultimate strength was 4499 lbs. with a coefficient of variation of 6%. Four of these joints survived the cyclic tests and were ramped to failure following the cycles. Five of the joints failed during the cycles. All of these failed during the third step of the load cycle. One of these joints was eliminated from the study because of bad deflection data caused by a current surge in the power supply (See Table B-2b). The results of this test suggest significant degradation took place (p-value = 0.0003). Since the first two stages of this test are less severe than C16 (which showed no degradation), it can be concluded that most of this additional strength degradation occurred due to the third and final stage of the loading.

Figures 4-15 and 4-16 show a typical load-deflection curve and the isolated hysteresis loops for the same test (C132-4).

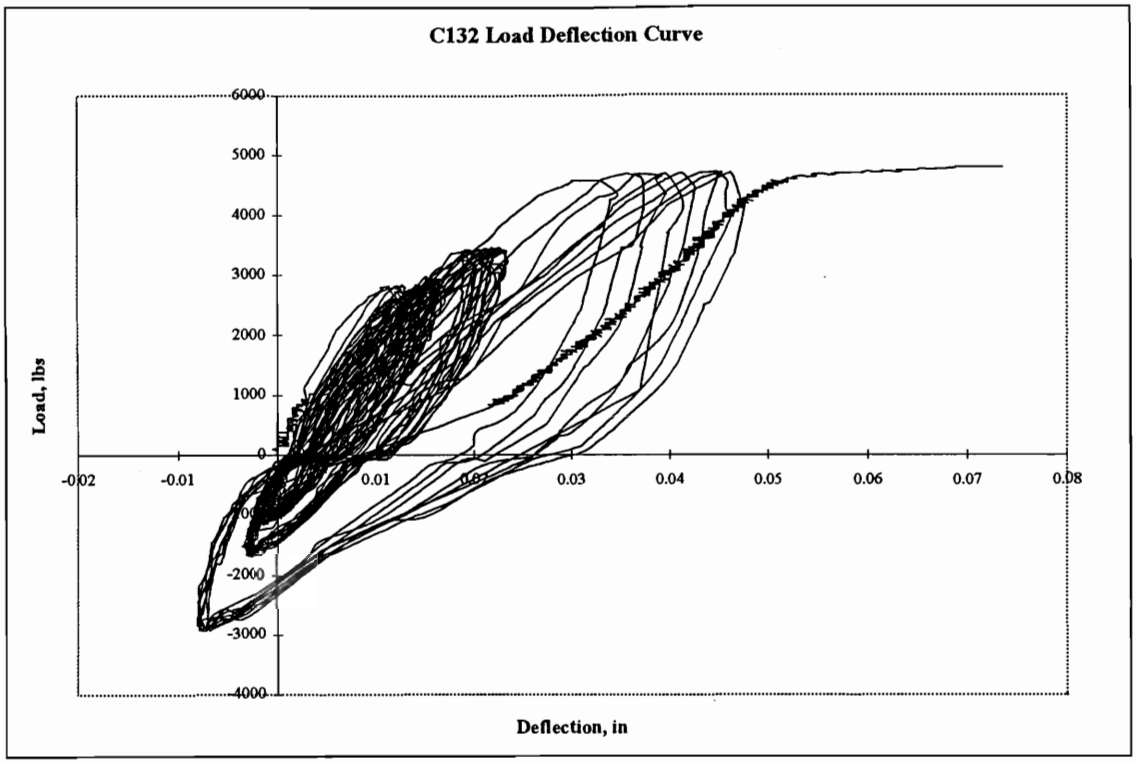

Figure 4- 15. Complete Load-Deflection Curve for Typical C132 Test (test C132-4).

The average Dead Load Stiffness was 2.57×10^5 lb./in. and the average Design Load Stiffness was 0.98×10^5 lb./in. (COV = 30% and 21%). There was a 75% decrease in stiffness from the Dead Load Stiffness to the Design Load Stiffness. This is a significant increase in stiffness degradation compared to the previous tests. The average decrease in stiffness during the first stage of the test was 16.2%, 18.7% in the second stage, and 14.2% in the third stage. The similarity of the stiffness degradation in the stages suggests that the increased magnitude of the last stage compensated for the decrease in the number of cycles between the stages. This confirms the idea that stiffness degradation is related to both the number of cycles and the magnitude of the load.

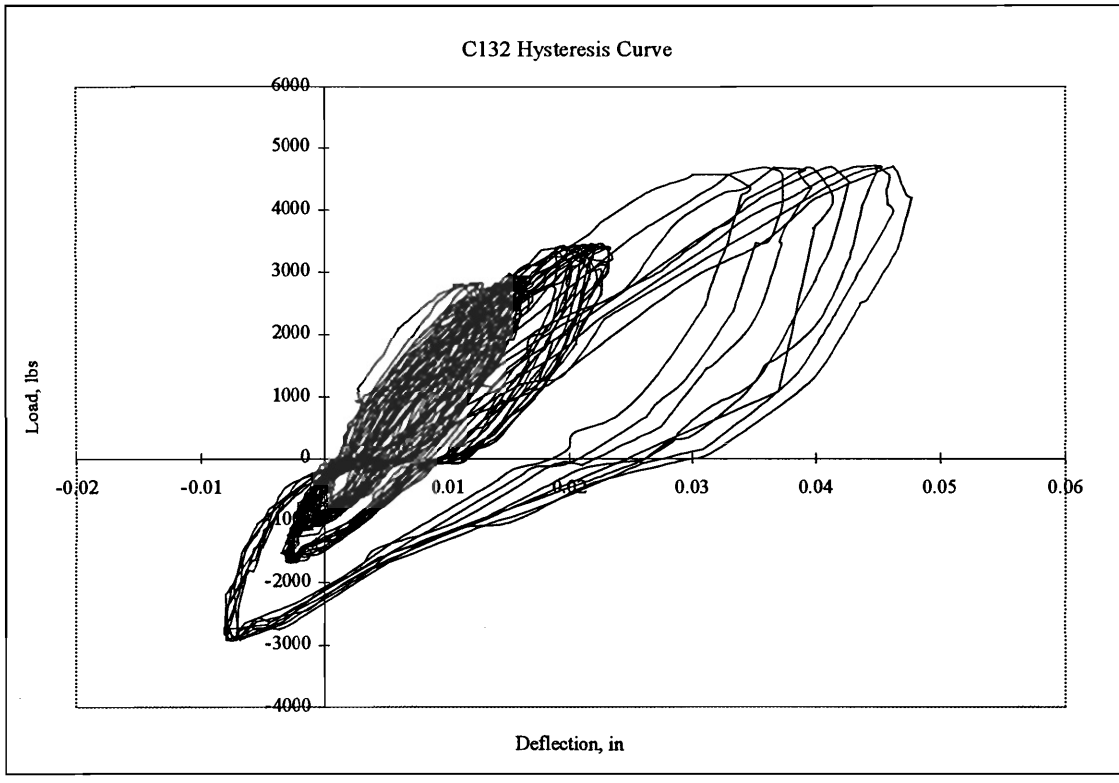

Figure 4- 16. Isolated Hysteresis Curves for Typical C132 Test (test C132-4).

The average ultimate displacement of the joint at failure was 0.035 inches. The average cyclic offset that occurred during the tests was 0.017 inches. These results are summarized in Table B-2b).

The energy dissipation increased by 123% between the first hysteresis loop and the final hysteresis loop of the first stage. The energy dissipation of the second stage increased 117% (from first cycle to last cycle of this stage), and the third stage increased 116% (from first cycle to last cycle of this stage). These results are summarized in Table B-3b. The energy dissipation of the first and second stages is similar to that observed in C16. Comparison of the second stages of these two tests is especially interesting since the magnitudes were clearly different for the same number of cycles. It would seem that the small change in magnitude (from 1.33 to 1.6 times the design load) had no significant impact on the energy dissipation. The energy

dissipation for the third stage of this test is nearly as high as the energy dissipation during the second stage (although the number of cycles is reduced in half). This may be due to two factors: 1) the increase in magnitude, or 2) the joint was already significantly weakened and does not adequately reflect the same characteristics as if it were tested at a high level immediately.

Figures 4-17 and 4-18 show typical stiffness degradation and energy dissipation versus the displacement in the joint. The statistical evidence does not suggest any relationships between stiffness and deflection, except in the third stage (R^2=0.856, 0.851, and 0.973 for each stage respectively)(Table B-3b). Statistically, the energy dissipation does not increase with deflection. Visual observation of the data does, however, suggest that stiffness and energy dissipation is related to deflection.

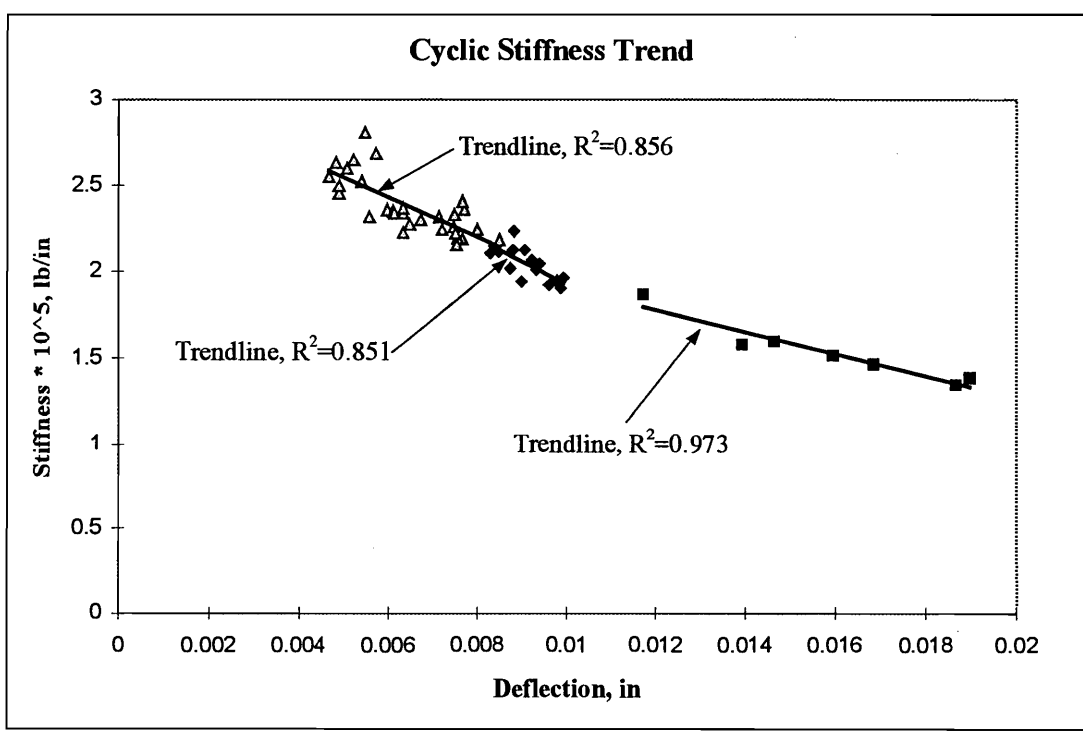

Figure 4- 17. Stiffness During Typical C132 Test (test C132-4).

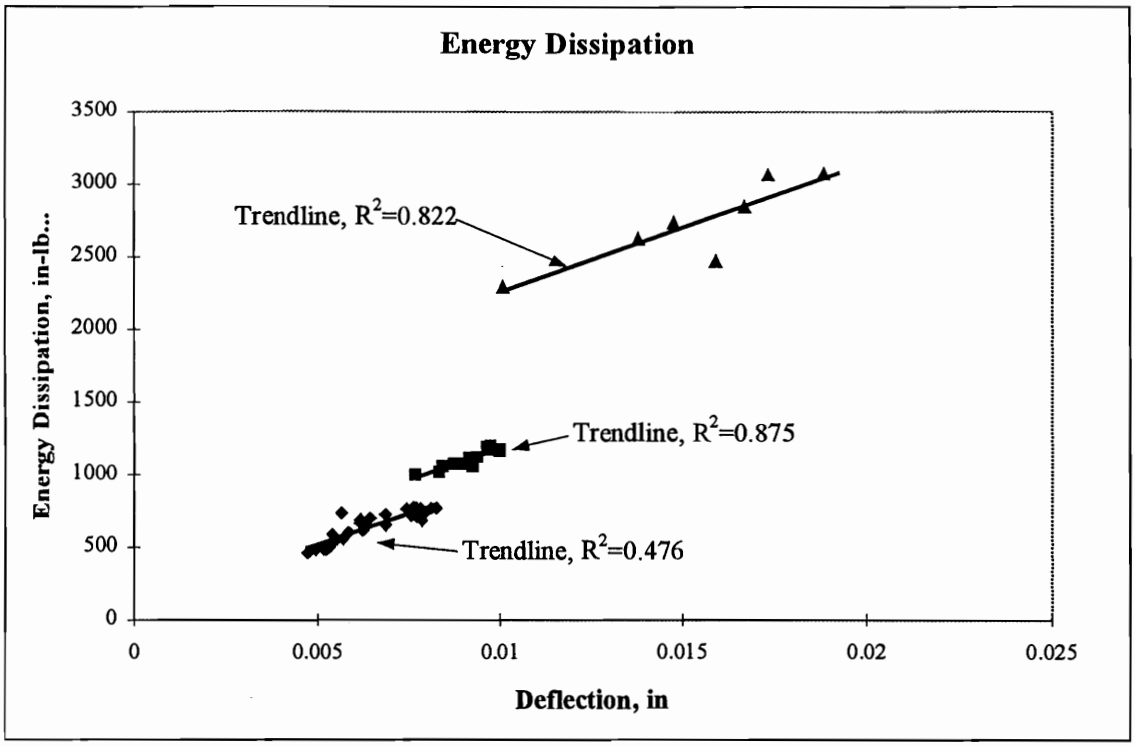

Figure 4- 18. Energy Dissipation During Typical C132 Test (test C132-4).

4.1.2.6.Cyclic Testing Results (C8)

A total of nine tension-splice joints were tested under the C8 loading. The average ultimate strength was 4794 lbs. with a coefficient of variation of 25%. Only one of these joints survived the cyclic tests and was ramped to failure following the cycles. Nine of the joints failed during the cycles. The high COV is due to the single joint that survived the tests. The p-value for the comparison of this test to the static test (p-value = 0.051) suggests a lack of confidence regarding the possibility of degradation. These results are summarized in Table B-2b.

Figures 4-19 and 4-20 show a typical load-deflection curve and the isolated hysteresis loops for the same test.

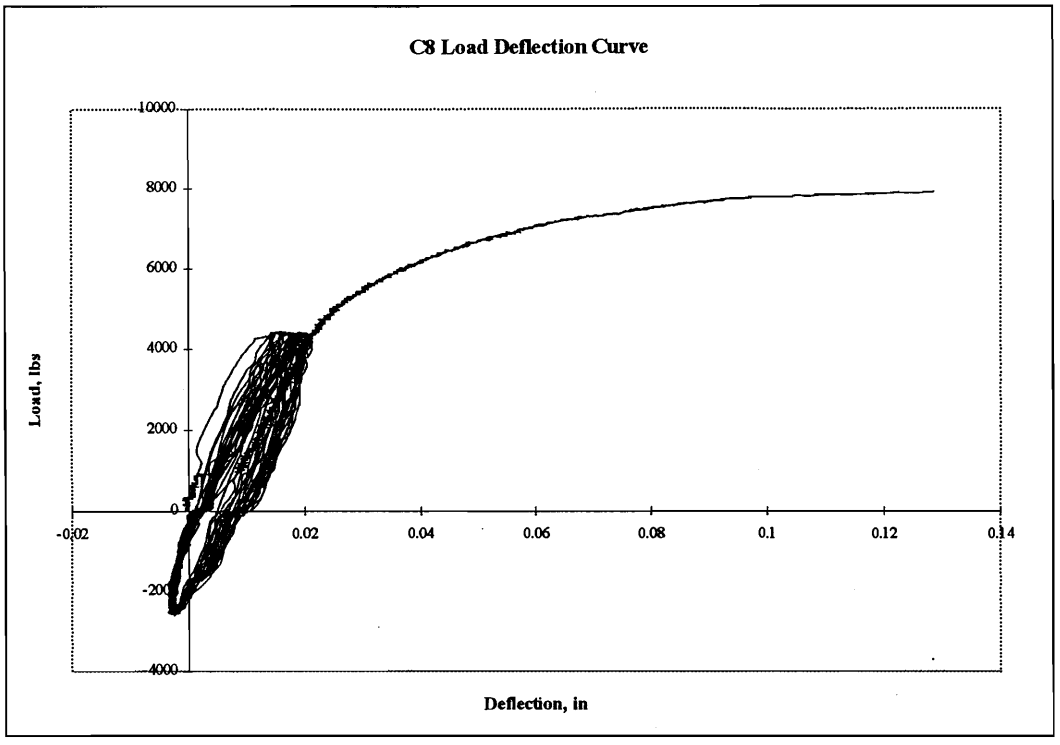

Figure 4- 19. Complete Load-Deflection Curve for Typical C8 Test (test C8-4).

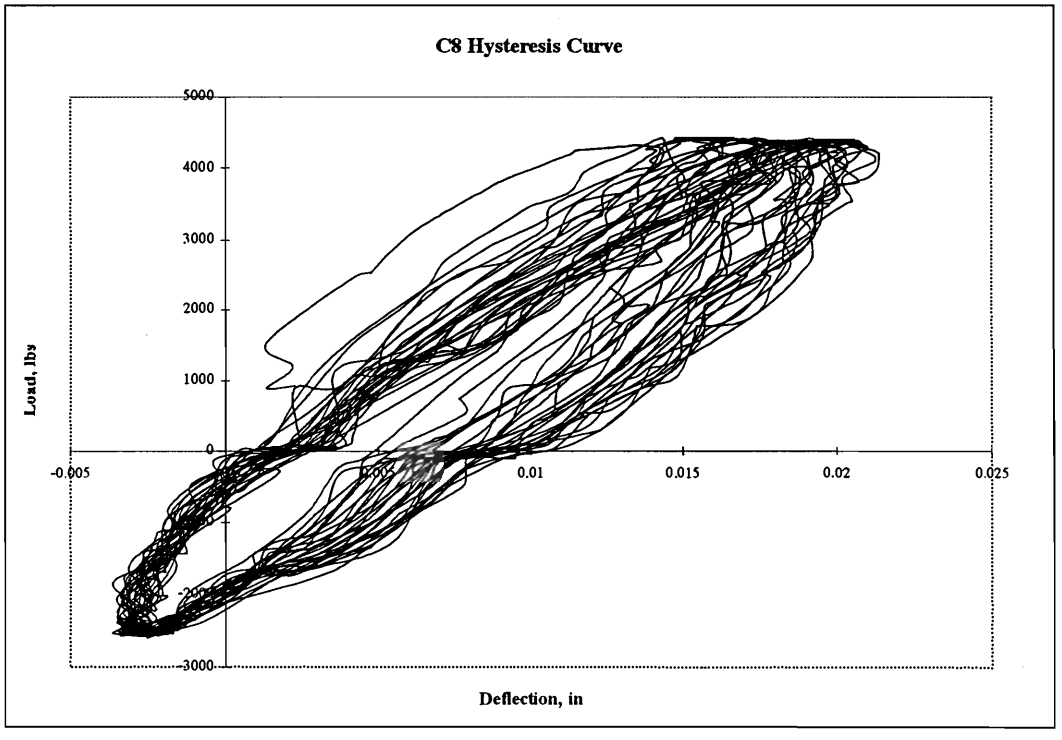

Figure 4- 20. Isolated Hysteresis Curves for Typical C8 Test (test C8-4).

The average Dead Load Stiffness was 2.71 x 10^5 lb./in. and the average Design Load Stiffness was 2.11 x 10^5 lb./in. (COV = 24% and N/A). There was a 92% decrease in stiffness from the Dead Load Stiffness to the Design Load Stiffness. The decrease in stiffness for the one test that survived was 22.1%. The average ultimate displacement of the joint at failure was 0.017 inches. The average cyclic offset that occurred during the tests was 0.007 inches (based on one measurement). These results are summarized in Table B-2b. Because only one joint survived this loading test, stiffness degradation conclusions are difficult to make.

The energy dissipation increased by 133% between the first and last cycle of this test. Since only one joint survived the tests, there was insufficient data to make any clear conclusions. These results are summarized in Table B-3b. In comparing the energy dissipation of these joints to that for the first stage of other tests, it seems as though the difference between 1.0 and 1.8 times the design load has little affect on the overall energy dissipation. The energy dissipation for 1.0 times the design load is very similar to the dissipation for 1.8 times the design load (p-value = 0.0002). This would suggest that the number of cycles is the major influence on energy dissipation (rather than magnitude).

Figures 4-21 and 4-22 show typical stiffness degradation and energy dissipation versus the displacement in the joint. The stiffness is related to deflection (R^2=0.923) and the energy dissipation is not statistically related to deflection (R^2 = 0.869). The general trend of the data does, however, suggest that energy dissipation increases with deflection.

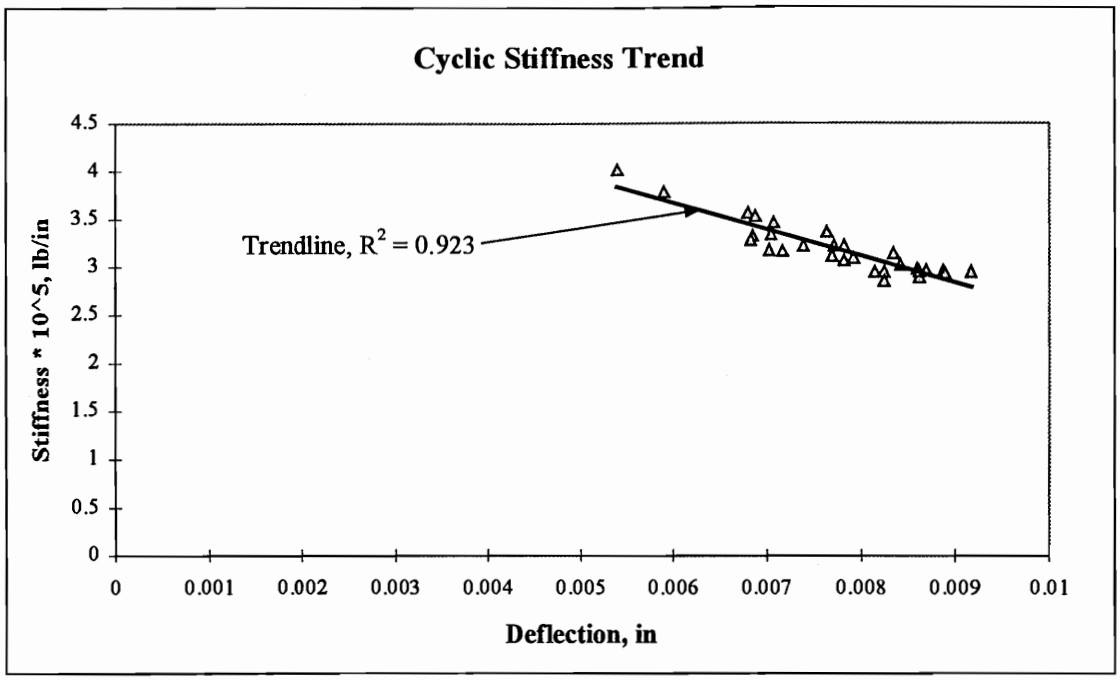

Figure 4- 21. Stiffness During Typical C8 Test (test C8-4).3

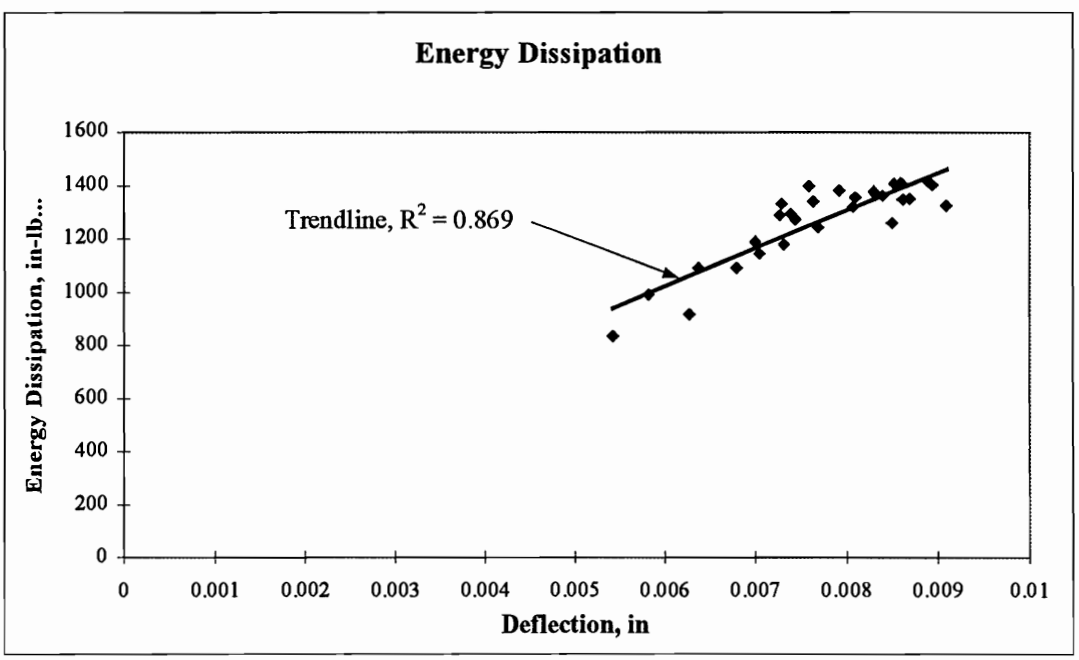

Figure 4- 22. Energy Dissipation During Typical C8 Test (test C8-4).

4.1.2.7.Cyclic Testing Results (C162)

A total of ten tension-splice joints were tested under the C162 loading. The average ultimate strength was 4924 lbs. with a coefficient of variation of 16%. Five of these joints survived the cyclic tests and were ramped to failure following the cycles (See Table B-2b). One of the joints was lost because of faulty load cell data at the end of the test caused by a poor wiring connection. The deflection and strength data from the early stages (1 and 2) were fine; therefore stiffness and deflection properties could be accurately determined for these stages. Five of the joints failed during the cycles. Two failed during the second load step and three failed during the third load step. There was significant evidence of strength degradation in this test (p-value = 0.0267). Since the first two stages are the same as C16, we can again conclude that most of the degradation occurred during the third and final stage of loading.

Figures 4-23 and 4-24 show a typical load-deflection curve and the isolated hysteresis loops for the same test.

The average Dead Load Stiffness was 2.89×10^5 lb./in. and the average Design Load Stiffness was 1.30×10^5 lb./in. (COV = 12% and 18%). There was a 77% decrease in stiffness from the Dead Load Stiffness to the Design Load Stiffness. The average decrease in stiffness during the first stage of the test was 22.9%, 16.9% in the second stage, and 0% in the third stage. The average ultimate displacement of the joint at failure was 0.048 inches. The average cyclic offset that occurred during the tests was 0.019 inches. These results are summarized in Table B-2b.

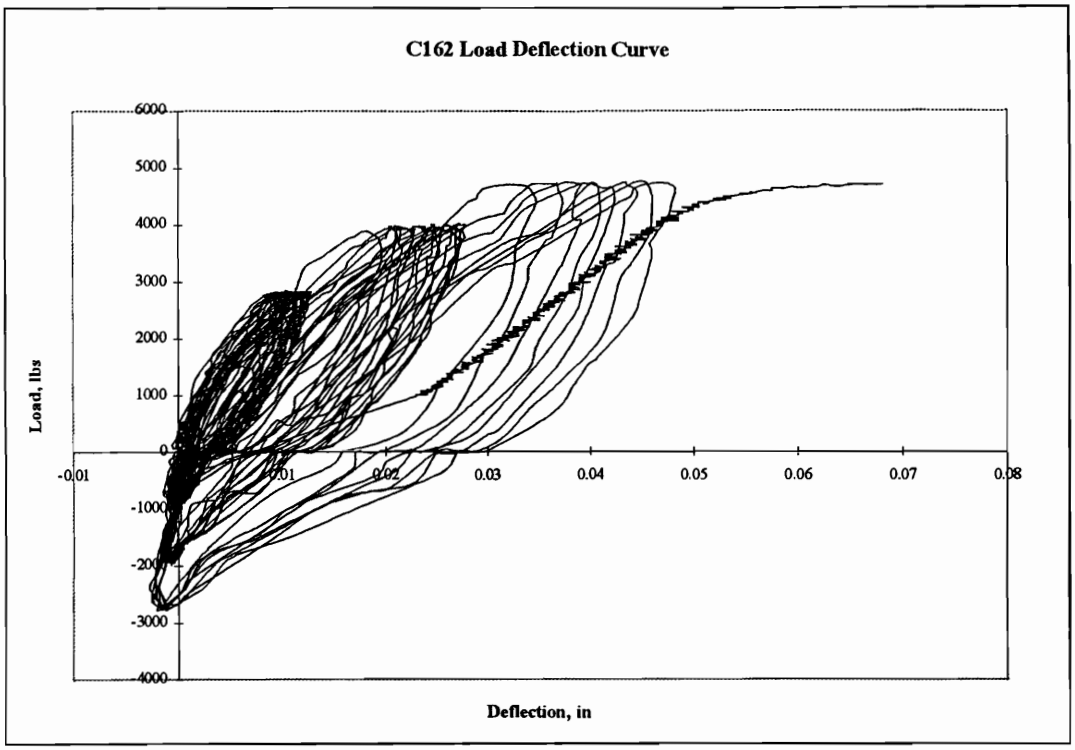

Figure 4- 23. Complete Load-Deflection for Typical C162 Test (test C162-6).

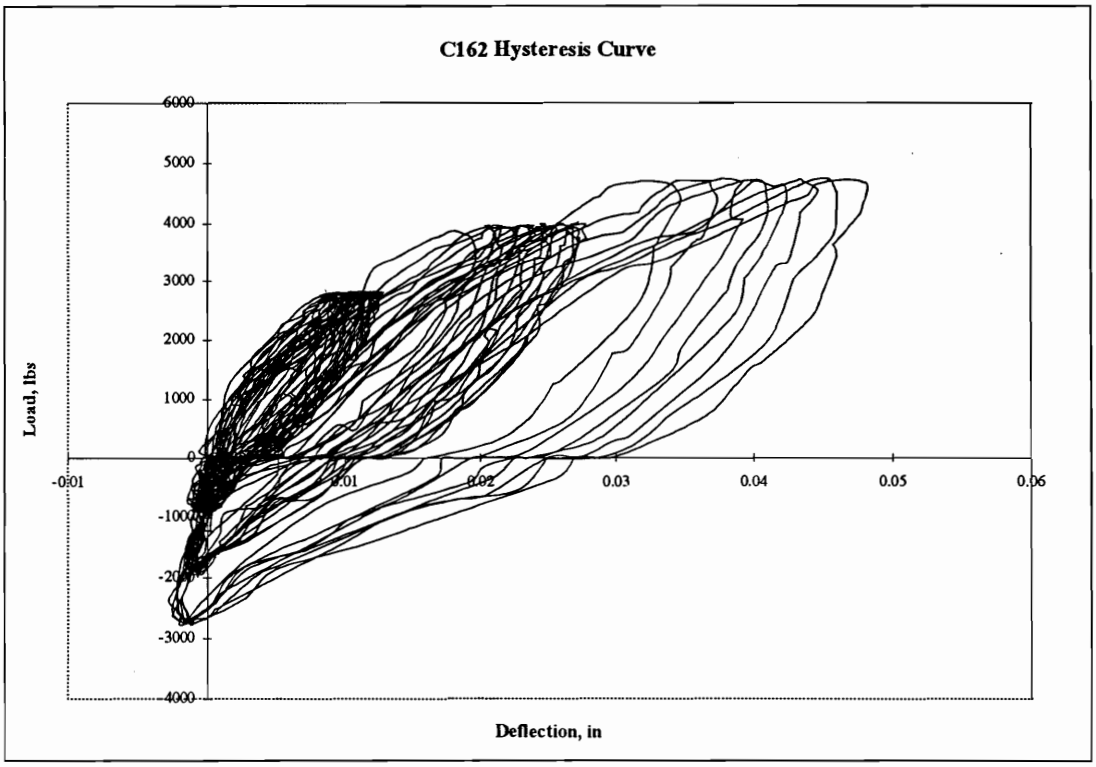

Figure 4- 24. Isolated Hysteresis Curves for Typical C162 Test (test C162-6).

The stiffness decrease (or lack there of) in the third stage is deceiving because a majority of the joints failed during the first or second cycle of the third stage. The total stiffness decrease in C162 is similar to the results for C132 (77% and 75%, respectively) (p-value = 0.48).

The energy dissipation increased by 160% between the first and last cycles of the first stage. The energy dissipation of the second stage increased 138% (between the first and last cycles of this stage), and the third stage increased 1% (between the first and last cycles of this stage). These results are summarized in Table B-3b. Again, the energy dissipation of the first and second stages are similar to the other cyclic tests presented earlier (apparently regardless of the cyclic magnitudes of the stages). The results from the third stage are misleading because very few joints survived into this stage and those that did failed after 1 or 2 cycles at this stage.

Figures 4-25 and 4-26 show typical stiffness degradation and energy dissipation versus the displacement in the joint. The stiffness and energy dissipation are not linearly related to the deflection. The R^2 values can be found on the plots of stiffness decrease and energy dissipation.

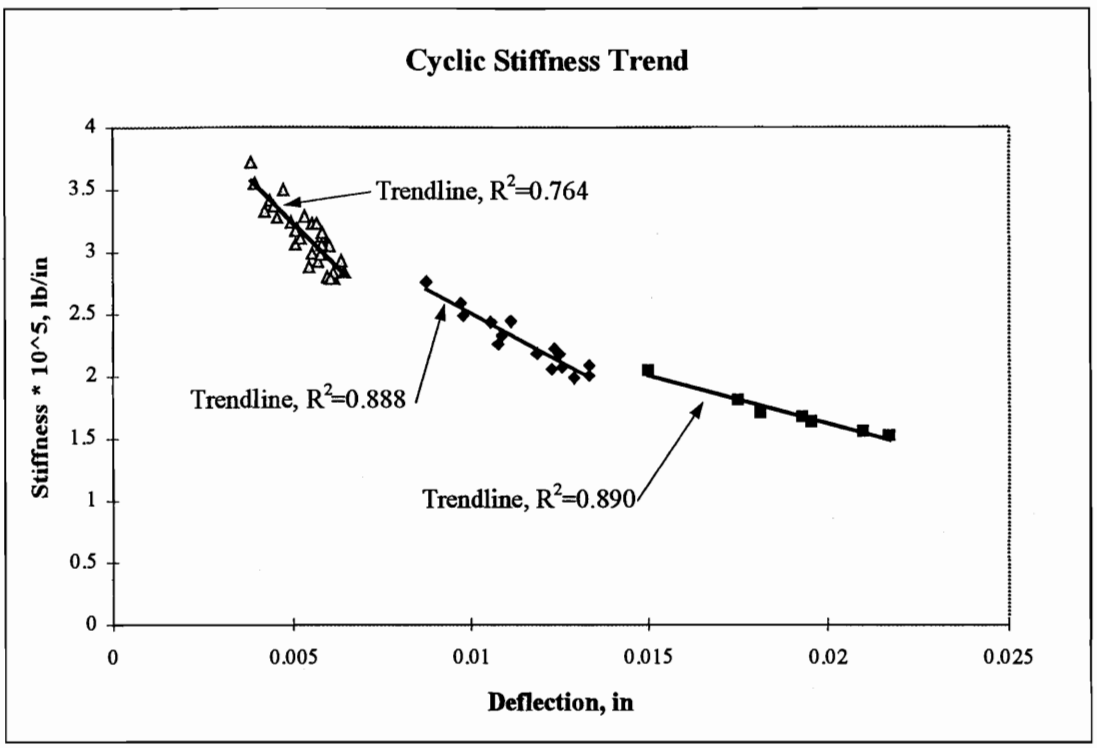

Figure 4- 25. Stiffness Decrease During Typical C162 Test (test C162-6).

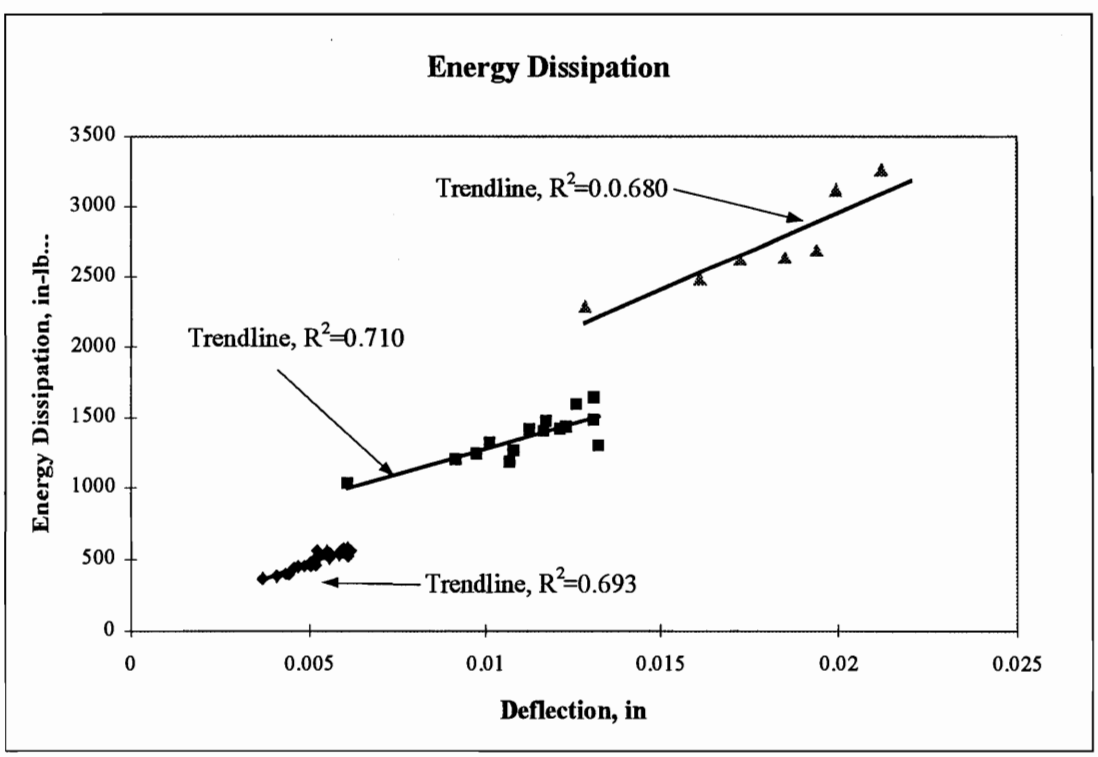

Figure 4- 26. Energy Dissipation During Typical C162 Test (test C162-6).

4.1.3. Discussion of Tension-Splice Joint Cyclic Testing Results

The results from these tests provide an insight into the duration of load factor for the tension-splice joint. The duration of load factor is based on strength properties, therefore; strength degradation of the MPC joints helps determine the appropriateness of the current duration of load factor. Detailed tables of the following testing information can be found in Appendix B. The average ultimate loads are shown in Figure 4-27.

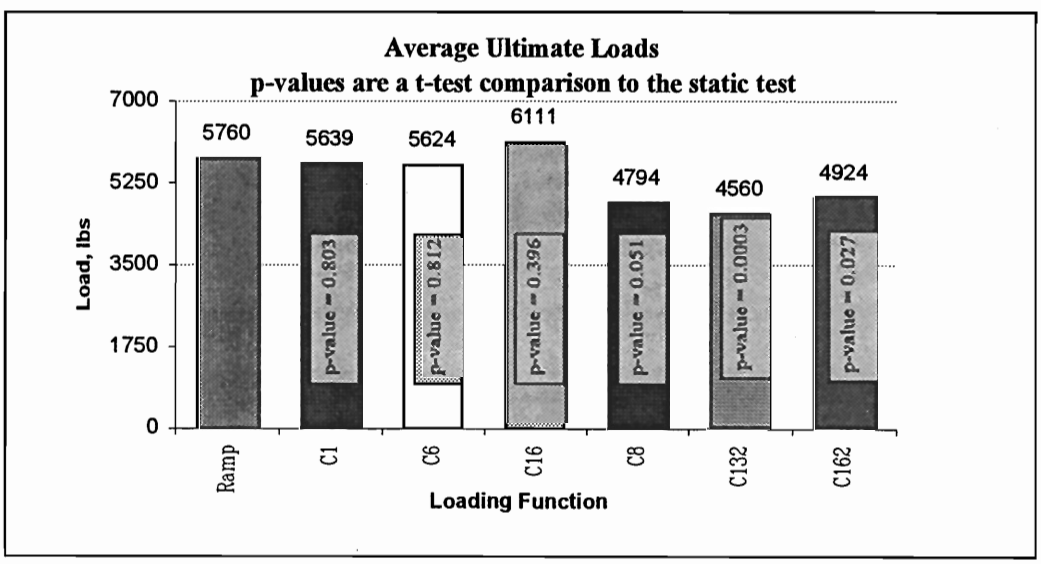

Figure 4- 27. Average Ultimate Load for Tension Splice Joints.

C6 is the simplest test examining the duration of load factor of 1.6. It basically implies a ten-year loading of 1.6 times the design load (assuming approximately 4 design level events. There was no evidence that strength degradation occurred in this test (2-sided p-value = 0.8121).

Table 4- 2. P-Values for Strength Comparisons

	Ramp Load	*C6*	*C8*	*C162*
C1	0.8028	0.9825	0.1617	NA
C6	0.8121	0	0.2185	NA
C16	0.3962	0.4432	NA	0.0140
C132	0.0003	NA	NA	0.2180
C8	0.0507	0.2185	0	NA
C162	0.0267	NA	NA	0

Test C1 assumes that C_D=1.0 or that there is no duration of load effect on the joints. C1 was done as a baseline for C6 and for all the other cyclic tests. As with the static ramp load test, C1 provides a baseline to compare the strength degradation of each cyclic test. In comparing C1 to the static ramp load, no strength degradation is evident. (2-sided p-value = 0.8028). The comparison between C1 and C6 also does not suggest any strength degradation (2-sided p-value = 0.9825). Because C6 showed no strength degradation, this would imply that C_D=1.6 may be a reasonable assumption. The rest of the cyclic tests of the tension-splice joint tests are more conservative and therefore increase our confidence that C_D could be conservatively taken as 1.6.

C162 attempts to simulate a number of events in the life of the joint (4 minor, 2 design, and 1 major) (based on Dolan (1994)). This could be looked upon as the most conservative investigation of C_D=1.6 that was accomplished in our tests. The comparison of C162 to the static ramp load suggests that some degradation may have occurred (2 sided p-value = 0.0267). Dolan (1994) found no strength degradation for nailed and bolted joints subjected to similar loading regimes. Therefore, MPC joints do not provide the same conservative level of confidence that nailed and bolted joints demonstrate (according to Dolan (1994)). If our results had shown no strength

degradation for C162, it could have been reasoned that C_D= 1.6 was sufficient (to the same level of confidence as in Dolan's research of nailed and bolted joints), but this did not occur. Our testing of C162 showed that some strength degradation may have occurred in the joint. C16 helped to pinpoint the stage that caused the degradation.

To help locate the source of the strength degradation in C162, C16 was performed. This test isolated the first two stages of C162. C16 did not show evidence of degradation (2-sided p-value = 0.3962). C16 produced some high ultimate loads and the average was actually higher than for the static ramp loading (but not statistically, p-value = 0.3962). In comparing C16 to C6, no degradation was observed (2-sided p-value = 0.4432), but degradation was observed between C16 and C162 (2-sided p-value = 0.0140). Combining these results would indicate that the degradation occurred during the stage involving 2.0 times the design load loading for 8 seconds and not during the first two steps of C162. In terms of duration of load, this would imply that a C_D=1.6 may still be acceptable, but not with the same confidence as for Dolan's results for nailed and bolted connections which showed no strength degradation at this level of loading.

C132 was done to investigate the duration of load factor of 1.33 previously used in both the NDS (AFPA 1993) and UBC (1985). In comparing C132 to the static ramp load, there is overwhelming evidence of degradation (2-sided p-value = 0.0003). By comparing C132 and C162, it is possible to predict any strength degradation that may have occurred due to the second stage (1.33 vs. 1.6) of the loading and compare any differences from the 1.33 duration of load factor and the current 1.6 duration of load factor. In comparing C132 and C162, no degradation was observed (2-sided p-value = 0.2180). The results for the C16 and C132 comparisons suggest that the first and second stages of the tests have little impact on the degradation of the joints. It is therefore suspected that most of the strength degradation occurs during the third stage (or the major event). Again, if we are trying to determine an adequate C_D factor, this test comparison suggests that the use of 1.6 is appropriate. By using 1.6, we gain an

increase in design capacity without sacrificing confidence in the joint's ability to withstand a cyclic event. We do not sacrifice any confidence because C132 showed the same degradation.

The final test, C8, investigates the possible upper bound of the duration of load factor. This test was chosen because C_D =1.8 fell between C_D=1.6 (current NDS (AFPA 1991) design value and highest value tested that showed no sign of strength degradation) and C_D=2.0 (the lowest value that showed strength degradation). Since 2.0 showed degradation and 1.6 did not, the testing of 1.8 seemed like a reasonable step. The comparison between C8 and the static ramp load suggests possible evidence of degradation (2-sided p-value = 0.0507). This higher p-value of 0.0507 reflects a lack of confidence the comparison between C8 and the static ramp load caused degradation. To adequately evaluate C8 a larger sample set would need to be tested. There is no evidence that C8 is statistically different than C6 (2-sided p-value = 0.2185). While C8 and C6 are statistically the same population, C6 does not show any strength degradation (compared to the static) and C8 possibly shows some strength degradation (compared to the static). This suggests that there is some slight strength degradation from C6 to C8 but it is statistically minor. More samples would need to be tested to determine if the duration of load factor could in fact be higher than 1.6 (such as 1.8).

In summary, the joints seem to have little strength degradation during the first and second steps of the loading function. While statistically there is no significant degradation, comparisons between some of the tests (i.e. C8 and C6) would suggest that some minor degradation may occur. Most of the degradation appears to occur during the third and final step of the loading function (major event). Based on the results of C8, it would seem that the upper bound to the duration of load factor is approximately 1.8. More joint tests would need to be performed to statistically confirm this conclusion. The significant result of this research is that using C_D=1.6 for the design of MPC joints subjected to seismic events seems appropriate.

Assuming the stiffness loss taken between the Dead Load Stiffness and Design Load Stiffness for the static ramp test is a baseline stiffness decrease for the case of no cyclic loading, all cyclic joints experienced varying degrees of stiffness degradation beyond that observed in the static case (excluding C1). Stiffness degradation was defined as the decrease between the Dead Load Stiffness and the Design Load Stiffness. The static ramp load test experienced a 32% decrease in stiffness (this is a reflection of the joint's nonlinear behavior). C6 experienced a 59% decrease. C1 experienced a 31% decrease. C162 and C16 experienced 77% and 43% decreases, respectively. C132 and C8 experienced 75% and 92% decreases, respectively. This suggests that all of the cyclic tests (C6, C16, C162, C132, and C8) experienced stiffness degradation beyond what would be expected due to loading without the cycles.

The stiffnesses of the cyclic tests did degrade. The stiffness degradation observed above suggests that both the magnitude and the number of cycles influence stiffness degradation. This can be observed by comparing the higher magnitude tests to the lower magnitude tests. All tests that contained 2.0 times the design loading experienced a significant level of stiffness degradation (> 75%). All other tests showed less degradation (<59%). This suggests that magnitude of the cycles has an impact on stiffness degradation. By looking closer and comparing tests individually, we can see that the number of cycles seems to impact stiffness degradation as well. The highest loading magnitude for C6 and C16 is the same but the stiffness degradation is 16% higher during C6, which contains more cycles at the higher magnitude. A similar conclusion can be drawn by comparing C162 and C132. The only difference is the magnitude of the second stage, and C162 stiffness degradation was slightly higher. Although the results here are less conclusive, the same result occurs (higher magnitude = increased stiffness degradation).

P-values associated with dead load stiffness, design load stiffness, and stiffness decrease were also calculated. As expected, the comparisons between the static ramp load case and each of the cyclic cases did not show any statistical differences for the dead load stiffness (Table 4-3).

Table 4- 3. P-Values for Dead Load Stiffness Comparisons.

Comparison	*P-Value*
C1 to Static	0.6262
C6 to Static	0.1043
C16 to Static	0.9383
C132 to Static	0.2566
C8 to Static	0.2146
C162 to Static	0.4085

Stiffness degradation was also examined by comparing the Design Load stiffnesses for the different testing regimes. Degradation was evident in three of the cases by this method. C1 and C16 did not show evidence of stiffness degradation (p-value = 0.105, 0.501, respectively), but C6, C132, and C162 did (p-value = 0.041, 0.00, 0.001, respectively). These results agree with the stiffness degradation results of the previous paragraph. These results suggested that both magnitude and the number of cycles influence stiffness degradation.

Table 4- 4. P-Values for Design Load Stiffness Comparisons.

	Ramp Load	*C6*	*C8*	*C162*
C1	0.105	0.012	0.0002	NA
C6	0.041	NA	0.008	NA
C16	0.501	0.274	NA	0.0145
C132	0.000	NA	NA	0.480
C8	0.000	0.000	NA	NA
C162	0.001	NA	NA	NA

Other comparisons were also investigated. The p-value for the comparison between C16 and C162 was 0.0145. This suggests that significant degradation occurred due to the added eight cycles at 2.0 times the design load. The p-value for the comparison of the static case with C8 showed degradation (p-value = 0.000). The comparison of C6 to C8 also showed degradation (p-value = 0.000). These results suggest that magnitude influenced the stiffness decrease observed in the Design Load Stiffness values. The comparisons between C6, C1 and the static case reveals that the Design Load Stiffness decreased with increased magnitude and the number of cycles. The p-values for these comparisons are in Table 4-3. These results support the conclusion that increased magnitude and number of cycles increase the stiffness degradation of the joints.

The energy dissipation from these tests suggests that energy dissipation is related to the number of cycles. All of the cyclic loadings showed significant energy dissipation as the test progressed.

Table 4- 5. P-Values for Stiffness Decrease Comparisons.

	Ramp Load	*C6*	*C8*	*C162*
C1	0.873	0.034	0.0002	NA
C6	0.005	NA	0.008	NA
C16	0.261	0.148	NA	0.0145
C1322	0.000	NA	NA	0.480
C8	0.000	0.000	NA	NA
C162	0.002	NA	NA	NA

4.1.4. Problems During Tension-Splice Joint Tests

Two of the original load cases were not correctly tested (C132 and C142). The control system was set incorrectly with amplitude offset before the tests began. As a result, one of these load cases (C132) was re-tested and the results from this case led to the elimination of the second case (C142) from the study. Appendix A briefly discusses these two load cases and the results obtained from them.

4.2. Heel Joint Results

The heel joint testing was limited because of a limited number of samples. The method of testing the heel joints changed during the research. In the original method, we attempted to replicate the conditions of an actual heel joint in a truss (including rotations). Several joints were tested using this method, but several problems occurred.

First, the joints were extremely difficult to position in the test frame. To accurately measure the rotation, the joint needed to be placed in the frame in such a way that the loading acted axially. Because of the difficulty associated with this orientation, the COV for the rotation was extremely large. The slightest variation in the alignment created significant changes in the rotation.

The second problem was a fundamental one involving the measurement of the rotation. The amount of rotation that a heel joint experiences is influenced by a number of geometric properties of the truss. These include the distribution of loads through the truss based on both the configuration of the truss members and the placement of loads and the size of the truss (i.e. the length of the upper chord). To accurately determine the rotational stiffness of a truss joint, the entire truss should be investigated. By measuring the rotation of the joint due to an axial load, we are only measuring the rotation caused by a slight moment (a direct result of a slightly off center axial load).

It was decided that the setup being used did not provide for control of all the variables associated with it and the rotation aspect of the research was eliminated. For this reason, a large number of the fabricated and tested joints were not used for the final testing program (having been tested incorrectly). The changes in the system dealt with the need to eliminate and/or reduce the rotational component that the heel joint tests were experiencing. To do this, numerous braces were added to the hydraulic unit and a string was stretched between the loading point and the working point of the joint. This helped to ensure a consistent alignment of the heel joints. The heel joints provided an interesting challenge in terms of alignment.

A summary of heel joint test results is provided here and individual test results are discussed in the following sections and sub-sections. Table 4-6 shows the average strength and stiffness for heel joints under static and three different types of cyclic loading conditions. The strength is after the cyclic loading. The stiffness reported here is the Design Load Stiffness. The coefficient of variation (COV) for the strength results only slightly.

Table 4- 6. Heel Joint Test Summary.

Test	*Strength, lbs. (N, COV)*	*Design Stiffness, $*10^5$ lbs./in (N, COV)*	*Offset Stiffness, $*10^5$ lbs./in (N, COV)*
Static	5760 (10, 6%)	1.05 (9, 14%)	1.03 (9, 14%)
C16	5553 (10, 10%)	0.35 (8, 65%)	0.51 (8, 65%)
C162	5328 (10, 17%)	0.99 (4, 72%)	0.97 (4, 72%)
C18	5643 (10, 9%)	1.02 (8, 29%)	1.03 (8, 29%)

4.2.1. General Characteristics

Several general characteristics regarding each joint were recorded. The characteristics that were recorded and investigated included ultimate load, modulus of elasticity, moisture content, specific gravity, rings per inch, percent latewood, grain orientation, Dead Load Stiffness, Design Load Stiffness, Dead/Design Stiffness Decrease, ultimate displacement and cyclic offset. These characteristics are defined in the same manner as for the tension-splice joints with the only variation being the value of the dead load (1550 lbs. vs. 900 lbs.) (see Appendix B). A tooth withdrawal failure mode was observed for all of the heel joint tests (Figure 4-28).

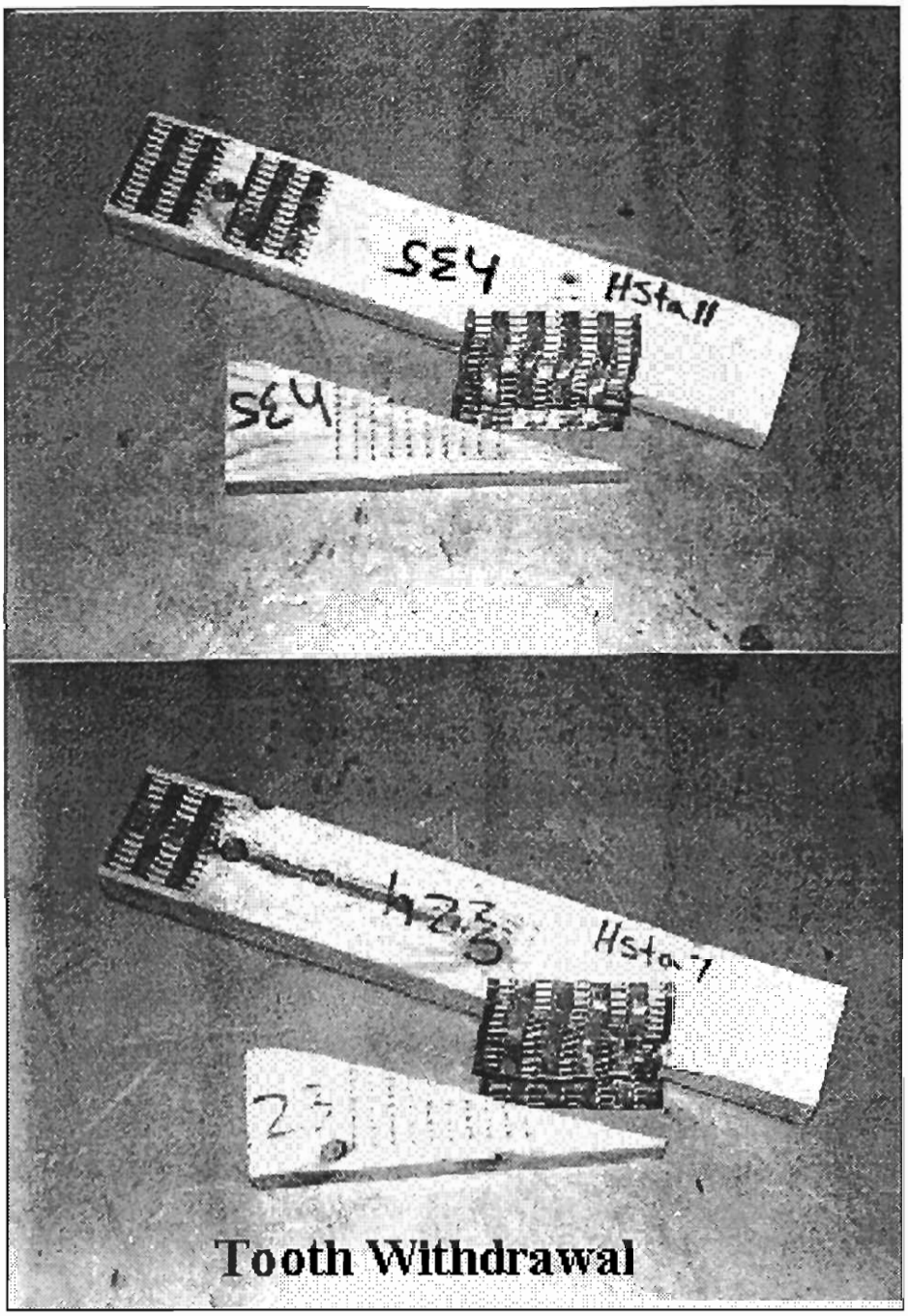

Figure 4- 28. Heel Joint Failure Mode.

4.2.2. Heel Joint Tests

4.2.2.1.Static Results

A total of ten heel joints were tested statically. The average ultimate strength was 5763 lbs. with a coefficient of variation of 6%. The design load for the heel joints was determined by dividing the average ultimate strength for all the static tests by 3 (AFPA 1991). This results in an average design load of 1920 lbs. Interestingly, this is the same design load as for the tension-splice joints. Of the two methods recommended in the 1991 NDS, the heel joint design load was controlled by dividing the average ultimate load by 3 (same as for the tension-splice joints). The slip critical method was applied to the heel joint by measuring the slip of the upper chord. All of the statically loaded heel joints failed in tooth withdrawal. A typical load-deflection curve (from test HL-10) is presented in Figure 4-29.

Dead Load Stiffness and Design Load Stiffness for the heel joints are defined in a similar manner as for the tension-splice joints. The Dead Load Stiffness was defined as the slope of the secant line between the base (or beginning) of the load deflection curve and the dead load (1550 lbs.). The Design Load Stiffness was defined as the slope of the secant line between the dead load value after the cyclic portion of the test to the average design load from the static tests. For the static joints, there was no cyclic portion of the test, so the stiffness was taken between the dead load and the design load.

The average Dead Load Stiffness was 2.22×10^5 lb./in. and the average Design Load Stiffness was 1.05×10^5 lb./in. (COV = 12% and 14%). There was approximately a 52% decrease in stiffness from the Dead Load Stiffness to the Design Load Stiffness. The average ultimate displacement of the joint at failure was 0.198 inches.

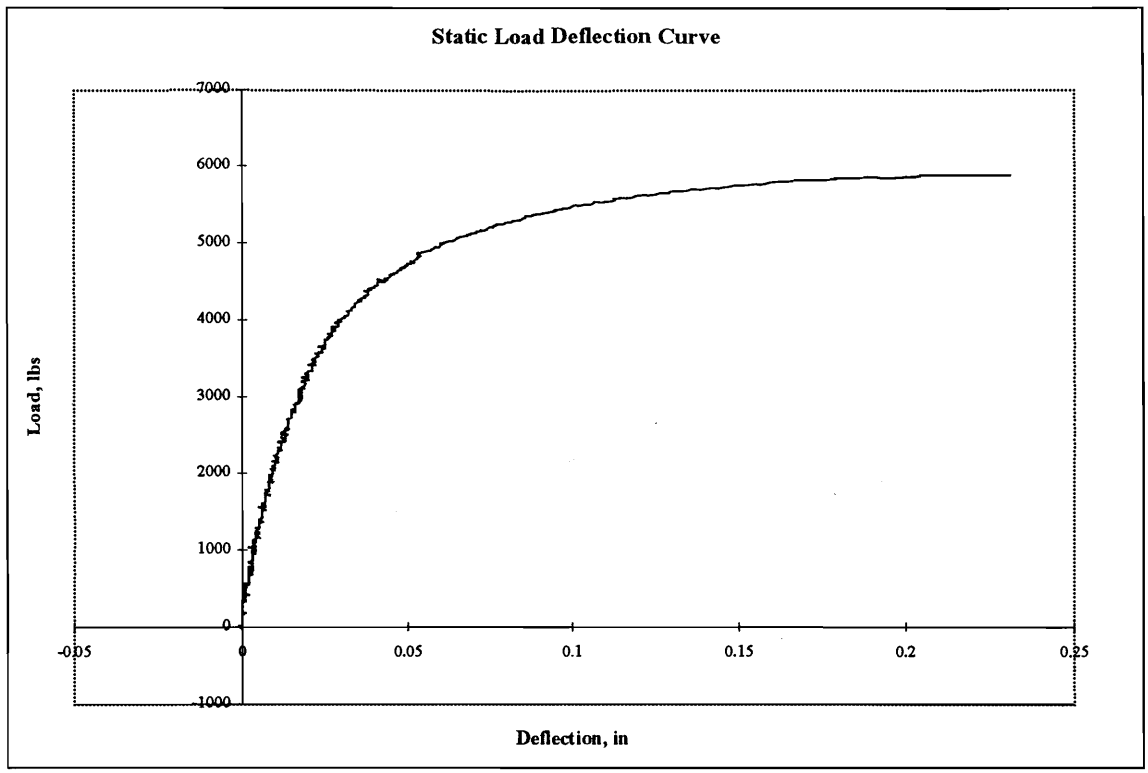

Figure 4- 29. Static Load-Deflection Curve For a Typical Heel Joint (test HL-10).

4.2.2.2. Cyclic Testing Results (CH16)

A total of ten heel joints were tested under CH16. The average ultimate strength was 5551 lbs. with a coefficient of variation of 10%. All ten of these joints survived the cyclic tests and were ramped to failure following the cycles. These results indicate that there was no strength loss from this test. The p-value was greater than 0.05 when compared to the ultimate strength population for CH16 to the ultimate strength population from the static tests (p-value = 0.340).

Figures 4-30 and 4-31 are plots of the complete load-deflection curve and the isolated hysteresis curves for a typical CH16 test (test CH16-1).

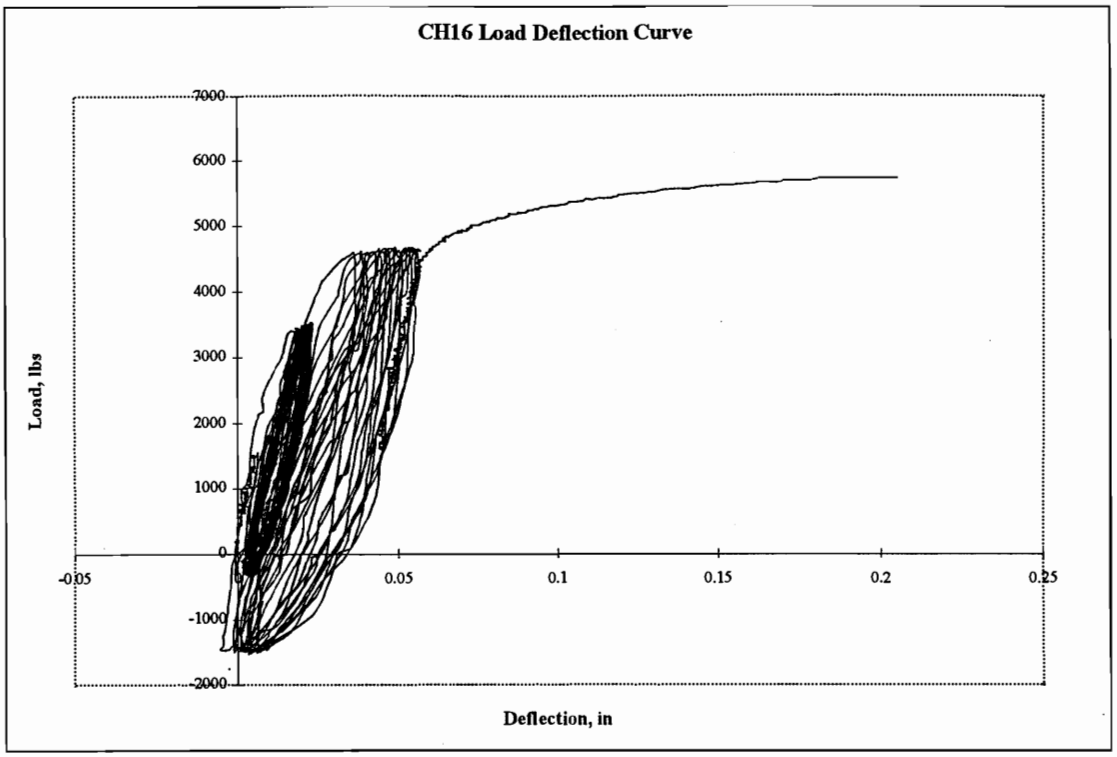

Figure 4- 30. Complete Load-Deflection Curve for Typical CH16 Test (test CH16-1).

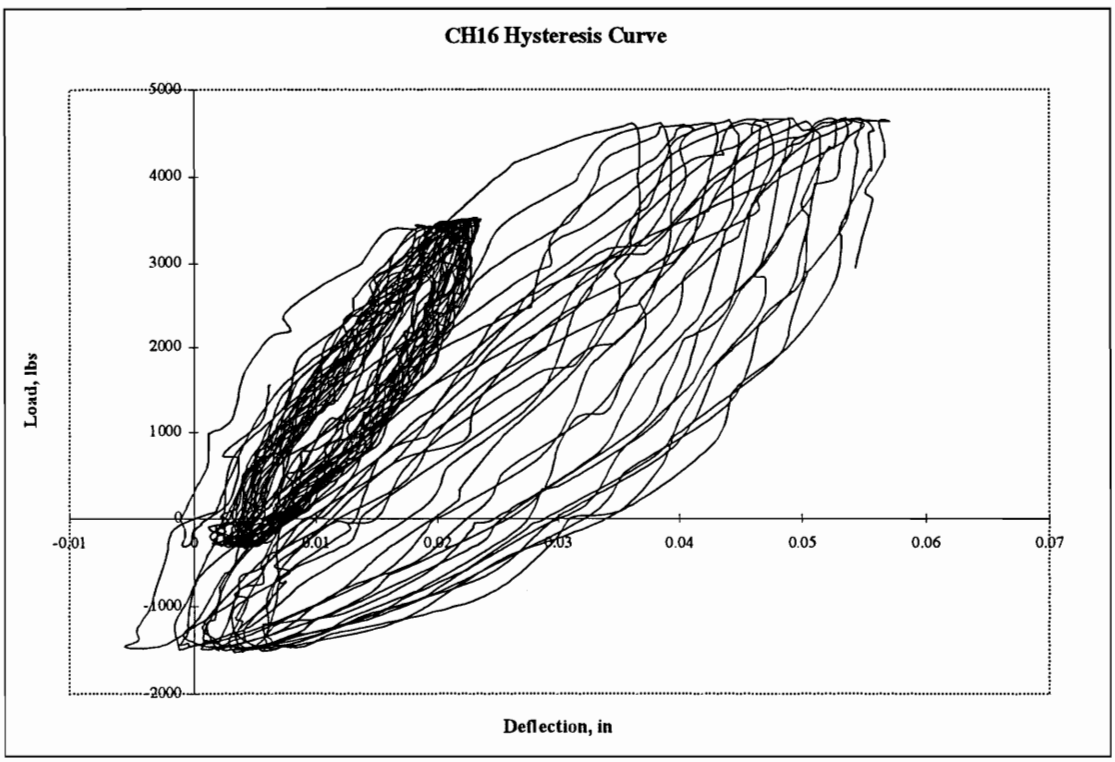

Figure 4- 31. Isolated Hysteresis Curves for Typical CH16 Test (test CH16-1).

The average Dead Load Stiffness was 2.15 x 10^5 lb./in. and the average Design Load Stiffness was 0.35 x 10^5 lb./in. (COV were 23% and 133%, respectively). There was an 80% decrease in stiffness from the Dead Load Stiffness to the Design Load Stiffness. The average ultimate displacement of the joint at failure was 0.207 inches. The average cyclic offset that occurred during the tests was 0.059 inches. The Dead Load stiffness was similar to the static load case. The Design Load stiffness suggests that significant degradation took place (p-values = 0.001 between the Design Load Stiffness and the static load case stiffness).

Figure 4-32 shows the stiffness degradation that was observed during the cyclic portion of a typical test and Figure 4-33 shows the change in the energy dissipation of the joint as the cycles progressed. From a statistical viewpoint, these characteristics had very low R^2 values, but the plots of these characteristics do show a clearly decreasing trend that becomes more linear as the individual test progressed. The average decrease in stiffness during the first stage of the test was 11.2% and 18.1% in the second stage. The energy dissipation increased by 348% by the end of the first stage from the first cycle of the stage. These results demonstrate that the heel joints of this study had a high energy dissipation ability (when compared to the tension-splice joint).

4.2.2.3.Cyclic Testing Results (CH162)

Ten heel joints were tested under CH162 loading conditions. These tests were designed to be a conservative evaluation of C_D=1.6. It provides an approximation of the loads that may be expected during the life of a typical structure. The average ultimate strength was 5317 lbs. with a coefficient of variation of 17%. All ten of these joints survived the cyclic tests and were ramped to failure following the cycles. The CH162 results do not indicate any strength degradation. The p-value is greater than 0.05 for the comparison between the ultimate strength population of CH162 and the ultimate strength population of the static heel joints (p-value = 0.203).

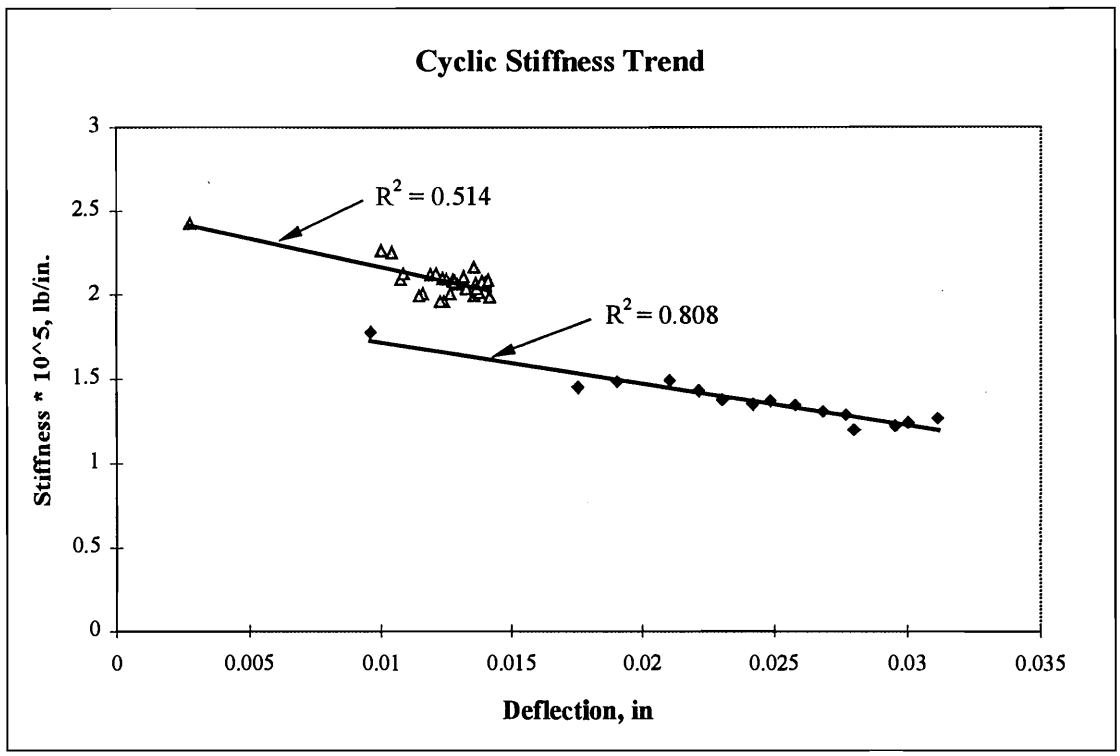

Figure 4- 32. Stiffness During a Typical CH16 Test (test CH16-1).

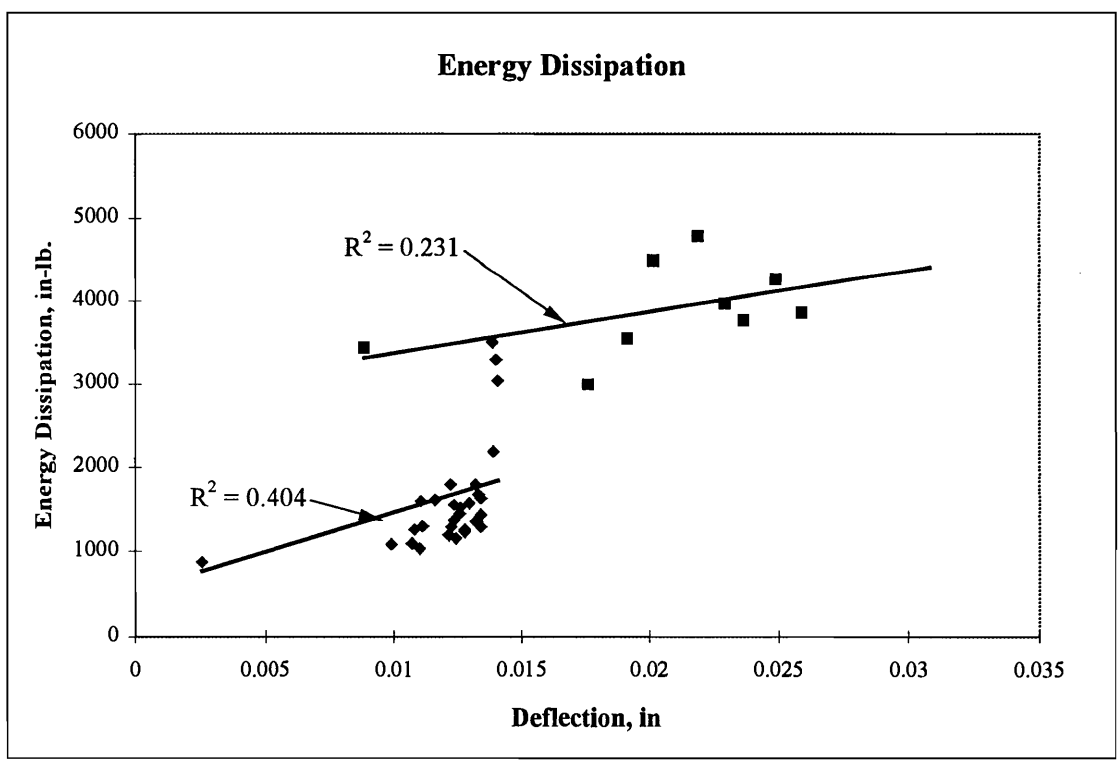

Figure 4- 33. Energy Dissipation During a Typical CH16 Test (test CH16-1).

This would seem to indicate that C_D=1.6 is adequate for the design of heel joints. Figures 4-34 and 4-35 are plots of the complete load-deflection curve and isolated hysteresis curves of a typical CH162 test.

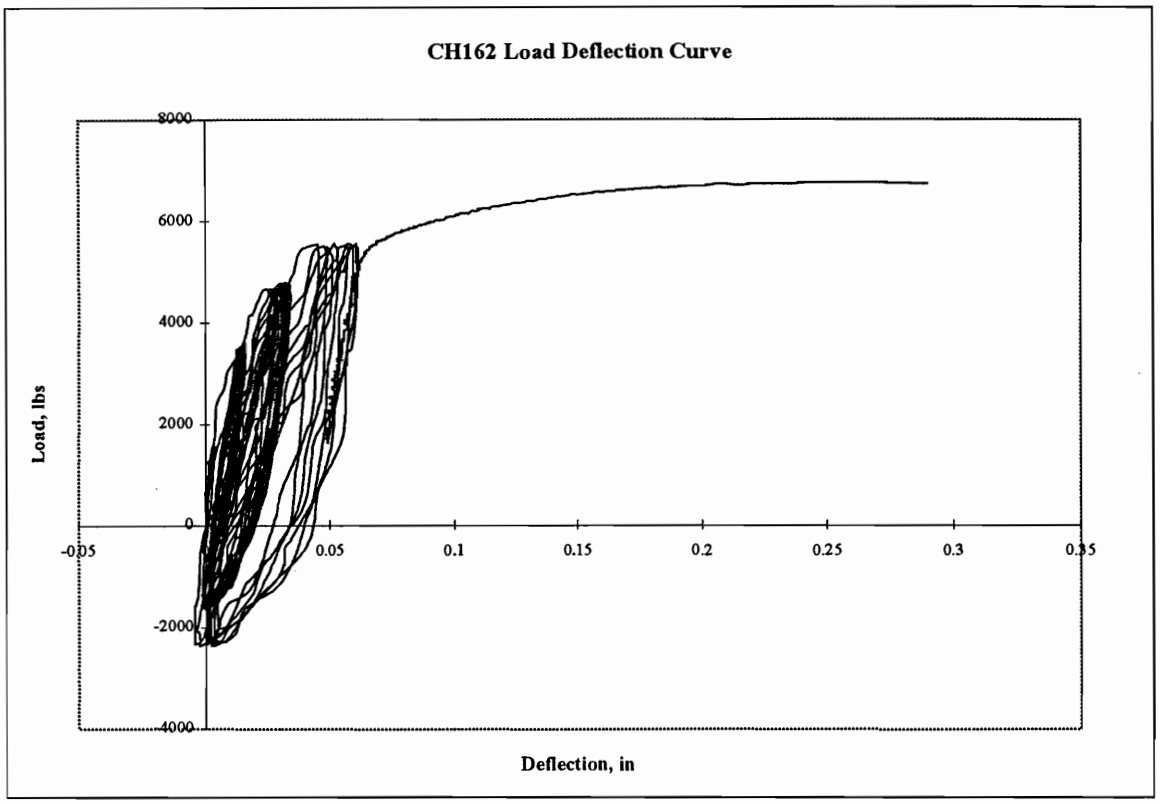

Figure 4- 34. Complete Load-Deflection Curve for Typical CH162 Test (CH162-4).

The average Dead Load Stiffness was 2.27 x 10^5 lb./in. and the average Design Load Stiffness was 0.99 x 10^5 lb./in. (COV = 27% and 72%, respectively). There was an 86% decrease in stiffness from the Dead Load Stiffness to the Design Load Stiffness. The average ultimate displacement of the joint at failure was 0.293 inches. The average cyclic offset that occurred during the tests was 0.135 inches. The average decrease in stiffness during the first stage of the test was 13.7%, 24.5% in the second stage and 4.1% in the third stage.

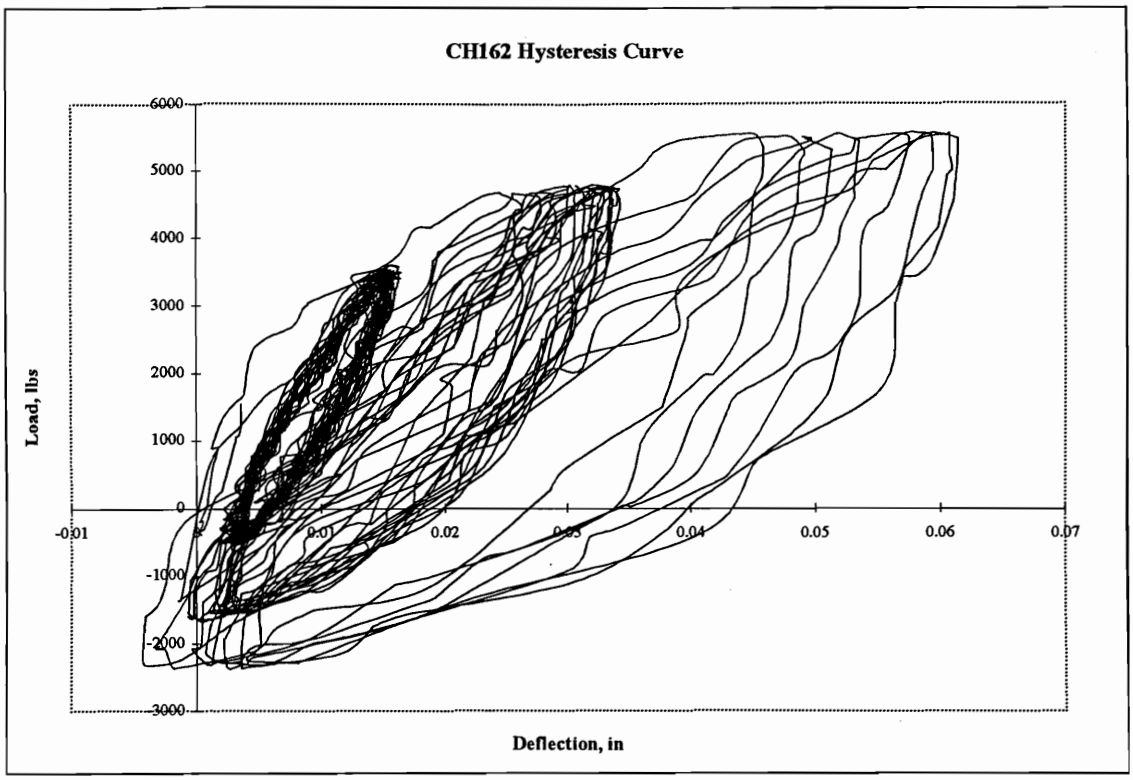

Figure 4- 35. Isolated Hysteresis Curves for Typical CH162 Test (CH162-4).

The amount of stiffness decrease did not significantly increase between CH16 and CH162. This would suggest that the major event (2.0 times the design load) does not affect the heel joint in the same manner as the tension-splice joint. The energy dissipation increased by 292% between the first and last cycle of the first stage. During the second stage, the energy dissipation increased by another 162%. For CH162, the first stage had a significantly higher energy dissipation. Figure 4-36 and 4-37 present the plots of the stiffness decrease and the energy dissipation, respectively.

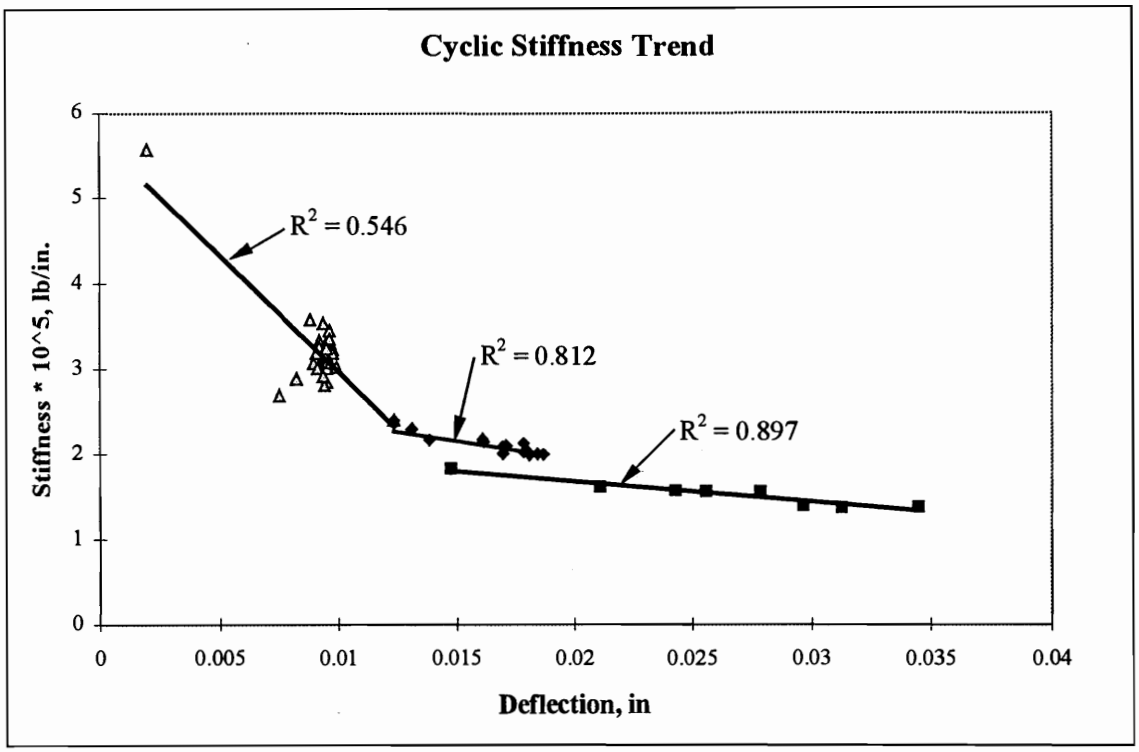

Figure 4- 36. Stiffness During a Typical CH162 Test (test CH162-4).

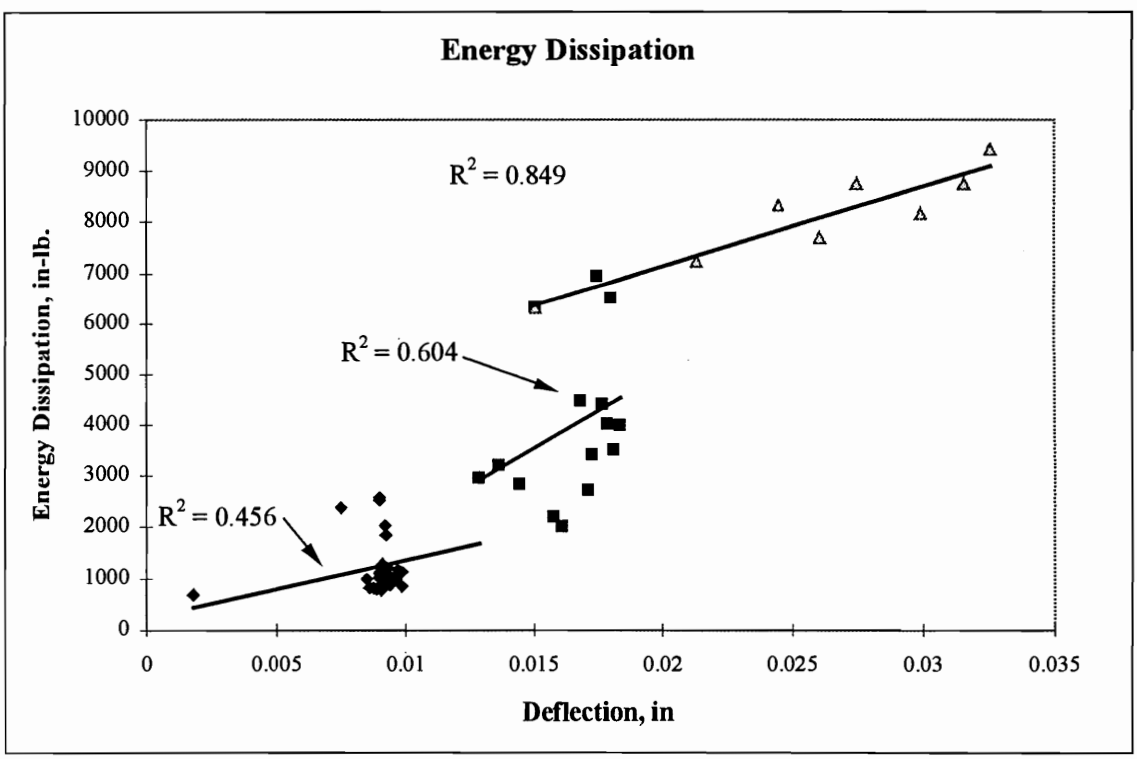

Figure 4- 37. Energy Dissipation During a Typical CH162 Test (test CH162-4).

4.2.2.4.Cyclic Testing Results (CH18)

Ten heel joints were tested the under CH18 loading condition. These tests were designed to investigate C_D=1.8. The average ultimate strength was 5640 lbs. with a coefficient of variation of 9%. All ten of these joints survived the cyclic tests and were ramped to failure following the cycles. CH18 did not suggest any strength degradation when compared to the static loading case (p-value = 0.589)

Figures 4-38 and 4-39 are plots of the complete load-deflection curve and isolated hysteresis curves for a typical CH18 test.

The average Dead Load Stiffness was 2.33×10^5 lb./in. and the average Design Load Stiffness was 1.02×10^5 lb./in. (COV = 31% and 29%, respectively). There was a 56% decrease in stiffness from the Dead Load Stiffness to the Design Load Stiffness. The average ultimate displacement of the joint at failure was 0.256 inches. The average cyclic offset that occurred during the tests was 0.075 inches. The average decrease in stiffness during the first stage of the test was 23.6% and 30.6% in the second stage (see Figure 4-40). There is not a significant increase in the amount of stiffness decrease for the CH18 load case (compared to CH16 and CH162). For this reason, making conclusions regarding the stiffness decrease is difficult. The energy dissipation increased by 422% between the first and last cycles of the first stage. During the second stage (between the first and last cycle), the energy dissipation increased by another 123% (see Figure 4-41). Since the magnitude of loading varies only slightly, the results for CH18 reinforce the CH162 results that the number of cycles is the greatest influence on energy dissipation.

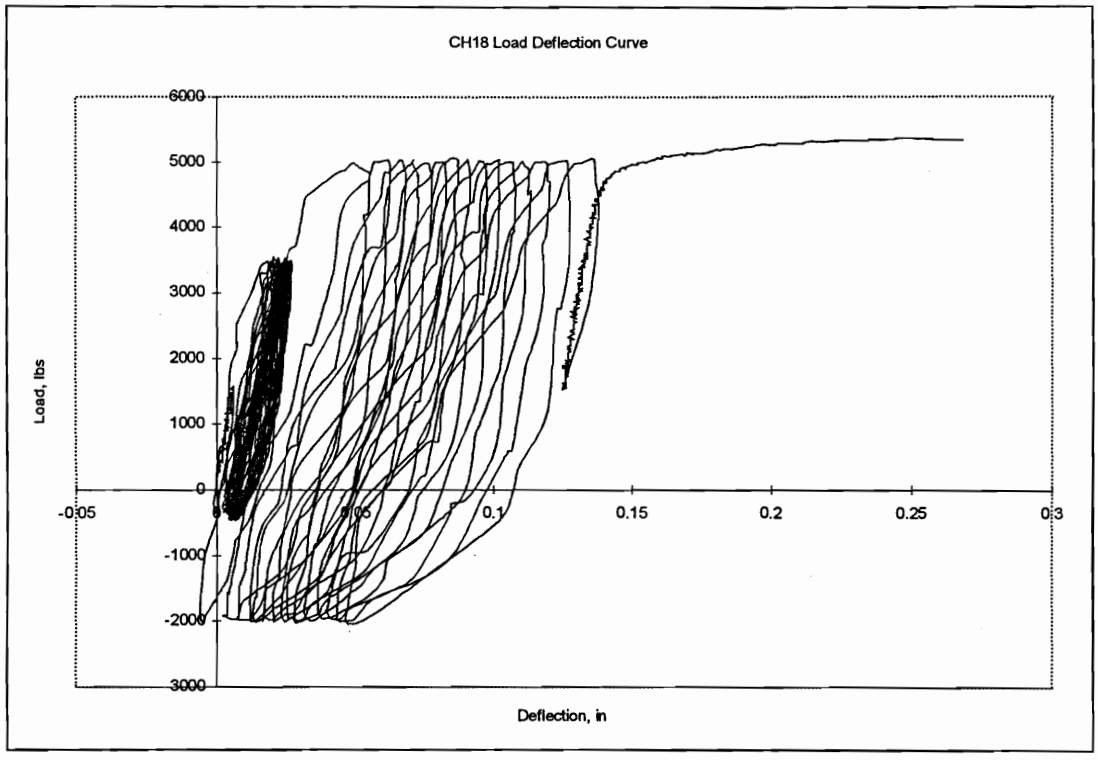

Figure 4- 38. Complete Load-Deflection Curve for Typical CH18 Test (test CH18-2).

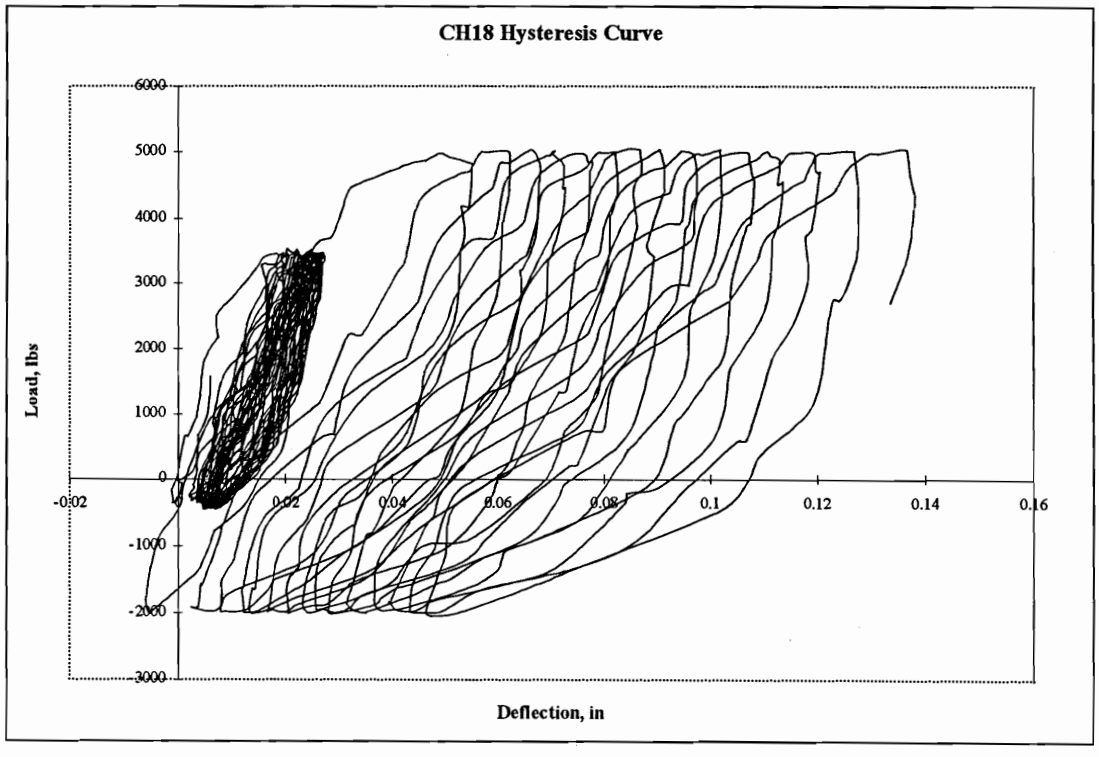

Figure 4- 39. Isolated Hysteresis Curves for Typical CH18 Test (test CH18-2).

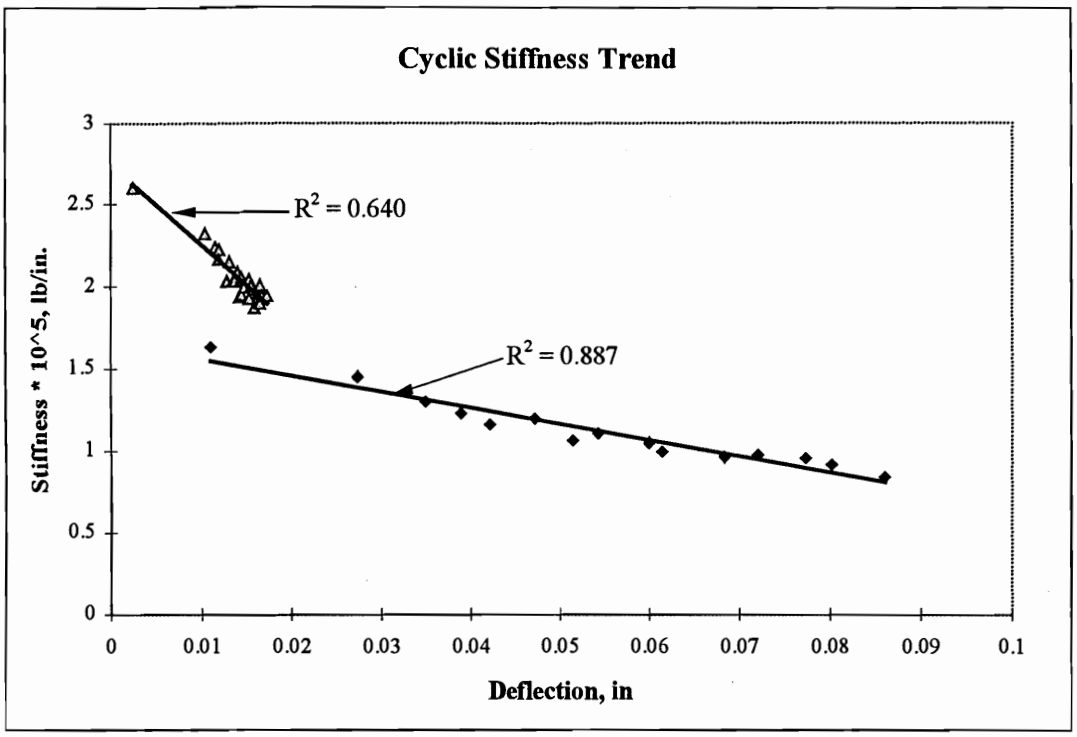

Figure 4- 40. Stiffness During a Typical CH18 Test (test CH18-2).

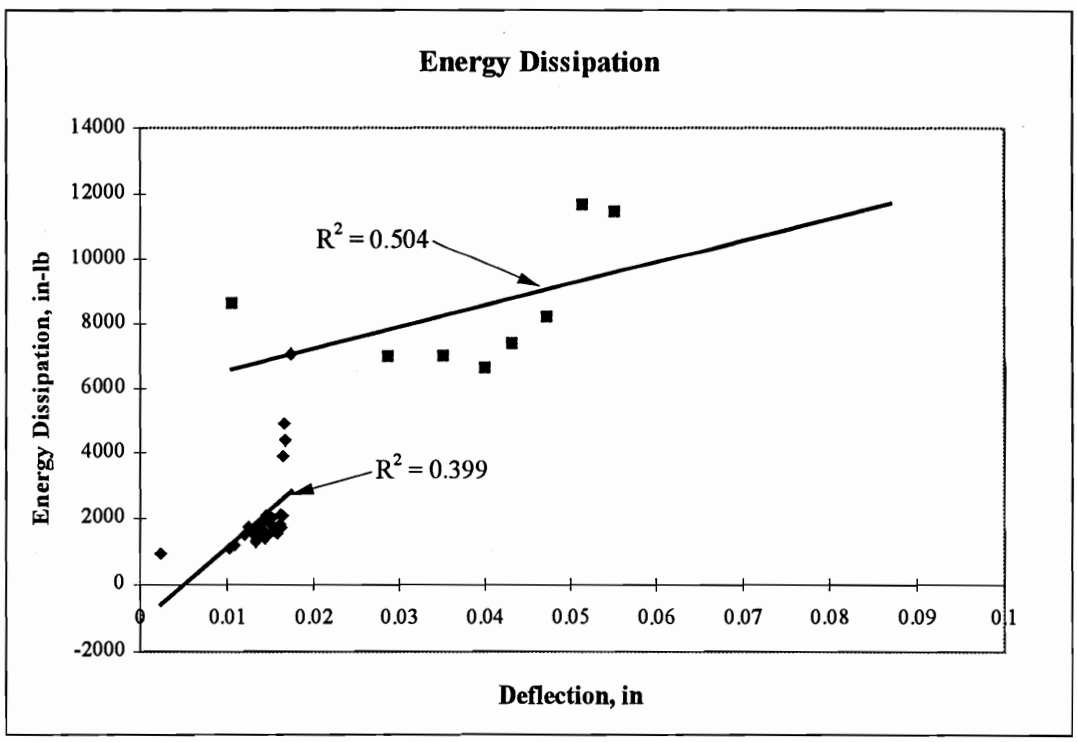

Figure 4- 41. Energy Dissipation During a Typical CH18 Test (test CH18-2).

4.2.3. Discussion of Heel Joint Cyclic Testing Results

The results from the heel joint tests indicate that C_D=1.6 is adequate for the design of these joints. The most conservative test of C_D=1.6 (CH162) does not experience any strength degradation. None of the testing regimes showed significant strength degradation (all p-values > 0.05) (Figure 4-42).

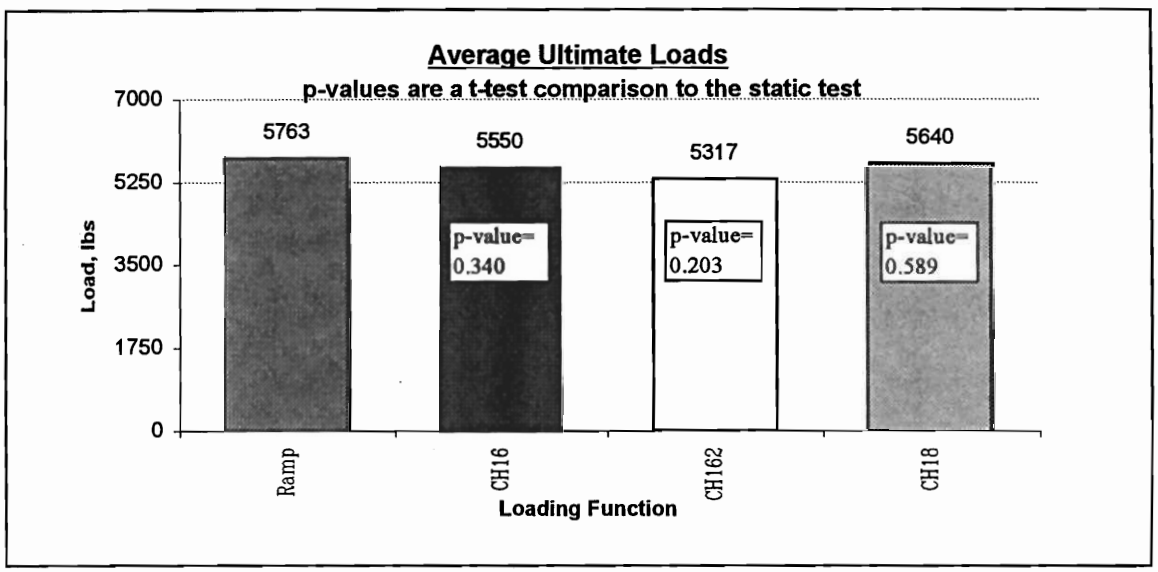

Figure 4- 42. Ultimate Loads for Heel Joints.

The stiffness degradation was not consistent between testing regimes. The p-values for stiffness degradations are given in Table 4-7. CH16 showed significant stiffness degradation (p-value = 0.0008 for CH16/Static comparison), but CH162 and CH18 did not show any degradation when compared to CH16 (p-values = 0.8805 and 0.8137, respectively). CH16 and CH162 did show a greater stiffness decrease when compared to the static case (P-values = 0.0089 and 0.0006 respectively). These results are inconsistent but the isolated cases of degradation (CH16, CH162) suggest slight

degradation in the stiffness does occur (See Table 4-7). In order to adequately investigate the stiffness properties of MPC heel joints, more detailed tests need to be performed that include more variations of the load levels done (such as CH132 and CH6).

Table 4- 7. Stiffness P-Values for Heel Joints.

	Compared to Static	*Compared to CH16*
CH16	0.0008	NA
CH162	0.0089	0.8805
CH18	0.0006	0.8137

On the other hand, conclusions can be made regarding the cyclic stiffness results. In all the load cases, stiffness decreased as the cycles progressed. There was a 52% decrease in stiffness for CH16. The percent decrease was determined in the same manner as for the tension-splice joints. The percent decrease in stiffness was taken as the percent change between the Dead Load Stiffness and the Design Load Stiffness. CH162 cyclic stiffness decreased by 54.8% and CH18 decreased by 60.4%. A majority of the stiffness decrease occurred during the transitions between the cycles. This was determined by looking at the final stiffness of one loading stage compared to the initial stiffness of the next loading stage. The decrease in stiffness for each of these load case was relatively consistent between one another.

Based on the percent increase in energy dissipation, it seems that the energy dissipation of the joint increased dramatically during the tests. Most of the increase occurred during the first stage for each test where there were a greater number of cycles at a lower magnitude. The stages that had higher magnitudes and fewer cycles did not dissipate as much energy. Therefore, energy dissipation seems to be related to the number of cycles rather than magnitudes.

5. Conclusions and Recommendations

5.1. Duration of Load Factor For Metal-Plate-Connected Truss Joints

The objective of this study was to evaluate the duration of load factor of 1.6 for metal-plate-connected truss joints by subjecting tension-splice joints and heel joints to a cyclic loading that has been proposed to simulate seismic events. To do this, this study investigated strength and stiffness degradation of the joint from this cyclic loading. Seventy tension-splice joints and forty heel joints were tested under several cyclic loading regimes of varying magnitude and number of cycles. The results were analyzed using t-test and regression comparisons of the strength and stiffness degradation trends.

The duration of load results from the tension-splice joints and heel joints suggest consistency with the current NDS code use of C_D=1.6. The most conservative test regime, C162 caused strength degradation. For C162, it appeared that most of the degradation occurred during the last stage (2.0 times the design load). Because most of the degradation occurs during the final stage of the loading (regardless of the magnitude of the load used in the second stage), the use of C_D=1.6 seems appropriate for tension-splice joints.

The results for the heel joints support the premise that C_D=1.6. None of the testing cases showed any strength degradation. This would suggest that C_D=1.6 is adequate considering CH16 and CH162. The insignificant amount of strength degradation observed during CH162 would suggest that a higher C_D may be acceptable, but the limited heel joint tests that were done do not indicate what that value should be.

There was significant stiffness degradation for both the tension-splice joints and the heel joints. Although no strength degradation was observed, this would suggest that structural damage does occur in the form of stiffness degradation. Stiffness degradation increased with the severity of the test.

The energy dissipation observed in both the tension-splice joints and heel joints increases as the testing progresses. The energy dissipation is a force travelling over a specific distance. An increase in displacement would increase the energy dissipation of the joint as long as the joint had the strength to withstand the loading.

5.2. Recommendations for Further Study

There are several recommendations for further study. The most important would be to investigate other methods to determine of duration of load effects. The method used in this research approximated the loading on a structure during its lifetime, but there are no standards or other methods to gauge this approximate method. Other possible methods may be based on a more accurate approximation of the loading during the life of a structure or be based on an actual record of testing over a structure's lifetime. This would lead to a more accurate determination of the duration of load factor. The second would be to investigate the influence of over-pressing and joint alignment on joint performance. The comparison of results from this research with Kent (1995) suggests that variations exist due to differences in the manufacturing of these joints that can cause strength reductions. A study of this area could lead to ways of improving the manufacturing process for MPC joints. Third, a study looking specifically at the influence of and failure mechanisms due to different rates of loading on the strength of MPC joints. By varying the loading rates, the impact of the higher frequencies (common in seismic events) could be more closely observed and evaluated.

Bibliography

American Forest & Paper Association. 1991. National Design Specification for Wood Construction. Washington, D.C.

American Forest & Paper Association. 1993. Commentary on the 1991 National Design Specification for Wood Construction. Washington, D.C.

American Society for Testing and Materials. 1994. Standard methods of testing mechanical fasteners in wood. ASTM D 1761-88, ASTM D2395-93, ASTM D4442-92, & ASTM D2915, Annual Book of ASTM Standards. ASTM, West Conshohocken, Pa. pg. 280-281.

American Society of Civil Engineers. 1961. Manuals and Reports on Engineering Practice. American Society of Civil Engineers. New York, NY.

American Society of Civil Engineers. 1995. Minimum Design Loads For Buildings and Other Structures, ASCE 7-95. American Society of Civil Engineers. New York, NY.

Arbek, T. 1979. " The Effect of Time on the Strength of Truss Plate Joints." Bachelor of Science of Forestry Thesis. Department of Civil Engineering, Carleton University. Ottawa, Canada.

Barrett and R.O. Foschi. 1978. Duration of Load and Failure Probability of Wood. Part II: Constant, Ramp and Cyclic Loads. Canadian Journal of Civil Engineering 5(4):515-532.

Bodig, J. and B.J. Farquhar. 1988. Behavior of Mechanical Joints of Wood at Accelerated Strain Rates. Proceedings of the International Conference on Timber Engineering. 2:455-463.

Buchanan A.H. and J. Dean. 1994. Practical Design of Timber Structures To Resist Earthquakes. Proceedings from the Pacific Timber Engineering Conference, Gold Coast, Australia, pg. 813-822.

Ceccotti, A., A. Vignoli and S. Giordana. 1994. Seismic Tests of Full-Scale Timber Structures. Proceedings from the Pacific Timber Engineering Conference, Gold Coast, Australia. Vol. 1, pg. 232-240.

Cramer, S.M., D. Shrestha and W.B. Fohrell. 1990. Theoretical Considerations of Metal-Plate-Connected Wood-Splice Joints. Journal of Structural Engineering, ASCE, 116(12): 3458-3475

Dagher, H.J., V. Caccese, Y. Hsu, R. Wolfe and M. Ritter. 1991. Fatigue Strength of Metal Connector Plates. Technical Report, Department of Civil Engineering, University of Maine, Orono, Maine.

Davenport, A.G., D. Surry and T. Stathopoulos. 1977. Wind Loads on Low Rise Buildings, Final Report Phases I and II, BLWT-SS8-1977. University of Western Ontario, London, Ontario, Canada.

Davenport, A.G., D. Surry and T. Stathopoulos. 1978. Wind Loads on Low Rise Buildings, Final Report Phases IIII, BLWT-SS8-1978. University of Western Ontario, London, Ontario, Canada.

Deam, B. and A. King. 1994. The Seismic Behavior of Timber Structures. Proceedings from the Pacific Timber Engineering Conference, Gold Coast, Australia. Vol. 1, pg. 215-221.

Dinwoodie, J.M. 1975. Timber-A Review of the Structure-Mechanical Property Relationship. Journal of Microscopy. 104(1): 3-32.

Dolan, J.D. 1995a. Re: Personal E-mail. Dated Aug. 3, 1995. Jddolan@vt.edu. Virginia Polytechnic Institute and State University, Blacksburg, Virginia.

Dolan, J.D. 1995b. Re: Load Controlled Cyclic Testing. Personal E-mail. Dated Sept. 22, 1995. Jddolan@vt.edu. Virginia Polytechnic Institute and State University, Blacksburg, Virginia.

Dolan, J.D. 1994. Proposed Test Method for Dynamic Properties of Connections Assembled With Mechanical Fasteners. ASTM Journal of Testing and Evaluation. 22(6): 542-547.

Dolan, J.D. 1989. The Dynamic Response of Timber Shear Walls, Ph.D. Dissertation, Department of Civil Engineering, University of British Columbia, Canada

Dolan, J.D. and T.E. McLain. 1995. Proposed Test Method For Dynamic Properties of Connections Assembled With Mechanical Fasteners. International Council For Building Research Studies and Documentation Working Commission W18-timber Structures. Meeting Twenty-six, Aug.

Dolan, J.D., S.T. Gutshall and T.E. McLain. 1995. Monotonic and Cyclic Tests to Determine Short-Term Duration of Load Performance of Nail and Bolt Connections, Volume I: Summary Report. Virginia Polytechnic Institute and State University Timber Engineering, Report No. TE-1994-001, Oct.

Emerson, R.N. and K.J. Fridley. 1996. Resistance of Metal-Plate-Connected Truss Joints to Dynamic Loading. Forest Products Journal. 46(5): 83-90.

Foliente, G.C. and E.G. Zacher. 1994. Performance Tests of Timber Structural Systems Under Seismic Loads. Proceedings of a Research Needs Workshop: Analysis, Design and Testing of Timber Structures Under Seismic Loads. (Editor: G.C. Foliente), University of California, Forest Products Laboratory, Richmond, CA.

Foschi, R.O. and F.Z. Yao. 1986. Another look at three duration of load models. Report by Working Commission W18-Timber Structures, International Council for Building Research Studies and Documentation, Florence, Italy.

Foschi, R.O. 1982. Load Duration Effects in Western Hemlock Lumber. Journal of Structural Engineering, ASCE. 108(7): 1494-1510.

Gerhards, C.C. 1979. Time-Related Effects of Loading on Wood Strength: A Linear Cumulative Damage Theory. Wood Science. 11(3): 139-144.

Gerhards, C.C and Link, C.L. 1987. Effect of Grade on Load Duration of Douglas-fir in Bending. Wood and Fiber Science. 19(2): 147-164.

Girhammar, U.A. and H. Anderson. 1988. Effect of Loading Rate on Nailed Timber Joint Capacity. Journal of Structural Engineering, ASCE. 114(11): 2439-2456.

Groom, Leslie, and A. Polensek. 1992. Nonlinear Modeling of Truss-Plate Joints. Journal of Structural Engineering, 118(9):2514-2531. Sept.

Gupta, R. 1994. Metal-Plate-Connected Tension Joints Under Different Loading Conditions. Wood and Fiber Science, 26(2):212-222.

Gupta, R., and K.G. Gebremedhin. 1992. Resistance distributions of a metal-plate-connected wood truss. Forest Products Journal. 42(7/8):11-16.

Gupta, R., K.G. Gebremedhin, M.D. Grigoriu. 1992. Characterizing the Strength of Wood Truss Joints. Transactions of the ASAE. 35(4):1286-1290.

Gupta, R., K.G. Gebremedhin. 1990. Destructive Testing of Metal-Plate-Connected Wood Truss Joints. Journal of Structural Engineering, ASCE. 116(7):1971-1982.

Gupta, R., K.G. Gebremedhin, J.R. Cooke. 1992. Analysis of Metal-Plate-Connected Wood Trusses With Semi-Rigid Joints. Transactions of the ASAE. 35,3:1011-1018.

Gutshall, S.T. 1994. Monotonic and Cyclic Short-Term Performance of Nailed and Bolted Timber Connections. MS Thesis. Virginia Polytechnic Institute and State University, Blacksburg, Virginia.

Hayashi, T. and H. Sasaki. 1979. Fatigue Properties of Nailed Wood-Metal Tension Joints. Presentation Summary at the 28th Annual Meeting of the Japan Wood Research Society, Japan: 253.

Hayashi, T., H. Sasaki and M. Masuda. 1980. Fatigue properties of wood butt joints with metal plate connectors. Forest Products Journal. 30(2):49-54.

Kent, S. 1995. Dynamic Behavior of Metal-Plate-Connected Wood Truss Joints. MS Thesis. Oregon State University. Corvallis, OR.

Leiva, L. 1994. Racking Behavior of Timber-Framed Shear Walls. Proceedings from the Pacific Timber Engineering Conference. Gold Coast, Australia. Vol. 1, pg. 168-176.

Liu, H. 1991. Wind Engineering: A Handbook for Structural Engineers. Prentice Hall, Englewood Cliffs, NJ.

Madsen, B. 1973. Duration of Load Tests for Dry Lumber in Bending. Forest Products Journal 23(2):33-40.

Madsen, B., K. Johns. 1982. Duration of Load Effects in Lumber. Part II, Experimental Data. Canadian Journal of Civil Engineering. 9:515-525.

Polensek, A., B.D. Schimel, 1991. Dynamic Properties of Light-Framed Wood Subsystems. Journal of Structural Engineering, ASCE. 117(4): 1079-1095.

Porter, M.L. 1987. Sequential phased displacement (SPD) procedure for TCCMAR testing. Proceedings of the Third Meeting of the Joint Technical Coordinating committee on Masonry Research, U.S.-Japan Coordinated Earthquake Research Program. Tomamu, Japan.

Reyer and Oji. 1991. Timber Structures-Joints Made With Mechanical Fasteners, A Proposed Test Procedure. Presentation at the Meeting of the RILEM TC 109 TSA Meeting in Watford, England.

Rosowsky, D. 1992. A Static-Fatigue Damage Accumulation Model For Wood Connections Subject to Cyclic Loads. Structural Engineering Report, CE-STR 92-9. Purdue University. West Lafayette, Ind.

Rosowsky, D., K.J. Fridley. 1992. Stochastic Damage Accumulation and Reliability of Wood Members. Wood and Fiber Science. 24(4):401-412.

Rosowsky, D., K.J. Fridley. 1995. Directions For Duration of Load Research. Forest Products Journal. 45(3):85-88.

Sletteland, N.T., G.L. Pratt, R.T. Schuler. 1977. Fatigue Life of Metal Connector Plates. American Society of Agricultural Engineers. June 26-29. Paper No. 77-4037.

Soltis, L.A., P. Mtgenga. 1985. Strength of Nailed Wood Joints Subjected to Dynamic Load. Forest Products Journal. 35(11/12):14-18.

Tokuda, M., M. Takeshita, H. Sugiyama. 1977. The Behaviors of Metal Plate Connector Joints Subjected to Repetitive Tension Force. Journal of the Japan Wood Research Society. 25(6):408-413.

Truss Plate Institute. 1985. Design Specification for Metal Plate Connected Wood Trusses. TPI:85. Madison, WI.

Uniform Building Code (UBC), 1985/1994. International Conference Building Officials, Whittier,CA.

USDA. 1987. Forest Products Laboratory Agricultural Handbook 72, Wood Handbook: Wood as an Engineering Material. Washington, D.C.: U.S. Department of Agriculture.

Wolfe, M. Hall, D. Lyles. 1991. Test Apparatus for Simulation Interactive Loads on Metal Plate Wood Connections. Journal of Testing and Evaluation, JTEVA, 19:421-428.

Wood, L.W. 1951. Relation of strength of wood to duration of load. Report No. 1916. Madison, WI: U.S. Department of Agriculture, Forest Service, Forest Products Laboratory, revised 1960.

Workbench 2.0. 1991. Strawberry Tree Incorporated.

Appendices

Appendix A. Preliminary Tension Splice Joint Tests.

Testing Procedures and Inaccuracies in C132 and C142.

The inaccuracies in C132 and C142 were due to improper calibration of the hydraulic control system before and during the tests. Following the tests, it was apparent that the load experienced by the joint did not reach the total compressive load intended. It is possible that the damage done to the joint was lower than it would have been. For this reason, a second set of C132 was done with corrected calibration.

The original C132 test was intended to investigate the conservative use of a duration of load factor of 1.33 in the same manner that C162 tests the conservative use of 1.6 as the duration of load factor. The C132 test regime applies a dead load of 900 lbs. at a rate of 780 lbs./min. before beginning the cyclic portion of the test. After the dead load is reached, a 1 Hz cyclic load of 1.0 times the design load is applied for 30 seconds, 1.33 times the design load is applied at 1 Hz for 15 seconds, and 2.0 times the design load at 1 Hz for 8 seconds. This test simulates 4 minor events, 2 design events (at NDS/UBC design level) and 1 major event. If the joint survived the test, it was ramped to failure at a rate of 780 lbs./min. This loading function is shown in Figure A-1. The C142 test was intended to investigate the conservative use of a duration of load factor of 1.4. The previous test (original C132) indicated that there was no degradation (in contrast to the second C132). The purpose of this test was to investigate a duration of load factor between 1.33 and 1.6 (1.4). The C142 load regime applies a dead load of 900 lbs. at a rate of 780 lbs./min. before beginning the cyclic portion of the test. After the dead load is reached, a 1 Hz cyclic load

of 1.0 times the design load is applied for 30 seconds, 1.4 times the design load is applied at 1 Hz for 15 seconds, and finally 2.0 times the design load is applied at 1 Hz for 8 seconds. This test simulates 3 minor events, 2 design events (based on old NDS and current UBC (AFPA 1991 and UBC 1985) duration of load value of 1.33), and 1 major event. If the joint survived the test, it was ramped to failure at a rate of 780 lbs./min. This loading function is shown in Figure A-2.

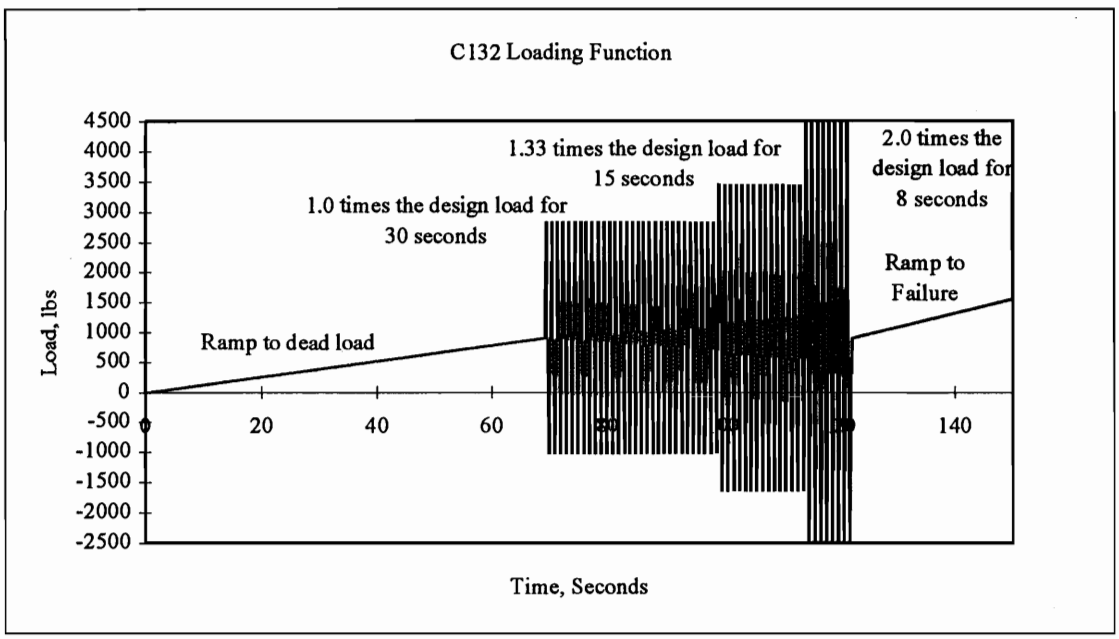

Figure A- 1. C132 Loading Function.

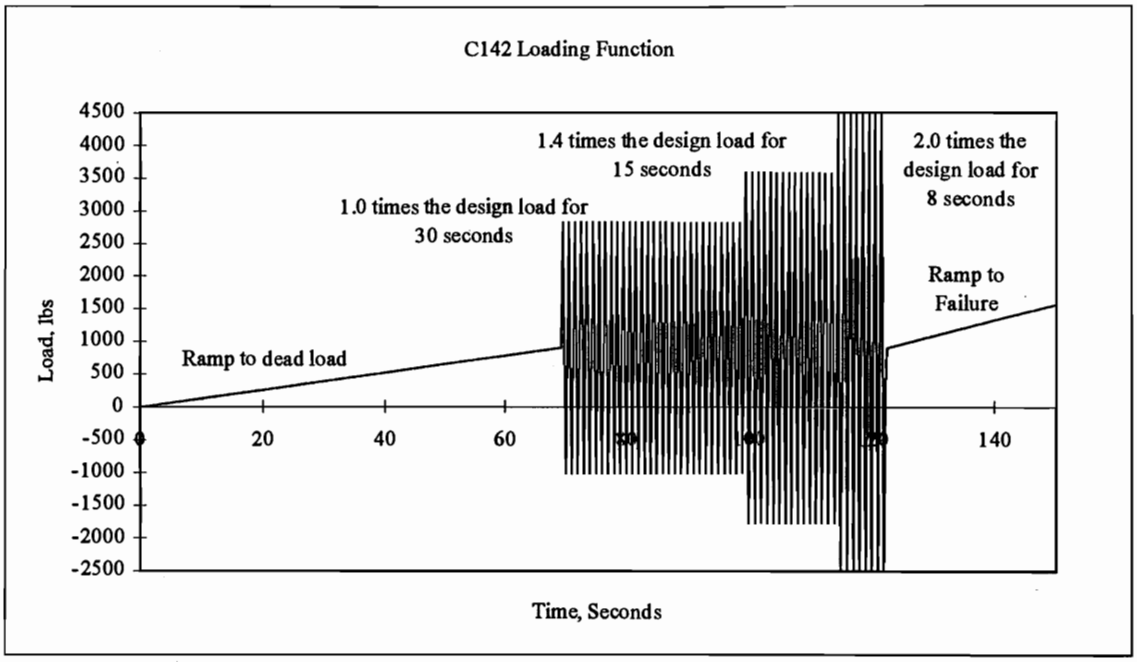

Figure A- 2. C142 Loading Function.

Duration of Load Results

Duration of Load Results (C132)

A total of ten tension splice joints were tested under the original C132 loading function. The average ultimate strength was 5489 lbs. with a coefficient of variation of 24%. Seven of these joints survived the cyclic tests and were ramped to failure following the cycles. Three of the joints failed during the cycles. All of these failed during the third step of the loading function. One of these joints was also eliminated from the study because of poor deflection data. The poor deflection data was caused by an initial offset of the LVDT used for measuring deflections. The offset was caused by voltage irregularities.
The average Dead Load Stiffness was 3.15×10^5 lb./in. The average Design Load Stiffness was 1.39×10^5 lb./in. The average ultimate displacement of the joint at failure was 0.064 inches. The average cyclic offset that occurred during

the tests was 0.016 inches. There was a 71% decrease in stiffness from the Dead Load Stiffness to the Design Load Stiffness.
Other material properties were also determined. The average specific gravity was 0.49. The average Modulus of Elasticity was 2.10 lb/in^2.

Duration of Load Results (C142)

A total of ten C142 tension splice joints were tested under the C142 loading function. The average ultimate strength was 4792 lbs. with a coefficient of variation of 23%. Five of these joints survived the cyclic tests and were ramped to failure following the cycles. Four of the joints failed during the cycles. All of these failed during the third step of the loading function. One joint was eliminated from the study because of poor load cell data. The poor load cell data was caused by an initial offset in the load cell calibration.
The average Dead Load Stiffness was 2.92 x 10^5 lb./in. The Design Load Stiffness was 1.15 x 10^5 lb./in. The average ultimate displacement of the joint at failure was 0.051 inches. The average cyclic offset that occurred during the tests was 0.025 inches. There was an 80% decrease in stiffness from the Dead Load Stiffness to the Design Load Stiffness.

Other material properties were also determined. The average specific gravity was 0.49. The average Modulus of Elasticity was 2.10 lb/in^2.

Appendix B. Tension-Splice Joint Data

Definitions of Column Headings

No.: The serial number. The number of samples used in averaging is equal to the number of values listed, unless there is an asterisk next to the number. Asterisked values were dropped from analysis due to problems with data acquisition.

Test Number: The name of the raw data file containing the data.

Load Case: The load case refers to the loading regime for the particular data set. This column also includes the date that the testing was done.

Joint ID: Joint ID refers to which board the joint came from (each board produced approximately 3 joints). This value was used to track the modulus of elasticity for the board and therefore the joint.

Ultimate Load: The load at which the particular joint failed. If the joint did not survive the cycles, the ultimate load is the highest load experienced by the joint during the loading cycles. If the joint survived the cycles it was ramped to failure.

Modulus of Elasticity: The modulus of elasticity in psi * 106. This was recorded for each 10-foot board before the joints were cut. This was done with an E-computer (Metriguard, Model 390).

Moisture Content: Moisture content was determined by taking the wet weight minus the dry weight divided by the dry weight. This was done using ASTM D2395-93 (Method A, Volume by Measurement) and ASTM D4442-92 (Method A, Oven-Drying Primary).

Specific Gravity: The specific gravity was determined on a dry basis (dry weight divided by the volume after drying). This was done using ASTM D2395-93 (Method A, Volume by Measurement) and ASTM D4442-92 (Method A, Oven-Drying Primary).

Ring Count: The ring count refers to the number of rings per inch.

Percent Latewood: The percent latewood was a visual approximation of the percent latewood in a typical growth ring.

Grain Orientation: The grain orientation was the angle of the line tangent to a growth ring near the center of the 2 x 4 sample measured from the vertical axis.

Ultimate Displacement: The ultimate displacement is the longitudinal displacement when the joint failed.

Cyclic Offset: Cyclic offset refers to the amount of displacement that occurred due to the cyclic portion of the test. The offset was taken as the

difference between the displacement before the cycles began and the displacement after the cycles was complete.

Dead Load Stiffness: Dead load stiffness refers to the stiffness determined by taking the slope of the secant line between zero load and the dead load (900 lbs. for tension splice joints and 1550 lbs. for heel joints) on the load/deflection curve.

Design Load Stiffness: Design load stiffness refers to the stiffness determined by taking the slope of the secant line between the point when the cycles stopped and the design load (1920 lbs. for both the tension splice joints and the heel joints) on the load-deflection curve.

Dead/Design Decrease: The percent decrease in stiffness between the measured dead load stiffness and the design stiffness.

" FDC:" This refers to failed during cycles and therefore data is not available.

Cond.: Cond. or " condition" refers to the visual observation of the plate condition before the test. This is a qualitative observation as to the embed most of the plate into the wood. " VG" signifies very good. " O.K." signifies fair condition. " N/A" signifies that an observation was not taken. " Q" signifies that the joint was in question.

Stiffness at Start/End Stage X: The cyclic stiffness determined from the second hysteresis curve at the start of the stage and the cyclic stiffness determined from the second to the last hysteresis curve at the end of each stage.

Energy Dissipation at Start/End Stage X: The energy dissipation from the second hysteresis curve at the start of the stage and the energy dissipation determined from the second to the last hysteresis curve at the end of each stage.

Slope of Regression: The slope of regression is the slope of the regression line taken from the stiffness or energy dissipation data points for each cycle. This value is calculated for each stage of a particular loading function.

R-squared value for each stage: It is a measure of the statistical linearity of the stiffness trend and/or energy dissipation change during each stage of a loading function.

Table B-1 a. Tension-Splice Joint Characteristics.

No.	Test Number	Load Case	Joint ID	Ultimate Load lbs	Modulus of Elasticity psi * 10^6	Moisture Content %	Specific Gravity Dry Based	Ring Count per Inch	Percent Latewood %	Grain Orientation Degrees
1	TS-1	Static	T6	6781	2.08	12%	0.49	25.0	50%	14
2	TS-2	3/11/96	T22	5758	1.66	13%	0.41	7.0	25%	0
3	TS-3		T26	6101	2.21	14%	0.52	15.0	50%	11
4	TS-5		T17	5601	2.5	13%	0.51	21.0	50%	9
5	TS-6		T2	5307	2.12	13%	0.56	11.0	33%	17
6	TS-7		T3	4295	2.53	13%	0.51	9.0	33%	26
7	TS-8		T27	6285	2.3	12%	0.51	5.0	33%	0
8	TS-9		T14	5458	1.75	12%	0.40	5.0	25%	0
9	TS-10		T31	5775	1.84	12%	0.44	18.0	25%	9
10	TS-11		T26	6240	2.21	14%	0.52	12.0	50%	17
	Average			5760	2.12	13%	0.49	12.8	37%	10.3
Average Design				1920						
	CV %			12%	14%	6%	10%	53%	30%	84%
1	C1-1	C1	T5	7150	1.91	12%	0.59	6.0	40%	56
2	C1-2	3/14/96	T13	6130	1.82	12%	0.51	6.0	50%	33
3	C1-3		T30	6213	1.84	12%	0.42	5.0	20%	0
4	C1-4		T31	6026	1.84	11%	0.44	20.0	50%	10
5	C1-5		T3	2859	2.53	13%	0.51	9.0	50%	29
6	C1-6		T15	7383	1.97	13%	0.55	13.0	33%	10
7	C1-7		T32	4444	1.77	13%	0.41	5.0	25%	17
8	C1-8		T34	4934	2.05	13%	0.44	10.0	40%	12
9	C1-9		T14	5136	1.75	12%	0.41	5.0	33%	0
10	C1-10		T4	6117	1.87	12%	0.46	10.0	33%	0
	Average			5639	1.94	12%	0.47	8.9	37%	16.7
	CV %			24%	12%	5%	13%	54%	28%	108%
1	C6-1	C6	T7	7413	1.74	13%	0.54	13.0	50%	7
2	C6-2	3/13/96	T27	5722	2.3	12%	0.58	12.0	40%	9
3	C6-3		T36	4059	2.17	13%	0.48	7.0	40%	0
4	C6-4		T25	3989	2.24	13%	0.50	7.0	30%	0
5	C6-5		T15	7580	1.97	13%	0.53	20.0	40%	15
6	C6-6		T34	4208	2.05	13%	0.47	10.0	25%	23
7	C6-7		T30	6785	1.84	12%	0.46	5.5	30%	0
8	C6-8		T34	5311	2.05	12%	0.45	7.5	25%	12
9	C6-9		T28	7638	2.15	12%	0.49	7.0	50%	10
10	C6-10		T35	3538	2.27	14%	0.58	12.0	40%	14
	Average			5624	2.08	13%	0.51	10.1	37%	9.0
	CV %			29%	9%	6%	9%	43%	25%	84%
1	C16-1	C16	T31	4014	1.84	11%	0.44	22.0	50%	14
2	C16-2	3/15/96	T24	7503	2.4	13%	0.51	13.0	40%	10
3	C16-3		T16	6830	1.85	13%	0.46	5.0	33%	14
4	C16-4		T19	6464	1.82	12%	0.45	5.0	33%	0
5	C16-5		T10	6925	2.17	13%	0.57	15.0	50%	10
6	C16-6		T28	6736	2.15	12%	0.48	6.0	45%	0
7	C16-7		T18	5987	1.71	12%	0.41	5.0	25%	0
8	C16-8		T7	6466	1.74	13%	0.46	13.0	20%	16
9	C16-9		T18	4838	1.71	12%	0.39	5.0	25%	0
10	C16-10		T8	5344	1.73	12%	0.46	6.0	40%	0
	Average			6111	1.91	12%	0.46	9.5	36%	6.4
	CV %			18%	13%	5%	11%	62%	30%	109%

Table B-1 b. Tension-Splice Joint Characteristics.

No.	Test Number	Load Type	Joint ID	Ultimate Load	Modulus of Elasticity	Moisture Content	Specific Gravity	Ring Count	Percent Latewood	Grain Orientation
				lbs	psi	%	Dry Based	per Inch	%	Degrees
1	C132-1	C132	T40	---	---	13%	0.57	25.0	60%	32
2	C132-2	3/28/96	T41	4379	1.8	12%	0.46	7.0	40%	14
3	C132-3	Set 2	T29	4773	1.73	13%	0.44	13.0	40%	10
4	C132-4		T4	4791	1.87	12%	0.45	11.0	40%	0
5	C132-5		T12	4607	2.51	13%	0.53	28.0	33%	31
6	C132-6		T37	4330	3.24	12%	0.46	9.5	40%	25
7	C132-7		T23	4712	2.24	13%	0.46	7.5	33%	2
8	C132-8		T2	4338	2.12	13%	0.52	10.0	50%	7
9	C132-9		T36	4548	2.17	13%	0.48	7.5	25%	0
	Average			4499	2.04	12%	0.48	12.4	38%	12
	CV %			6%	14%	6%	11%	63%	30%	107%
1	C8-1	C8	T40	4159	2.44	12%	0.60	19.0	50%	35
2	C8-2	3/29/96	T25	4530	2.24	13%	0.50	6.0	50%	20
3	C8-3		T38	4187	2.35	12%	0.46	8.0	33%	43
4	C8-4		T39	7909	2.87	14%	0.69	20.0	55%	5
5	C8-5		T9	4430	1.85	13%	0.44	6.0	50%	2
6	C8-6		T34	4536	2.05	12%	0.45	9.0	25%	32
7	C8-7		T26	4458	2.21	14%	0.53	12.0	33%	19
8	C8-8		T37	4526	2.24	11%	0.46	10.0	40%	5
9	C8-9		T38	4412	2.35	12%	0.45	7.0	40%	42
	Average			4794	2.29	13%	0.51	10.8	42%	23
	CV %			25%	12%	7%	17%	49%	24%	72%
1	C162-1	C162	T32	3985	1.77	12%	0.43	5.0	25%	11
2	C162-2	3/14/96	T14	4756	1.75	11%	0.40	6.0	33%	19
3	C162-3		T23	4742	2.24	12%	0.45	7.0	25%	7
4	C162-4		T16*	3981	1.85	13%	0.51	6.0	45%	13
5	C162-5		T30	5907	1.84	11%	0.44	5.0	15%	0
6	C162-6		T35	4703	2.27	14%	0.58	12.0	50%	17
7	C162-7		T11	4799	2.33	13%	0.51	10.0	40%	33
8	C162-8		T24*	7405*		13%	0.53	13.0	15%	0
9	C162-9		T13	6423	1.82	13%	0.55	5.5	70%	23
10	C162-10		T19	5020	1.82	12%	0.45	7.0	33%	0
	Average			4924	1.97	12%	0.48	7.7	35%	12.3
	CV %			16%	12%	8%	12%	38%	48%	90%

Table B-2 a. Tension-Splice Joint Stiffness Summary.

No.	Test Number	Load Type	Joint ID	Ultimate Load	Ult. Disp.	Cyclic Offset	Dead Load Stiffness	Design Load Stiffness	Dead/Design Decrease	Cond.	Survival
				lbs	in.	in.	10^5 lb/in	10^5 lb/in	Percent		
1	TS-1	Static	T6	6781	0.086	N/A	3.10	2.18	30%		
2	TS-2	3/11/96	T22	5758	0.064	N/A	2.77	1.74	37%		
3	TS-3		T26	6101	0.078	N/A	3.76	1.96	48%		
4	TS-5		T17	5601	0.085	N/A	3.22	2.40	25%		
5	TS-6		T2	5307	0.064	N/A	2.91	1.96	33%		
6	TS-7		T3	4295	0.057	N/A	2.05	1.40	32%		
7	TS-8		T27	6285	0.053	N/A	3.42	2.53	26%		
8	TS-9		T14	5458	0.081	N/A	2.81	1.85	34%		
9	TS-10		T31	5775	0.077	N/A	2.98	2.30	23%		
10	TS-11		T26	6240	0.097	N/A	3.54	2.32	34%		
	Average			5760	0.074		3.06	2.06	32%		
	Average Design			1920.0							
	CV %			12%	19%		16%	17%	22%		
1	C1-1	C1	T5	7150	0.088	0.005	3.83	2.99	22%	VG	Y
2	C1-2	3/14/96	T13	6130	0.072	0.004	2.73	2.38	13%	OK	Y
3	C1-3		T30	6213	0.091	0.009	2.77	2.28	18%	OK	Y
4	C1-4		T31	6026	0.053	0.003	4.64	3.68	21%	VG	Y
5	C1-5		T3	2859	0.004		2.12	FDC	100%	Q	N
6	C1-6		T15	7383	0.081	0.003	4.01	3.61	10%	VG	Y
7	C1-7		T32	4444	0.070	0.010	3.71	1.58	57%	VG	Y
8	C1-8		T34	4934	.009*	.001*	33.22*	15.27*		OK	Y
9	C1-9		T14	5136	0.078	0.013	2.04	1.85	9%	OK	Y
10	C1-10		T4	6117	0.064	0.007	3.15	2.36	25%	OK	Y
	Average			5639	0.067	0.006	3.22	2.59	31%		
	CV %			24%	39%	58%	28%	30%	98%		
1	C6-1	C6	T7	7413	0.107	0.007	3.03	1.72	43%	VG	Y
2	C6-2	3/13/96	T27	5722	0.057	0.015	3.28	1.74	47%	OK	Y
3	C6-3		T36	4059	0.001		5.85	FDC	100%	N/A	N
4	C6-4		T25	3989	0.002		4.35	FDC	100%	Q	N
5	C6-5		T15	7580	0.108	0.006	3.99	2.27	43%	VG	Y
6	C6-6		T34	4208	0.084	0.039	2.81	0.98	65%	Q	Y
7	C6-7		T30	6785	0.090	0.009	2.96	1.62	45%	OK	Y
8	C6-8		T34	5311	0.076	0.019	2.57	1.51	41%	OK	Y
9	C6-9		T28	7638	0.100	0.005	3.52	2.09	41%	VG	Y
10	C6-10		T35	3538	0.146	0.018	4.23	1.31	69%	Q	Y
	Average			5624	0.077	0.015	3.66	1.66	59%		
	CV %			29%	60%	76%	27%	25%	40%		
1	C16-1	C16	T31	4014	0.003		2.61		100%	VG	N
2	C16-2	3/15/96	T24	7503	0.110	0.006	3.55	2.47	30%	OK	Y
3	C16-3		T16	6830	0.068	0.007	4.19	2.98	29%	OK	Y
4	C16-4		T19	6464	0.078	0.011	2.34	1.77	24%	OK	Y
5	C16-5		T10	6925	0.106	0.010	3.28	1.92	41%	OK	Y
6	C16-6		T28	6736	0.083	0.009	2.95	1.74	41%	OK	Y
7	C16-7		T18	5987	0.097	0.017	3.16	1.55	51%	OK	Y
8	C16-8		T7	6466	0.073	0.009	4.27	2.12	50%	OK	Y
9	C16-9		T18	4838	0.081	0.023	2.97	1.21	59%	OK	Y
10	C16-10		T8	5344	0.095	0.024	1.48	1.50	-1%	OK	Y
	Average			6111	0.079	0.013	3.08	1.92	43%		
	CV %			18%	38%	53%	27%	28%	62%		

Table B-2 b. Tension-Splice Joint Stiffness Summary.

No.	Test Number	Load Case	Joint ID	Ultimate Load	Ult. Disp.	Cyclic Offset	Dead Load Stiffness	Design Load Stiffness	Dead/Design Decrease	Cond.	Survival
				lbs	in.	in.	10^5 lb/in	10^5 lb/in	Percent		
1	C132-1	C1322	T40		0.006		1.57	FDC	100%	Q	N
2	C132-2	3/28/96	T41	4379	0.085	0.025	3.20	0.68	79%	OK	Y
3	C132-3	Set 2	T29	4773	0.004		2.57	FDC	100%	Q	N
4	C132-4		T4	4791	0.074	0.020	2.78	1.13	59%	V	Y
5	C132-5		T12	4607	0.003		2.51	FDC	100%	Q	N
6	C132-6		T37	4330	0.076	0.031	2.46	0.95	61%	OK	Y
7	C132-7		T23	4712	.0003*		21.82*	BDD		OK	N
8	C132-8		T2	4338	0.062	0.002	4.05	0.92	77%	OK	Y
9	C132-9		T36	4548	0.003		2.52	FDC	100%	Q	N
	Average			4499	0.035	0.017	2.57	0.98	75%		
	CV %			6%	1.077	0.736	30%	21%	44%		
1	C8-1	C8	T40	4159	0.003		2.95	FDC	100%	K	N
2	C8-2	3/29/96	T25	4530	0.003		3.79	FDC	100%	OK	N
3	C8-3		T38	4187	0.004		2.4	FDC	100%	Q	N
4	C8-4		T39	7909	0.129	0.007	2.99	2.11	29%	VG	Y
5	C8-5		T9	4430	0.004		2.19	FDC	100%	OK	N
6	C8-6		T34	4536	0.004		1.64	FDC	100%	OK	N
7	C8-7		T26	4458	0.003		2.55	FDC	100%	OK	N
8	C8-8		T37	4526	0.003		2.48	FDC	100%	OK	N
9	C8-9		T38	4412	0.003		3.42	FDC	100%	OK	N
	Average			4794	0.017	0.007	2.71	2.11	92%		
	CV %			25%	2.460		24%		26%		
1	C162-1	C162	T32	3985	0.003		2.79	FDC	100%	Q	N
2	C162-2	3/14/96	T14	4756	0.003		3.27	FDC	100%	OK	N
3	C162-3		T23	4742	.00023*		33.14*	BDD		VG	N
4	C162-4		T16*	3981	0.004		2.63	FDC	100%	Q	N
5	C162-5		T30	5907	0.063	0.015	2.76	1.60	42%	VG	Y
6	C162-6		T35	4703	0.068	0.021	3.09	1.16	62%	Q	Y
7	C162-7		T11	4799	0.003		3.26	FDC	100%	OK	N
8	C162-8		T24*	7405*	0.111	0.016	*			VG	Y-Throw
9	C162-9		T13	6423	0.104	0.014	3.04	1.36	55%	OK	Y
10	C162-10		T19	5020	0.077	0.032	2.30	1.09	53%	VG	Y
	Average			4924	0.048	0.019	2.89	1.30	77%		
	CV %			16%	95%	39%	12%	18%	34%		

Table B-3 a. Tension-Splice Joint Hysteresis Summary.

No.	Test Number	Stiffness at Start of Stage 1 10^5 lb/in	Stiffness at End of Stage 1 10^5 lb/in	Stiffness at Start of Stage 2 10^5 lb/in	Stiffness at End of Stage 2 10^5 lb/in	Stiffness at Start of Stage 3 10^5 lb/in	Stiffness at End of Stage 3 10^5 lb/in	Slope of Regression Stage 1	Slope of Regression Stage 2	Slope of Regression Stage 3	R Squared Value Stage 1	R Squared Value Stage 2	R Squared Value Stage 3
1	C1-1	4.02	3.70					-0.009			0.368		
2	C1-2	3.22	3.07					-0.012			0.565		
3	C1-3	2.92	2.40					-0.019			0.768		
4	C1-4	3.64	2.91					-0.025			0.839		
5	C1-5	1.89	1.82					-0.012			0.696		
6	C1-6	5.39	4.77					-0.022			0.561		
7	C1-7	3.14	1.69					-0.046			0.924		
8	C1-8	2.74	1.51					-0.040			0.914		
9	C1-9	2.37	2.26					-0.007			0.574		
10	C1-10	3.19	2.85					-0.011			0.591		
	Average	3.25	2.70					-0.020			0.680		
	CV %	30%	37%					-66%			26%		
1	C6-1	3.02	2.00					-0.037			0.947		
2	C6-2	2.82	1.84					-0.032			0.923		
3	C6-3	2.34						-0.123			0.968		
4	C6-4	2.51						-0.076			0.971		
5	C6-5	4.32	2.88					-0.042			0.881		
6	C6-6	2.09	0.86					-0.040			0.933		
7	C6-7	3.33	2.07					-0.042			0.827		
8	C6-8	2.69	1.57					-0.037			0.929		
9	C6-9	4.18	2.75					-0.042			0.847		
10	C6-10	3.71	1.71					-0.063			0.932		
	Average	3.10	1.96					-0.053			0.916		
	CV %	25%	33%					-52%			5%		
1	C16-1	2.65	1.90	1.65				-0.022	-0.062		0.902	0.982	
2	C16-2	4.51	4.07	3.79	2.85			-0.021	-0.062		0.605	0.816	
3	C16-3	3.54	2.80	2.71	2.06			-0.024	-0.047		0.701	0.874	
4	C16-4	3.43	2.97	2.63	2.21			-0.020	-0.038		0.672	0.908	
5	C16-5	4.27	3.35	3.08	2.35			-0.019	-0.060		0.612	0.946	
6	C16-6	3.35	2.77	2.50	2.11			-0.021	-0.033		0.699	0.848	
7	C16-7	2.73	2.14	1.94	1.58			-0.019	-0.030		0.823	0.901	
8	C16-8	4.08	3.23	3.13	2.52			-0.026	-0.048		0.753	0.872	
9	C16-9	2.75	2.04	1.81	1.30			-0.027	-0.042		0.897	0.978	
10	C16-10	2.78	2.24	1.95	1.54			-0.015	-0.036		0.778	0.922	
	Average	3.41	2.75	2.52	2.06			-0.021	-0.046		0.744	0.905	
	CV %	20%	25%	27%	24%			-17%	-27%		14%	6%	

Table B-3 b. Tension-Splice Joint Hysteresis Summary.

No.	Test Number	Stiffness at Start of Stage 1 10^5 lb/in	Stiffness at End of Stage 1 10^5 lb/in	Stiffness at Start of Stage 2 10^5 lb/in	Stiffness at End of Stage 2 10^5 lb/in	Stiffness at Start of Stage 3 10^5 lb/in	Stiffness at End of Stage 3 10^5 lb/in	Slope of Regression Stage 1	Slope of Regression Stage 2	Slope of Regression Stage 3	R Squared Value Stage 1	R Squared Value Stage 2	R Squared Value Stage 3
1	C132-1	0.98						-0.143			0.985		
2	C132-2	3.15	2.28	2.30	1.48	1.38	0.99	-0.025	-0.072	-0.077	0.857	0.952	0.996
3	C132-3	2.31	1.50	1.57	1.35	1.18		-0.027	-0.020	-0.254	0.891	0.899	0.963
4	C132-4	2.68	2.15	2.10	1.96	1.58	1.35	-0.016	-0.018	-0.053	0.741	0.782	0.943
5	C132-5	2.26	1.73	1.54	1.23			-0.020	-0.025		0.872	0.904	
6	C132-6	2.81	2.26	2.20	1.78	1.53	1.19	-0.024	-0.025	-0.072	0.853	0.712	0.958
7	C132-7	2.26	2.08	1.83	1.61	1.23		-0.011	-0.024	-0.224	0.737	0.827	1.000
8	C132-8	3.73	3.06	2.91	2.46	2.01	1.55	-0.029	-0.039	-0.094	0.851	0.807	0.980
9	C132-9	2.59	1.90	1.79	1.32			-0.023	-0.037		0.915	0.924	
	Average	2.53	2.12	2.03	1.65	1.48	1.27	-0.035	-0.033	-0.129	0.856	0.851	0.973
	CV %	30%	22%	22%	25%	20%	19%	-115%	-54%	-67%	9%	10%	2%
1	C8-1	Failed during first cycle, no accurate data obtained.											
2	C8-2	2.64						-0.056			0.862		
3	C8-3	Failed during first cycle, no accurate data obtained.											
4	C8-4	3.79	2.95					-0.025			0.803		
5	C8-5	Data lost											
6	C8-6	1.53						-0.088			0.974		
7	C8-7	2.07						-0.145			0.988		
8	C8-8	2.33						-0.058			0.942		
9	C8-9	1.98						-0.191			0.973		
	Average	2.39	2.95					-0.094			0.923		
	CV %	33%						-67%			8%		
1	C162-1	2.95	1.85					-0.041			0.893		
2	C162-2	2.89	1.96	1.71	1.19	1.00		-0.026	-0.041		0.839	0.959	
3	C162-3	3.05	2.41	2.29	1.78	1.65		-0.020	-0.041	-0.127	0.813	0.906	0.966
4	C162-4	2.39	1.65	1.43				-0.024	-0.064		0.869	0.992	
5	C162-5	3.29	2.77	2.72	2.28	2.23	1.98	-0.018	-0.032	-0.059	0.726	0.845	0.811
6	C162-6	3.55	2.84	2.59	2.00	1.81	1.52	-0.023	-0.046	-0.052	0.813	0.939	0.898
7	C162-7	2.94	2.23	1.85	1.40	1.21		-0.021	-0.036	-0.089	0.835	0.918	0.999
8	C162-8	4.04	3.46	3.43	2.81	2.65	2.31	-0.011	-0.044	-0.055	0.339	0.776	0.796
9	C162-9	3.74	2.86	2.76	2.27	2.16	1.92	-0.023	-0.034	-0.044	0.706	0.763	0.833
10	C162-10	2.67	2.29	2.01	1.59	1.43	1.21	-0.013	-0.031	-0.044	0.806	0.894	0.923
	Average	3.15	2.43	2.31	1.92	1.77	1.79	-0.022	-0.041	-0.067	0.764	0.888	0.890
	CV %	16%	23%	27%	28%	32%	24%	-38%	-25%	-45%	21%	9%	9%

Table B-4 a. Tension-Splice Joint Energy Dissipation Summary.

No.	Test Number	Energy Dissipation Start of Stage 1	Energy Dissipation End of Stage 1	Energy Dissipation Start of Stage 2	Energy Dissipation End of Stage 2	Energy Dissipation Start of Stage 3	Energy Dissipation End of Stage 3	Slope of Regression Stage 1	Slope of Regression Stage 2	Slope of Regression Stage 3	R Squared Value Stage 1	R Squared Value Stage 2
1	C1-1	398	498					3.222			0.538	
2	C1-2	400	557					4.837			0.706	
3	C1-3	477	833					12.363			0.820	
4	C1-4	371	648					9.113			0.921	
5	C1-5	835	2662					40.421			0.780	
6	C1-6	291	362					2.691			0.543	
7	C1-7	458	954					18.102			0.907	
8	C1-8	496	1132					21.436			0.962	
9	C1-9	759	1026					9.515			0.334	
10	C1-10	497	611					4.102			0.406	
	Average	498	928					12.580			0.692	
	CV%	34%	71%					93%			32%	
1	C6-1	805	1518					24.206			0.876	
2	C6-2	1069	1780					20.887			0.643	
3	C6-3	1474						243.383			0.948	
4	C6-4	1315						138.413			0.952	
5	C6-5	696	1077					13.278			0.716	
6	C6-6	1415	3842					88.965			0.972	
7	C6-7	767	1587					25.705			0.796	
8	C6-8	1145	2258					40.999			0.838	
9	C6-9	605	1079					17.166			0.835	
10	C6-10	791	2170					48.693			0.981	
	Average	1008	1914					66.170			0.856	
	CV%	31%	47%					111%			13%	
1	C16-1	693	2055	2648				18.726	0.727		0.323	0.727
2	C16-2	298	385	870	1170			2.331	0.696		0.382	0.696
3	C16-3	383	575	1217	1426			7.667	0.536		0.851	0.536
4	C16-4	465	624	1338	1514			6.511	0.407		0.676	0.407
5	C16-5	318	458	1002	1357			5.031	0.913		0.835	0.913
6	C16-6	427	559	1168	1429			4.653	0.647		0.608	0.647
7	C16-7	516	806	1628	2166			10.777	0.949		0.795	0.949
8	C16-8	357	499	1089	1513			3.846	0.885		0.605	0.885
9	C16-9	524	884	1964	2768			11.916	0.918		0.844	0.918
10	C16-10	702	1066	2040	2755			12.719	0.936		0.849	0.936
	Average	468	791	1494	1789			8.418	0.761		0.677	0.761
	CV%	30%	62%	38%	34%			60%	25%		29%	25%

Table B-4 b. Tension-Splice Joint Energy Dissipation Summary.

No.	Test Num.	Energy Diss. Start of Stage 1	Energy Diss. End of Stage 1	Energy Diss. Start of Stage 2	Energy Diss. End of Stage 2	Energy Diss. Start of Stage 3	Energy Diss. End of Stage 3	Slope of Regression Stage 1	Slope of Regression Stage 2	Slope of Regression Stage 3	R Squared Value Stage 1	R Squared Value Stage 2	R Squared Value Stage 3
1	C132-1	1576						120.697			0.990		
2	C132-2	521	662	908	984	2966	4570	5.596	0.089	391.077	0.571	0.089	0.930
3	C132-3	665	999	1504	1822	4288		12.572	0.747		0.906	0.747	
4	C132-4	526	713	1056	1172	2735	3071	10.321	0.718	127.069	0.670	0.718	0.635
5	C132-5	706	1100	1761	1973			16.567	0.477		0.852	0.477	
6	C132-6	528	745	1210	1284	2893	4330	9.543	0.518	342.678	0.910	0.518	0.952
7	C132-7	590	931	1417	1987	3859		12.083	0.261		0.770	0.261	
8	C132-8	347	550	834	923	2411	2853	6.911	0.441	114.807	0.944	0.441	0.982
9	C132-9	588	921	1541	1873			9.609	0.509		0.783	0.509	
	Average	672	828	1279	1502	3192		22.655	0.470	243.908	0.822	0.470	0.875
	CV %	53%	23%	26%	30%	23%		163%	46%	59%	17%	46%	18%
1	C8-1	Failed during first cycle, no accurate data obtained.											
2	C8-2	1553						120.561			0.955		
3	C8-3	Failed during first cycle, no accurate data obtained.											
4	C8-4	994	1323					12.804			0.651		
5	C8-5	Data lost											
6	C8-6	2599						256.314			0.973		
7	C8-7	1876						223.223			0.842		
8	C8-8	1722						109.377			0.942		
9	C8-9	1942						337.249			0.853		
	Average	1781	1323					176.588			0.869		
	CV %	29%						66%			14%		
1	C162-1	521	1246					32.892			0.526		
2	C162-2	592	945	2069	3992			11.359	0.875		0.792	0.875	
3	C162-3	530	838	1682	2077	3303		11.462	0.922		0.822	0.922	
4	C162-4	602	1034	2365				11.846	0.816		0.731	0.816	
5	C162-5	421	511	1172	1328	2332	2548	4.857	0.440	56.297	0.673	0.440	0.779
6	C162-6	382	563	1244	1299	2623	3264	6.986	0.441	175.618	0.845	0.441	0.855
7	C162-7	583	886	1896	2398	4419		11.347	0.887		0.790	0.887	
8	C162-8	418	587	1083	1529	2288	2677	5.290	0.563	71.285	0.523	0.563	0.415
9	C162-9	413	612	1168	1811	2502	2799	6.666	0.748	69.118	0.714	0.748	0.630
10	C162-10	532	788	1650	3101	3520	3830	6.505	0.699	99.351	0.512	0.699	0.720
	Average	500	801	1592	2192	2998		10.921	0.710	94.334	0.693	0.710	0.680
	CV %	17%	30%	29%	43%	26%		75%	26%	51%	19%	26%	25%

Appendix C. Heel Joint Data.

The definitions for the heel joint tables are the same as the definitions of the tension splice joints. The displacement used for the heel joint is the longitudinal displacement of the top chord.

Table C- 1. Heel Joint Characteristics.

No.	Test Number	Load Type	Joint ID	Ultimate Load	Modulus of Elasticity	Moisture Content	Specific Gravity	Ring Count	Percent Latewood	Grain Orientation
				lbs	psi	%	Dry Based	per Inch	%	Degrees
1	HL-2	Static	H8	5890	2.15	12%	0.52	5.0	33%	0
2	HL-3	5/31/96	H19	5397	1.74	12%	0.39	4.0	40%	5
3	HL-5		H25	6114	2.96	12%	0.57	10.5	33%	2
4	HL-6		H28	5882	1.65	13%	0.39	5.0	25%	0
5	HL-7		H35	6360	1.73	10%	0.49	5.5	40%	9
6	HL-8		H14	5256	2.15	12%	0.49	12.5	33%	23
7	HL-9		S2.18	5799	2.18	13%	0.47	11.5	50%	0
8	HL-10		H24	5874	1.83	12%	0.43	6.0	50%	32
9	HL-11		H18	5408	1.76	14%	0.57	5.0	45%	25
10	HL-12		H26	5650	2.27	12%	0.51	7.5	25%	25
	Average			5763	2.0	12%	0.48	7.3	38%	12
	Average Design			1921						
	CV %			6%	19%	7%	13%	43%	25%	105%
1	CH16-1	CH16	H20	5731	1.71	12%	0.54	5.5	60%	0
2	CH16-2	6/2/96	H1	6225	1.91	13%	0.46	4.5	12%	12
3	CH16-3		H33	5456	1.72	12%	0.44	6.5	50%	66
4	CH16-4		H21	5490	1.98	12%	0.46	16.0	33%	8
5	CH16-5		H16	4764	1.75	12%	0.44	4.0	33%	22
6	CH16-6		H9	5969	2.15	12%	0.44	21.0	33%	5
7	CH16-7		H28	5036	1.65	11%	0.38	5.0	33%	7
8	CH16-8		H29	4802	2.63	12%	0.52	5.0	50%	0
9	CH16-9		S1.88	6001	1.88	12%	0.47	12.0	50%	0
10	CH16-10		S1.98	6031	1.98	13%	0.53			
	Average			5551	1.94	12%	0.47	8.8	37%	13
	CV %			10%	15%	4%	11%	69%	36%	157%
1	CH162-1*	Cy162	H35	4766*	1.73	12%	0.43	6.0	50%	10
2	CH162-2	6/4/96	S2.78	5482	2.78	12%	0.56	26.0	33%	5
3	CH162-3		H16	4709	1.75	12%	0.42	5.0	33%	10
4	CH162-4		H3	6738	1.68	12%	0.53	4.0	50%	14
5	CH162-5		H34	5430	2.48	12%	0.46	7.0	40%	7
6	CH162-6		H16	5474	1.75	12%	0.43	4.0	40%	13
7	CH162-7		H7	6177	1.71	14%	0.52	4.0	33%	5
8	CH162-8		H18	4996	1.76	13%	0.52	9.5	40%	30
9	CH162-9		H20	5341	1.71	11%	0.44	6.0	40%	14
10	CH162-10		H4	3502	1.81	12%	0.44	6.5	60%	7
	Average			5317	1.92	12%	0.47	7.8	41%	12
	CV %			17%	20%	5%	11%	85%	22%	64%
1	CH18-1	Cy18	H10	6029	2	13%	0.48	6.0	50%	14
2	CH18-2	6/10/96	H12	5327	1.85	12%	0.45	9.0	33%	0
3	CH18-3		H30	5077	1.83	12%	0.45	6.0	40%	0
4	CH18-4		H11	6023	1.77	11%	0.40	12.0	20%	20
5	CH18-5		S1.95	6189	1.95	13%	0.49	5.5	33%	2
6	CH18-6		H8	5981	2.15	13%	0.49	5.5	33%	4
7	CH18-7		H17	4972	2.15	13%	0.51	13.0	33%	3
8	CH18-8		H29	5038	2	13%	0.51	5.0	50%	7
9	CH18-9		S2.78	5727	2.63	12%	0.54	27.0	33%	4
10	CH18-10		H7	6039	1.71	13%	0.48	4.5	33%	1
	Average			5640	2.00	12%	0.48	9.4	34%	6
	CV %			9%	13%	4%	8%	74%	23%	119%

Table C- 2. Heel Joint Stiffness Summary.

No.	Test Number	Load Case	Joint ID	Ultimate Load lbs	Ult. Disp. in.	Cyclic Offset in.	Dead Load Stiffness 10^5 lb/in	Design Load Stiffness 10^5 lb/in	Dead/Design Decrease Percent	Survival
1	HL-2	Static	H8	5890	0.125	NA	2.49	1.10	56%	NA
2	HL-3	5/31/96	H19	5397		NA	Bad Deflection Data			NA
3	HL-5		H25	6114	0.21	NA	2.52	0.86	66%	NA
4	HL-6		H28	5882	0.17	NA	2.00	1.23	39%	NA
5	HL-7		H35	6360	0.236	NA	2.37	1.15	51%	NA
6	HL-8		H14	5256	0.215	NA	2.09	0.96	54%	NA
7	HL-9		S2.18	5799	0.234	NA	2.53	1.03	59%	NA
8	HL-10		H24	5874	0.231	NA	2.07	1.09	48%	NA
9	HL-11		H18	5408	0.173	NA	1.94	1.22	37%	NA
10	HL-12		H26	5650	0.185	NA	1.94	0.81	58%	NA
	Average			5763	0.198		2.22	1.05	52%	
	Average Design			1921						
	CV %			6%	19%		12%	14%	18%	
1	CH16-1	CH16	H20	5731	0.205	0.039	2.21	1.00	55%	Y
2	CH16-2	6/2/96	H1	6225	0.306	0.045	2.34	0.10	96%	Y
3	CH16-3		H33	5456	0.194	0.070	3.13	-0.45	114%	Y
4	CH16-4		H21	5490	0.224	0.072	1.77	0.70	60%	Y
5	CH16-5		H16	4764	0.211	0.129	2.01	0.44	78%	Y
6	CH16-6		H9	5969	0.106	0.038	2.64	0.38	86%	Y
7	CH16-7		H28	5036	0.165	0.056	1.26	0.87	31%	Y
8	CH16-8		H29	4802	0.148	0.076	2.20	0.08	96%	Y
9	CH16-9		S1.88	6001	0.255	0.034	1.94	0.54	72%	Y
10	CH16-10		S1.98	6031	0.251	0.035	2.00	-0.19	109%	Y
	Average			5551	0.207	0.059	2.15	0.35	80%	
	CV %			10%	28%	49%	23%	133%	33%	
1	CH162-1*	CH162	H35	4766*	0.267	0.228	2.31	0.25	89%	Y
2	CH162-2	6/4/96	S2.78	5482			1.49		100%	N
3	CH162-3		H16	4709			1.91		100%	N
4	CH162-4		H3	6738	0.29	0.045	3.21	1.82	43%	Y
5	CH162-5		H34	5430			1.88		100%	N
6	CH162-6		H16	5474			2.65		100%	N
7	CH162-7		H7	6177	0.304	0.062	2.78	0.58	79%	Y
8	CH162-8		H18	4996	0.311	0.203	2.70	1.31	51%	Y
9	CH162-9		H20	5341			2.45		100%	N
10	CH162-10		H4	3502			1.28		100%	N
	Average			5317	0.293	0.135	2.27	0.99	86%	
	CV %			17%	7%	70%	27%	72%	25%	
1	CH18-1	CH18	H10	6029	0.23	0.046	2.97	0.92	69%	Y
2	CH18-2	6/10/96	H12	5327	0.268	0.119	2.31	0.85	63%	Y
3	CH18-3		H30	5077			2.58		100%	N
4	CH18-4		H11	6023	0.237	0.057	2.92	0.95	68%	Y
5	CH18-5		S1.95	6189	0.348	0.080	2.23	1.15	49%	Y
6	CH18-6		H8	5981	0.28	0.076	2.42	1.46	40%	Y
7	CH18-7		H17	4972	0.223	0.128	2.88	0.78	73%	Y
8	CH18-8		H29	5038			2.15		100%	N
9	CH18-9		S2.78	5727	0.184	0.039	2.39	1.42	41%	N
10	CH18-10		H7	6039	0.278	0.051	0.46	0.63	-36%	Y
	Average			5640	0.256	0.075	2.33	1.02	56%	
	CV %			9%	19%	45%	31%	29%	69%	

Table C- 3. Heel Joint Hysteresis Summary.

No.	Test Number	Stiffness at Start of Stage 1 10^5 lb/in	Stiffness at End of Stage 1 10^5 lb/in	Stiffness at Start of Stage 2 10^5 lb/in	Stiffness at End of Stage 2 10^5 lb/in	Stiffness at Start of Stage 3 10^5 lb/in	Stiffness at End of Stage 3 10^5 lb/in	Slope of Regression Stage 1	Slope of Regression Stage 2	Slope of Regression Stage 3	R Squared Value Stage 1	R Squared Value Stage 2	R Squared Value Stage 3
1	CH16-1	2.26	2.03	1.45	1.24			-0.003	-0.023		0.111	0.917	
2	CH16-2	2.66	2.38	1.83	1.33			-0.018	-0.042		0.573	0.927	
3	CH16-3	2.75	2.15	1.74	1.23			-0.020	-0.032		0.729	0.240	
4	CH16-4	2.32	1.84	1.31	0.95			-0.014	-0.026		0.617	0.879	
5	CH16-5	2.37	1.96	1.26	0.64			-0.007	-0.056		0.334	0.821	
6	CH16-6	3.30	2.84	2.17	1.71			-0.014	-0.029		0.461	0.757	
7	CH16-7	2.09	1.68	1.29	0.89			-0.015	-0.031		0.708	0.967	
8	CH16-8	2.57	2.35	1.49	1.08			-0.013	-0.037		0.657	0.959	
9	CH16-9	2.54	2.19	1.79	1.46			-0.010	-0.028		0.633	0.906	
10	CH16-10	2.73	2.63	2.01	1.75			-0.009	-0.023		0.316	0.707	
	Average	2.56	2.21	1.63	1.23			-0.012	-0.033		0.514	0.808	
	CV %	13%	16%	20%	29%			-42%	-30%		39%	27%	
1	CH162-1*	Bad Deflection Data											
2	CH162-2	2.44	1.87	1.32	0.83			-0.012	-0.039		0.490	0.931	
3	CH162-3	3.57	2.91	2.40	2.00	1.61	1.37	-0.016	-0.029	-0.050	0.504	0.833	0.833
4	CH162-4	2.25	1.89	1.41	1.08	0.85		-0.009	-0.022	-0.063	0.425	0.894	0.922
5	CH162-5	2.69	2.10	1.74	1.51	1.05		-0.017	-0.017	-0.061	0.746	0.779	0.882
6	CH162-6	3.52	2.98	2.25	2.03	1.62	1.24	-0.015	-0.022	-0.063	0.429	0.536	0.794
7	CH162-7	2.61	2.45	1.93	1.62	1.34	0.91	-0.004	-0.026	-0.078	0.105	0.842	0.967
8	CH162-8	2.37	1.93	1.35	1.09	0.88		-0.014	-0.018	-0.093	0.708	0.873	0.983
9	CH162-9	1.25						-0.022			0.960		
10	CH162-10												
	Average	2.59	2.30	1.77	1.45	1.22	1.17	-0.014	-0.025	-0.068	0.546	0.812	0.897
	CV %	29%	21%	25%	32%	29%	20%	-39%	-31%	-22%	47%	16%	8%
1	CH18-1	3.15	2.56	1.90	1.39			-0.013	-0.041		0.498	0.910	
2	CH18-2	2.32	1.94	1.45	0.92			-0.010	-0.038		0.636	0.892	
3	CH18-3	2.70	1.84	1.23	0.73			-0.023	-0.040		0.792	0.956	
4	CH18-4	2.64	2.05	1.53	1.22			-0.015	-0.031		0.685	0.938	
5	CH18-5	2.65	2.15	1.57	1.16			-0.017	-0.027		0.652	0.806	
6	CH18-6	3.13	2.05	1.33	1.02			-0.021	-0.023		0.611	0.865	
7	CH18-7	3.02	2.12	1.92	0.97			-0.022	-0.059		0.765	0.829	
8	CH18-8	2.09	1.83	1.23				-0.007	-0.044		0.507	0.910	
9	CH18-9	3.03	2.39	1.93	1.34			-0.017	-0.052		0.615	0.880	
10	CH18-10	Bad Test Data											
	Average	2.75	2.10	1.57	1.09			-0.016	-0.039		0.640	0.887	
	CV %	14%	12%	19%	21%			-33%	-30%		16%	5%	

Table C- 4. Heel Joint Energy Dissipation Summary.

No.	Test Num.	Energy Disp. Start of Stage 1	Energy Disp. End of Stage 1	Energy Disp. Start of Stage 2	Energy Disp. End of Stage 2	Energy Disp. Start of Stage 3	Energy Disp. End of Stage 3	Slope of Regression Stage 1	Slope of Regression Stage 2	Slope of Regression Stage 3	R Squared Value Stage 1	R Squared Value Stage 2	R Squared Value Stage 3
		10^5 lb/in	10^5 lb/in	10^5 lb/in	10^5 lb/in	10^5 lb/in	10^5 lb/in						
1	CH16-1	1084	3295	2991				43.378	0.118		0.381	0.118	
2	CH16-2	909	4597	4408				23.202	0.023		0.065	0.023	
3	CH16-3	789	3302	2663				40.240	0.233		0.358	0.233	
4	CH16-4	1404	5212	5508				68.421	0.485		0.530	0.485	
5	CH16-5	1583	5587	6714				67.647	0.631		0.430	0.631	
6	CH16-6	881	3894	3416				45.951	0.269		0.375	0.269	
7	CH16-7	916	3121	4826				41.660	0.072		0.477	0.072	
8	CH16-8	1060	3161	6970				45.411	0.345		0.503	0.345	
9	CH16-9	1155	3203	4757				50.306	0.110		0.429	0.110	
10	CH16-10	1075	2492	4043				33.518	0.021		0.487	0.021	
	Average	1086	3786	4630				45.973	0.231		0.404	0.231	
	CV %	23%	27%	31%				30%	89%		33%	89%	
1	CH162-1*	Bad Deflection Data											
2	CH162-2	1678	6463	6210	7564			77.890	0.445		0.460	0.445	
3	CH162-3	793	2016	2956	6507	8722		29.516	0.580		0.277	0.580	
4	CH162-4	1547	4643	6005	4480	6939	9435	61.307	0.623		0.484	0.623	0.849
5	CH162-5	1159	5016	3655	6972	8029		63.704	0.628		0.391	0.628	
6	CH162-6	697	1934	2810	5573			27.461	0.671		0.441	0.671	
7	CH162-7	802	2509	3522	11010	5573	7510	29.782	0.695		0.418	0.695	0.971
8	CH162-8	1309	5291	4263	5557	8891	9359	64.930	0.588		0.357	0.588	0.819
9	CH162-9	2917						278.704			0.822		
10	CH162-10												
	Average	1363	3982	4203	6809	7631	8768	79.162	0.604		0.456	0.604	0.880
	CV %	53%	45%	33%	31%			105%	13%		35%	13%	
1	CH18-1	642	2769	4380	4846			44.456	0.297		0.426	0.297	
2	CH18-2	1092	4906	6995	8214			72.972	0.749		0.433	0.749	
3	CH18-3	1091	5665	5994	8242			78.295	0.857		0.361	0.857	
4	CH18-4	1092	3416	5344	6569			47.806	0.264		0.380	0.264	
5	CH18-5	1319	5156	5479	9540			71.223	0.929		0.429	0.929	
6	CH18-6	1404	6412	5165	6084			79.697	0.052		0.397	0.052	
7	CH18-7	869	4395	5262	8598			64.807	0.329		0.341	0.329	
8	CH18-8	1564	5993	9828				85.645	0.509		0.475	0.509	
9	CH18-9	740	2714	4160	5680			37.238	0.548		0.352	0.548	
10	CH18-10	Bad Test Data											
	Average	1090	4603	5845				64.682	0.504		0.399	0.504	
	CV %	28%	30%	29%				27%	59%		11%	59%	